

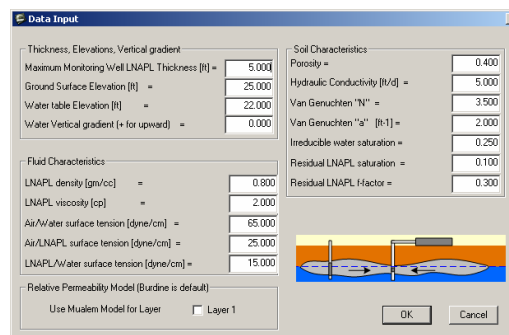
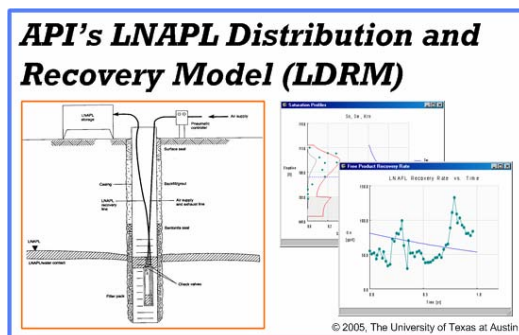


# LNAPL Distribution and Recovery Model (LDRM)

## Volume 2: User and Parameter Selection Guide

Regulatory and Scientific Affairs Department

API PUBLICATION 4760  
JANUARY 2007





# **LNAPL Distribution and Recovery Model (LDRM)**

## **Volume 2: User and Parameter Selection Guide**

**Regulatory and Scientific Affairs Department**

API PUBLICATION 4760  
JANUARY 2007

Prepared by:

Randall Charbeneau, Ph.D., P.E.  
The University of Texas at Austin  
Austin, Texas

G.D. Beckett, R.G., C.H.G.  
AQUI-VER, INC.  
Park City, Utah



## SPECIAL NOTES

API publications necessarily address problems of a general nature. With respect to particular circumstances, local, state, and federal laws and regulations should be reviewed.

Neither API nor any of API's employees, subcontractors, consultants, committees, or other assignees make any warranty or representation, either express or implied, with respect to the accuracy, completeness, or usefulness of the information contained herein, or assume any liability or responsibility for any use, or the results of such use, of any information or process disclosed in this publication. Neither API nor any of API's employees, subcontractors, consultants, or other assignees represent that use of this publication would not infringe upon privately owned rights.

API publications may be used by anyone desiring to do so. Every effort has been made by the Institute to assure the accuracy and reliability of the data contained in them; however, the Institute makes no representation, warranty, or guarantee in connection with this publication and hereby expressly disclaims any liability or responsibility for loss or damage resulting from its use or for the violation of any authorities having jurisdiction with which this publication may conflict.

API publications are published to facilitate the broad availability of proven, sound engineering and operating practices. These publications are not intended to obviate the need for applying sound engineering judgment regarding when and where these publications should be utilized. The formulation and publication of API publications is not intended in any way to inhibit anyone from using any other practices.

Any manufacturer marking equipment or materials in conformance with the marking requirements of an API standard is solely responsible for complying with all the applicable requirements of that standard. API does not represent, warrant, or guarantee that such products do in fact conform to the applicable API standard.

*All rights reserved. No part of this work may be reproduced, stored in a retrieval system, or transmitted by any means, electronic, mechanical, photocopying, recording, or otherwise, without prior written permission from the publisher. Contact the Publisher, API Publishing Services, 1220 L Street, N.W., Washington, D.C. 20005.*

## **FOREWARD**

Nothing contained in any API publication is to be construed as granting any right, by implication or otherwise, for the manufacture, sale, or use of any method, apparatus, or product covered by letters patent. Neither should anything contained in the publication be construed as insuring anyone against liability for infringement of letters patent.

Suggested revisions are invited and should be submitted to the Director of Regulatory and Scientific Affairs, API, 1220 L Street, NW, Washington, D.C. 20005.

## PREFACE

This manuscript documents use of the American Petroleum Institute LNAPL Distribution and Recovery Model (LDRM), and is presented as a supplement to API Publication Number 4682, *Free-Product Recovery of Petroleum Hydrocarbon Liquids*, which was published in June 1999, and to API Publication Number 4729, *Models for Design of Free-Product Recovery Systems for Petroleum Hydrocarbon Liquids; A User's Guide and Model Documentation*, which was published in August 2003 and included in the *API Interactive LNAPL Guide*. This manuscript is Volume 2 of a two volume series providing background and user information for LDRM. Guidance on use of the model is provided, along with information to help in parameter selection. The appendix presents results from an independent analysis of model performance. The API LDRM software can be downloaded from API's website at: [groundwater.api.org/lnapl](http://groundwater.api.org/lnapl).

# TABLE OF CONTENTS

<u>Section</u>		<u>Page</u>
1	INTRODUCTION.....	1
1.1	Background and Objectives.....	1
1.2	Scenarios for Free-Product Hydrocarbon Liquid Recovery.....	1
1.2.1	Scenarios for Recovery Well Systems.....	2
1.2.2	Scenario for LNAPL Recovery Using Trenches.....	3
1.3	Overview.....	4
2	USER GUIDE	
2.1	Workspace Setup .....	6
2.2	Starting the Application.....	7
2.3	Data Input Window .....	9
2.4	Menu Items.....	10
2.4.1	Add Field Data .....	13
2.4.2	LNAPL Recovery.....	15
2.4.3	Graphs Output.....	17
2.4.4	LNAPL Residual Saturation Models and Residual F-Factor Options .....	24
2.4.5	Piecewise Linear Model Breakpoint Options .....	25
2.4.6	Smear Correction Option .....	27
2.5	Model Output Options.....	29
2.5.1	Screen Output to the Main Application Window .....	29
2.5.2	File Output from LDRM Application .....	30
3	PARAMETER SELECTION AND PROBLEM SOLVING GUIDE .....	32
3.1	Objectives and Overview.....	32
3.2	Oil Recovery Experiences: Oilfield Production versus LNAPL Recovery .....	33
3.3	Parameter Limitations.....	34
3.4	Model Conceptualization .....	36
3.5	Multiphase Parameter Selection .....	38
3.5.1	Background to Multiphase Parameter Databases .....	38
3.5.2	Introduction to the API LNAPL Parameters Database.....	39
3.6	Example Problems .....	41
3.6.1	Problem #1: Simple Skimming Recovery Evaluation.....	43
3.6.1.1	Parameter Selection .....	43
3.6.1.2	Example Problem #1 Execution .....	44
3.6.2	Problem #2: Optimizing Remedial Options.....	49
3.6.2.1	Parameter Selection .....	49
3.6.3	Problem #3: Parameter Bracketing Problem .....	53
3.6.3.1	Parameter Selection Using the API LNAPL Parameter Database... ..	54
3.6.3.2	Example Problem #3: Execution .....	59
3.6.3.3	Problem #3: Conclusion .....	64
3.6.4	Problem #4: Case Study: LNAPL Recovery in Glacial Outwash Sands (Adapted from API Publication #4715).....	66
3.6.4.1	Problem Overview .....	66
3.6.4.2	Data Summary.....	67
3.6.4.3	Model Conceptualization Summary.....	68
3.6.4.4	Example Problem #4 Execution .....	69
3.6.4.5	Example Problem #4 Conclusions .....	76
4	REFERENCES.....	77
APPENDIX A	REVIEW OF THE LNAPL DISTRIBUTION & RECOVERY MODEL MATHEMATICAL VERIFICATION, CODE FIXES, & SENSITIVITY.....	79





# LIST OF FIGURES

<u>Figure</u>	<u>Page</u>
1.1	Monitoring Well LNAPL Thickness, $b_n$ ..... 2
1.2	Recovery Well System with 7 Recovery Wells Showing the Radius of Capture (Modified from Lefebvre, 2000)..... 3
1.3	Simple Trench System for LNAPL Recovery..... 4
2.1	Example Setup Folder Showing Project Workspace..... 6
2.2	API LDRM Logo..... 7
2.3	Terms and Conditions Window..... 7
2.4	Initiation Message Box..... 8
2.5	Standard Open File Dialog..... 8
2.6	Project Setup Dialog that Appears Only When “New” Simulation is Selected..... 9
2.7	Data Input Window for a 1 Layer Model..... 10
2.8	Standard File Menu Items..... 10
2.9	Data Menu Items..... 11
2.10	Recovery Menu Items..... 11
2.11	Graphs Menu Items..... 12
2.12	Options Menu Items..... 12
2.13	Help Menu Items..... 13
2.14	Input Field Data Options Message Window..... 14
2.15	Data Transfer Control Message Box..... 14
2.16	Application Folder with “field_data.csv” Spreadsheet..... 14
2.17	“field_data.csv” Spreadsheet with Data..... 15
2.18	Well Recovery Systems Data Entry Window..... 16
2.19	Interceptor Trench Data Entry Window..... 17
2.20	Data Input Window for Two-Layer Soil..... 18
2.21	Saturation Profiles Graph Output..... 18
2.22	Specific Volume/Transmissibility Graph Output..... 19
2.23	Free Product Thickness Graph Output..... 20
2.24	Drawdown/Buildup Graph Output..... 21
2.25	LNAPL Recovery Rate Graph Output..... 22
2.26	LNAPL Recovery Volume Graph Output..... 23
2.27	LNAPL Thickness Dialog Box for Later-Time Distributions..... 23
2.28	LNAPL Distribution Graph Output..... 24
2.29	Three Different LNAPL Residual Saturation Model Representations..... 25
2.30	LNAPL Distribution Output Graph with Variable LNAPL Residual Saturation..... 25
2.31	Pick Break Points: $bn_1$ , $bn_2$ Message Box..... 26
2.32	Piecewise Linear Model Representation with Alternative Breakpoints (Compare with Figure 2.22)..... 26
2.33	Initial LNAPL Saturation Distribution for Example with Smearing Option Selected..... 27
2.34	New LNAPL Layer Saturation Distribution Following Drawdown of the Water Table Using the Smear Correction Option..... 28
2.35	Summary Output Variables Written to the Main Window of the LDRM Application..... 30
2.36	Leading Part of the LDRM Simulation Output File..... 31
3.1	Simple Conceptual Site Model..... 37
3.2	Complex Cross-Section Showing Heterogeneity (Based on Combined Coring & Geophysics), Along with the Water Table Elevation Range and Site Investigation Locations..... 37
3.3	Startup Box, with Selection Shown..... 43
3.4	Startup Box, with Selection Shown..... 44

3.5	Input Parameters Controlling the LNAPL Distribution at Vertical Equilibrium.....	45
3.6	Results chart of Specific Volumes/Transmissibility for the Given Problem. Recall that $D_n$ is the specific volume, and $R_n$ is the recoverable volume. $T_n$ is the LNAPL transmissibility. Paralleling that is a linearized “fit” that can be tuned by the user as discussed in the text.....	46
3.7	Input Parameters for Skimming Recovery Portion of Problem #1 .....	47
3.8	Summary Output for Skimming Recovery Using the Constant Residual Saturation Option (Original Problem Definition) .....	48
3.9	Summary Output for the F-factor Residual Saturation Conditions, with Other Parameters Being the Basic Skimming Simulation.....	49
3.10	Data Input Screen for a Recovery Time of 2 Years .....	51
3.11	Results for Vacuum-Assisted Skimming .....	52
3.12	Site-specific Grain Size Data—Sample 1 .....	55
3.13	Site-specific Grain Size Data—Sample 2 .....	55
3.14	Capillary Fit Parameters for Samples with Soil Description.....	56
3.15	Capillary Fit Parameters for Given Conductivity Range .....	58
3.16	Grain Size Curves, Site Samples versus Database Samples .....	59
3.17	Initial Data Input Screen for Example Problem #3 .....	60
3.18	Saturation Profiles for Data Input in Figure 3.17 .....	61
3.19	Saturation Profile for $\alpha = 3.5 \times 10^{-2}$ 1/cm and $N=2.25$ .....	61
3.20	Saturation Profile for $\alpha = 7.8 \times 10^{-2}$ 1/cm and $N=1.50$ .....	62
3.21	Data Input Screen for Example Problem #4 .....	69
3.22	Saturation Profile for Example Problem #4 Input Data .....	70
3.23	Recovery Input Data for Example Problem #4 .....	71
3.24	Drawdown/Buildup Screen for Example Problem #4.....	71
3.25	Data Input for Model with Two Layers .....	72
3.26	Drawdown/Buildup for 2-Layer Model.....	73
3.27	LNAPL Recovery Rate versus Time .....	74
3.28	LNAPL Recovery Volume versus Time.....	75

## LIST OF TABLES

<u>Table</u>		<u>Page</u>
3.1	USDA Soil Types and Multiphase Parameters (from M.G. Schaap, U.S. Salinity Lab, 1999). Where: $N$ is the number of samples; $\theta_r$ is the residual volumetric moisture content; $\theta_s$ is the saturated volumetric moisture content (total porosity); $\log(\alpha)$ is the log of the van Genuchten model $\alpha$ parameter; $\log(n)$ is the log of the van Genuchten model $N$ parameter; and $K_s$ is the log of the saturated hydraulic conductivity. Abbreviations: S = sand; C = clay; L = loam; Si = silt.....	39
3.2	Results of Initial Optimization Simulations.....	51
3.3	Results for Vacuum-Assisted Skimming.....	51
3.4	Results of the Smear Zone Correction Problem.....	52
3.5	Site-Specific Grain Size Data.....	55



## EXECUTIVE SUMMARY

This document provides user and parameter selection guidance for application of the American Petroleum Institute LNAPL Distribution and Recovery Model (LDRM). This is Volume 2 of a two volume series; the first volume provides background information on distribution and recovery of petroleum hydrocarbon liquids in porous media, and is intended as an LNAPL primer. Section 1 of this volume discusses earlier releases of the API LNAPL Recovery Model and describes the new features of the current release of the model software application that is associated with this document series. Model scenarios (wells and trenches) are also described. Section 2 is a detailed guide to use of the LDRM software application. Workspace setup, program initiation, and data entry are described. The various menu items which provide the basic navigation tools through the application are discussed. Model options are described and model output using graphical screen output and text files are presented. Section 3 provides background information on model conceptualization, parameter selection (and limitations), and problem solving using the LDRM. Four example problem applications are presented which highlight model use, parameter estimation using the API LNAPL Parameters Database, and limitations of scenario-based models.



# 1 INTRODUCTION

## 1.1 BACKGROUND AND OBJECTIVES

The American Petroleum Institute (API) Publication Number 4682, *Free-Product Recovery of Petroleum Hydrocarbon Liquids* (Charbeneau et al., 1999), provides an overview of recovery technologies for petroleum hydrocarbon liquids that are released to the subsurface environment and accumulate near the water table. The primary recovery technologies include skimmer wells that produce hydrocarbon liquids and single- and dual-pump wells that produce both water and hydrocarbon liquids. Hydrocarbon liquid recovery rates may also be enhanced by applying a vacuum pressure to the well to increase the gradient towards the well within the hydrocarbon layer. API Publ 4682 describes two (Excel spreadsheet) models that may be used to characterize the subsurface distribution and mobility of liquid hydrocarbon (lighter-than-water nonaqueous phase liquids, LNAPL), and to calculate the potential recovery rate and time using single- and dual-pump wells, and vacuum-enhanced wells.

API Publication Number 4729, *Models for Design of Free-Product Recovery Systems for Petroleum Hydrocarbon Liquids* (Charbeneau, 2003) describes scenario-based models for LNAPL liquid recovery using skimmer wells, water and vacuum enhanced recovery wells, and trenches. Soil capillary pressure characteristics are described using the van Genuchten (1980) capillary pressure model (soil characteristics in API Publ 4682 are described using the Brooks and Corey (1964) capillary pressure model). Implementation of the models through use of four separate spreadsheets is presented, based on single or two-layer heterogeneity, and on selection of relative permeability model (Burdine, 1953, or Mualem, 1976).

The objective of the present manuscript is to provide necessary background and user information for application of scenario-based models describing LNAPL liquid recovery. Volume 1 of this two-volume series provides model background information including the effects of capillarity in porous media, distribution of LNAPL saturation under conditions of vertical equilibrium, potential movement of LNAPL liquid, and mathematical model formulation and solution. The model scope is similar to that presented in API Publ 4729, though the model formulation has been generalized and additional capabilities have been added. The present Volume 2 describes model implementation through a single executable program. This is a User Guide and includes information and guidance on parameter selection and model testing.

## 1.2 SCENARIOS FOR FREE-PRODUCT HYDROCARBON LIQUID RECOVERY

Proven technologies for free-product recovery of petroleum hydrocarbon liquids are described in API 4682. Models to provide quantitative estimates of system performance must necessarily be based on simplifying assumptions that will not be applicable to all field conditions. Nevertheless, the models provide insight and guidance that should be helpful in technology selection and system design, and in analysis of system performance. The model scenarios for well systems and trenches are discussed separately.

The subsurface porous media is assumed to be laterally homogeneous, but can have up to three distinct layers (numbered with Layer 1 on top) with different soil characteristic and permeability parameters. The vertical transition between layers is assumed to be abrupt. An example two-layer soil system is shown in Figure 1.1. This figure shows a monitoring well with an LNAPL layer located between the air-NAPL interface  $z_{an}$  and the NAPL-water interface  $z_{nw}$ . The total monitoring well LNAPL thickness is  $b_n$ . The elevation of the abrupt transition between the upper and lower soil layers is designated  $z_{12}$ . The elevation of the water table is designated  $z_{aw}$ . While the water table is not present because of the LNAPL layer, its elevation is easily determined from the elevations  $z_{an}$  and  $z_{nw}$ , and the LNAPL density  $\rho_n$  (see Section 2 of Volume 1).

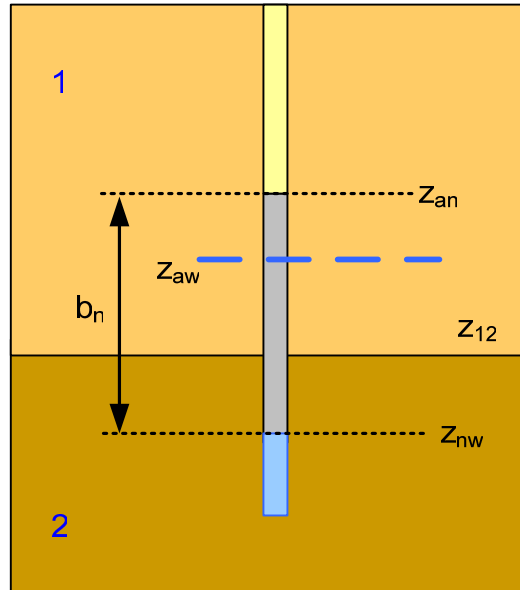


Figure 1.1—Monitoring Well LNAPL Thickness,  $b_n$

The soil texture characteristics that must be defined for each layer of the porous medium include the porosity  $n$ ; the (water phase) hydraulic conductivity  $K_w$ ; the van Genuchten parameters  $N$  and  $\alpha$ ; and the irreducible water saturation,  $S_{wr}$ . Selection of residual LNAPL saturation values remains an elusive issue, and various options are described in Section 2.4.4. Fluid properties include the LNAPL density,  $\rho_n$  (it is assumed that the water density is  $1 \text{ g/cm}^3$ ), and the water and LNAPL surface and interfacial tensions,  $\sigma_{aw}$ ,  $\sigma_{an}$ , and  $\sigma_{nw}$ .

### 1.2.1 Scenarios for Recovery Well Systems

The basic scenario for free-product recovery using well systems is the same for single- and dual-pump wells, vacuum-enhanced wells, and skimmer wells. The performance of each well is characterized in terms of its radius of capture  $R_c$ , with a typical scenario shown in Figure 1.2. This figure depicts a plan view of an LNAPL lens (in gray color) with 7 recovery wells located so that the pattern of wells with their radius of capture will cover most of the area of the lens. For single- and dual-pump well systems, the radius of capture could extend out to the radius of influence (water production) of the well. For vacuum-enhanced systems, the radius of influence of the vacuum extraction well (which is typically on the order of 30 – 40 feet) limits the radius of capture. For skimmer wells, the radius of capture is limited to a greater but unknown extent, which is probably on the order of 10 – 30 feet.



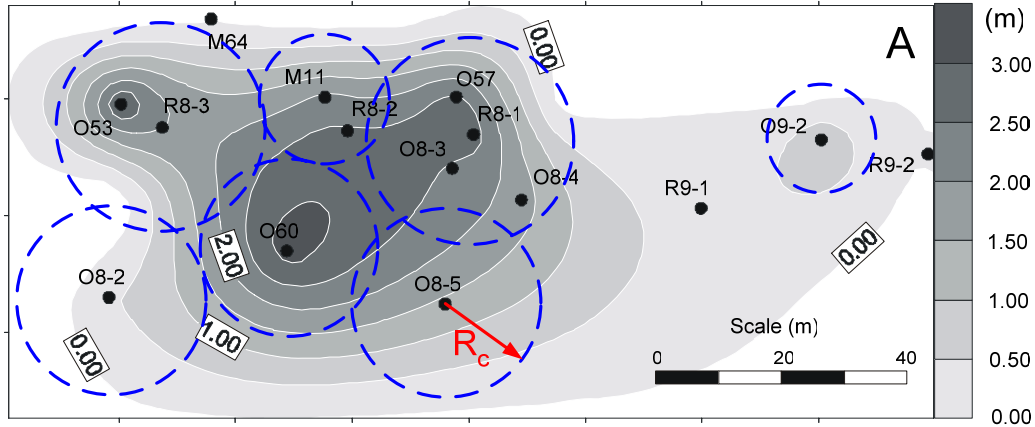


Figure 1.2—Recovery Well System with 7 Recovery Wells Showing the Radius of Capture. Scale on Right Side Shows Measured LNAPL Thickness in Wells. (Modified from Lefebvre, 2000)

The data required for analysis of recovery-well-system performance includes the radius of capture for the well, the LNAPL viscosity (the water viscosity is assumed to be 1 cp), and water production rate for a water-enhanced system or wellhead vacuum pressure for a vapor-enhanced system. For a water-enhanced system, the effective depth of penetration of the well into the aquifer must be specified, while for a vacuum-enhanced system, the screened interval of the vadose zone must be given. The effective relative permeability of the vadose zone due to the presence of residual soil water is assumed to be  $k_{ra} = 0.9$ . If zero water production and wellhead pressure are specified, then the well is assumed to function as a skimmer well.

### 1.2.2 Scenario for LNAPL Recovery Using Trenches

The modeling framework may also be used to represent a simple trench recovery system, such as shown in Figure 1.3. The trench has a length  $L_T$  transverse to the direction of groundwater flow. The LNAPL lens is assumed to be of rectangular shape with length  $L_T$  and width  $W_T$ . The natural groundwater hydraulic gradient  $J_w$  is transferred to the LNAPL layer and carries it into the trench where LNAPL is removed by skimmer wells or other technology. The rate of LNAPL discharge into the trench will depend on the effective lens thickness as observed in a monitoring well, soil texture, natural groundwater hydraulic gradient, and whether groundwater is also produced from the trench in order to increase the hydraulic gradient. If the trench cuts across an LNAPL lens, then the upstream and downstream sections of the lens must be analyzed separately, with  $J_w$  being negative on the downstream side.

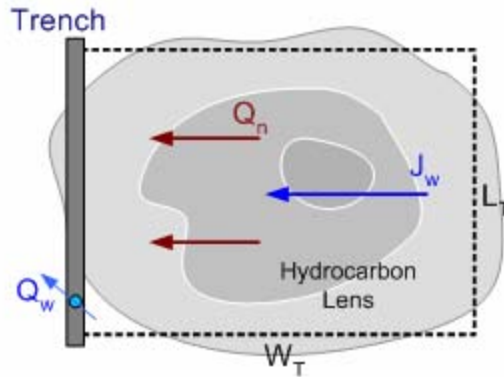


Figure 1.3—Simple Trench System for LNAPL Recovery

### 1.3 OVERVIEW

The new features included in this release of the API LDRM include the following:

- the model is a single, stand-alone executable application,
- one may select either US Customary or metric units,
- soil heterogeneity may be represented through use of 1, 2 or 3 soil layers,
- soil profile data may be represented either as elevation above a datum or as depth below the ground surface,
- the capability for simulating LNAPL smearing associated with water table drawdown has been added,
- three different representations for LNAPL residual saturation are available, and the user may change between representations during a modeling session,
- the effects of vertical hydraulic gradient through surface fine-grain soil layers on LNAPL distribution and recovery may be represented,
- either the Burdine or Mualem relative permeability model may be selected for individual soil layers,
- measured field data on LNAPL saturation, LNAPL thickness, LNAPL recovery volume, and LNAPL recovery rate may be added and displayed on model graphical output,
- model formulation through use of the LNAPL layer transmissibility function is both more rigorous and simpler than earlier model formulations,
- the user may more directly specify the breakpoints for the piecewise linear fit of the LNAPL transmissibility and specific volume functions,
- more extensive and useful model output capabilities have also been added.

Section 2 of this document provides detailed user information on application of LDRM. Model setup and data input are described. The user interacts with the application primarily through menu items that are selected on the main application window. These are described in Section 2.4. The method for adding field data is presented in Section 2.4.1, while the steps for simulating LNAPL recovery using wells or trenches are described in Section 2.4.2. Seven different graphical outputs are described in Section 2.4.3. Use of the different models for representing LNAPL residual saturation are discussed in Section 2.4.4, while selection of piecewise linear model breakpoints are described in Section 2.4.5. Section 2.4.6 discusses use of the smear correction option. Section 2.5 describes the model output.

Section 3 provides guidance for model conceptualization, parameter selection, and problem solving using the LDRM. Section 3.2 compares experience with oilfield production of hydrocarbon liquids with LNAPL recovery for environmental management. Section 3.3 discusses limitations that may be associated with LDRM input parameters. Section 3.4 discusses model conceptualization while Section 3.5 describes methods for parameter estimation when detailed site data is limited. Finally, Section 3.6 provides four example problems showing model application, methods for parameter estimation and bracketing, and an example where the scenario-based model might not be appropriate.

## **2 USER GUIDE**

The purpose of this section is to provide information on use of the API LNAPL Distribution and Recovery Model (LDRM) and its various options. Model input and graphical and text output are described. It is shown how field data may be entered and displayed on graphical output for model testing and calibration. Various options are explained and demonstrated. The output file format is also shown.

### **2.1 WORKSPACE SETUP**

The API LNAPL Distribution and Recovery Model (LDRM) consist of a single executable application that runs with the Windows™ operating system. It is assumed that the user is familiar with Windows, menus, the mouse, and folders for storage of files. The user should create a folder for storage of work and copy the executable application (LDRM.exe) to a desired location within the file structure (such as the primary work folder). Any additional input/output/data files that are supplied with the application should also be copied into the work folder. Subfolders can be created for each individual project. When running LDRM, the default folder for opening active projects is the folder containing the application, while the default folder for saving output is the active folder from which the input file was opened. An example setup is shown in Figure 2.1.

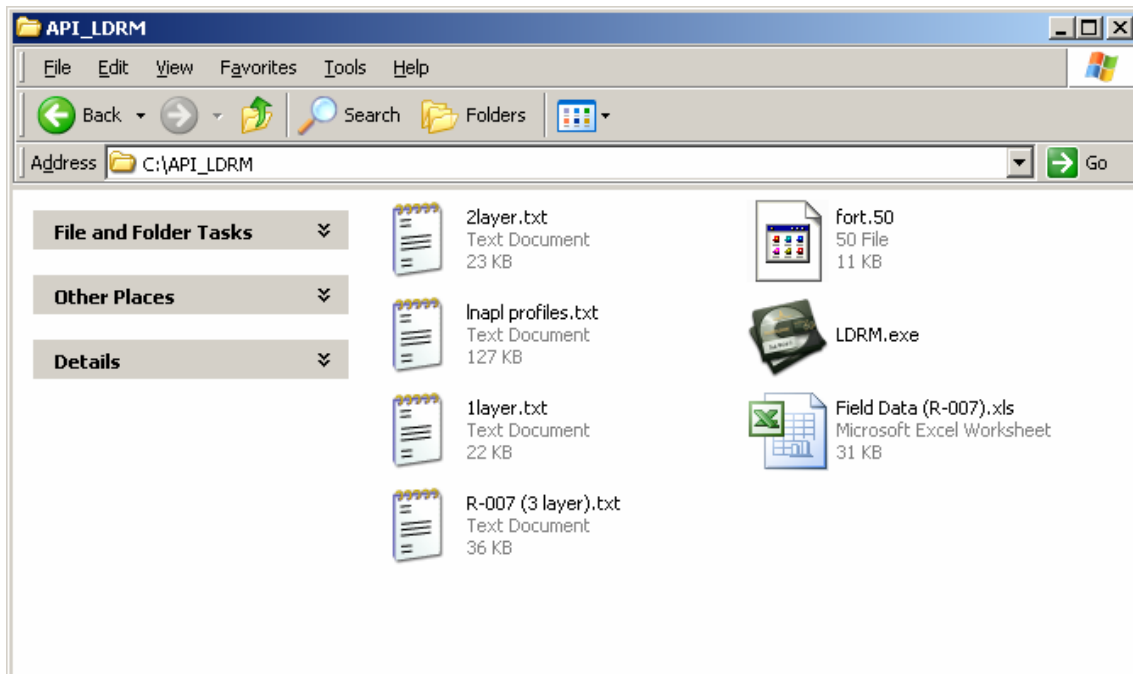


Figure 2.1—Example Setup Folder Showing Project Workspace

## 2.2 STARTING THE APPLICATION

Like all Windows applications, the LDRM model can be initiated by ‘clicking’ on the executable file icon (LDRM). The user is greeted briefly with the logo shown in Figure 2.2, and then is required to agree to Terms and Conditions of model use before the program is initiated, as shown in Figure 2.3.

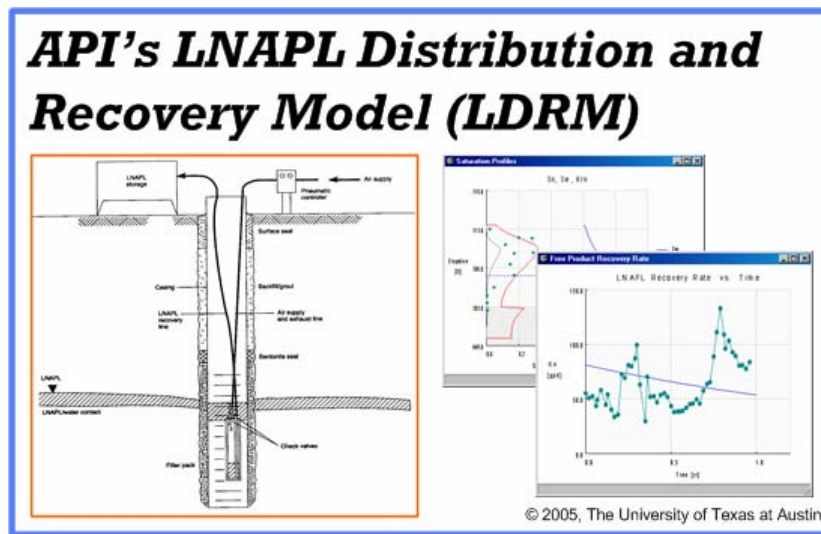


Figure 2.2—API LDRM Logo

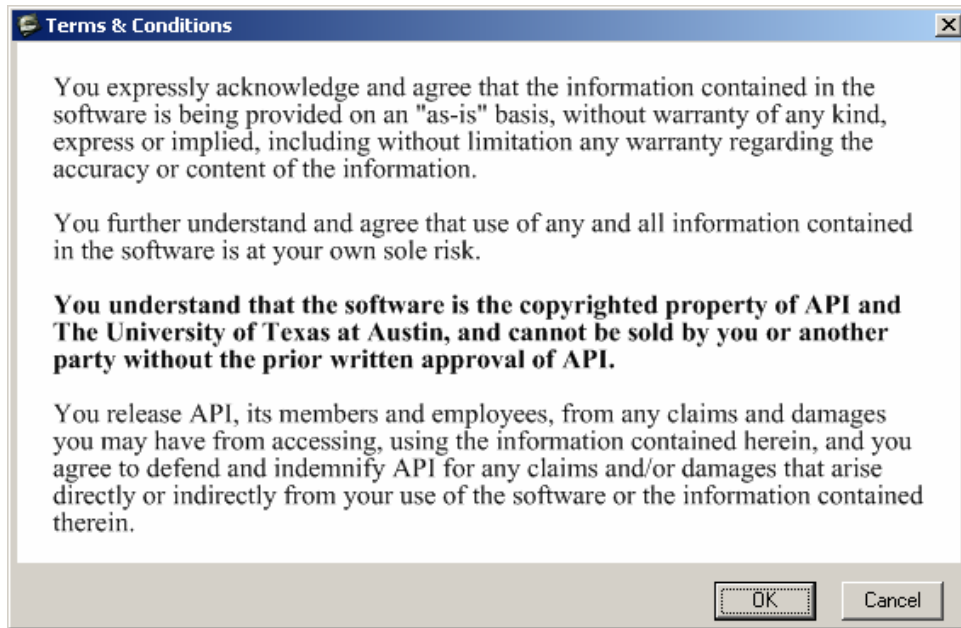


Figure 2.3—Terms and Conditions Window

Once the Terms and Conditions have been accepted (click on OK), the initiation message box shown in Figure 2.4 appears and provides the user with options on how to proceed. The user may open an existing simulation file, start a new simulation file, or exit the program. Select the appropriate item and click OK. If the user selection the Open option, then the standard Open File dialog appears (as shown in Figure 2.5), and one may navigate the file system and select the desired simulation file to open. Only files with the “\*.txt” extension may be used as input files. No options are provided for opening input files with another extension. Thus input files are standard ASCII text files and can be read and used by other text processing software, allowing the experienced user to edit input files without running the application.

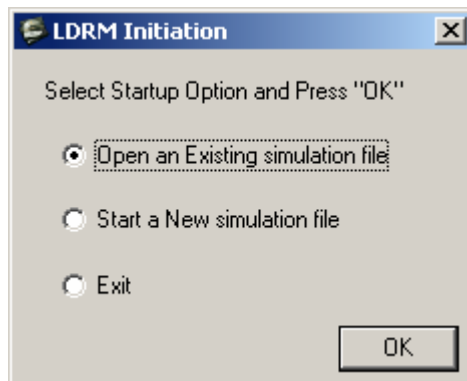


Figure 2.4—Initiation Message Box

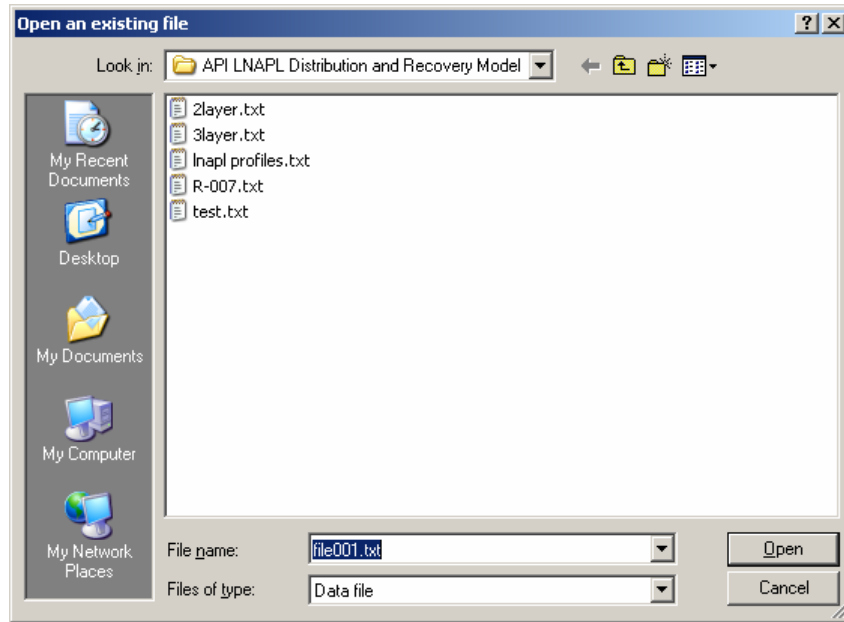


Figure 2.5—Standard Open File Dialog

If in the initiation message box (Figure 2.4) the user selects to start a new simulation file, then the Project Setup dialog appears, as shown in Figure 2.6. Basic choices for a given simulation can only be made through this dialog, and cannot be changed later (the user would have to start a new simulation). These choices include selection of units (English or Metric), number of layers (1, 2, or 3), and elevation representation (elevation above a selected datum or depth below ground surface, BGS). Other options that are selected through this dialog are whether to use a drawdown correction for LNAPL smearing and the LNAPL residual saturation representation. Both of these selections can be changed at a later time, and both are discussed in detail below (Smear Correction in Section 2.4.6; LNAPL Residual Saturation in Section 2.4.4). Click OK to continue.

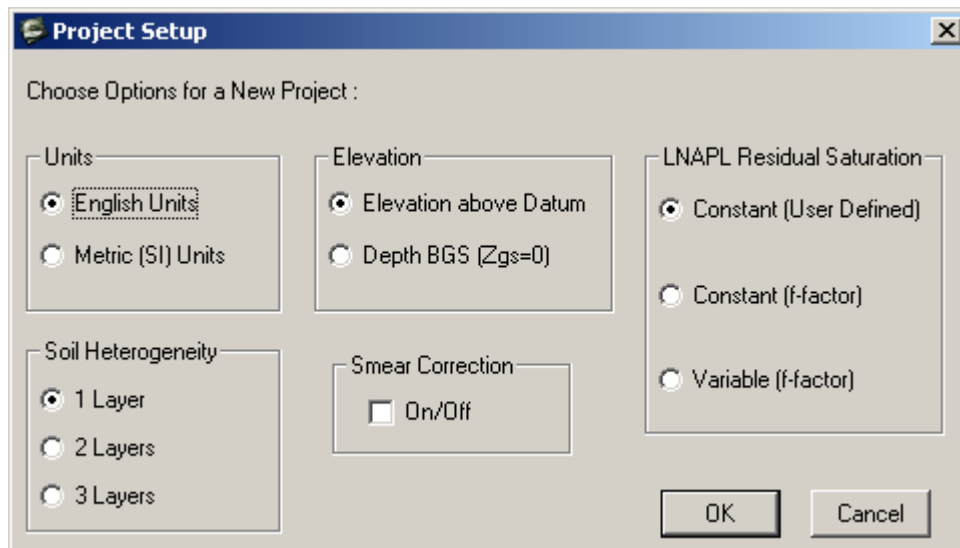


Figure 2.6—Project Setup Dialog that Appears Only When “New” Simulation is Selected

## 2.3 DATA INPUT WINDOW

Once a selection has been made to Open an existing simulation or start a new simulation, the Data Input window appears, such as shown in Figure 2.7. The appearance of this window differs depending on the selected options, in particular Soil Heterogeneity (number of layers) and Elevation representation. Figure 2.7 corresponds to English units, 1 layer, and Elevation above Datum (options shown in Figure 2.6). The Data Input windows for 2 layer and 3 layer simulations are shown in Figures 2.20 and 2.38 below. The basic data requirements should be straightforward, based on the background information presented in Volume 1. A couple of items are of note:

- If a vertical gradient is specified, then it applies only for the uppermost layer. There is no capability for specifying a vertical gradient in a lower layer.
- The Burdine (default) or Mualem relative permeability model may be selected for any layer, and a combination of models may be specified for a multiple-layer soil profile.
- Required Residual LNAPL Saturation and Residual LNAPL f-factor data requirements will vary with selected representation model, and these entry boxes may appear with “Constant” or “Variable” for other options.

Parameter	Value
Maximum Monitoring Well LNAPL Thickness [ft]	5.000
Ground Surface Elevation [ft]	25.000
Water table Elevation [ft]	22.000
Water Vertical gradient (+ for upward)	0.000
LNAPL density [gm/cc]	0.800
LNAPL viscosity [cp]	2.000
Air/Water surface tension [dyne/cm]	65.000
Air/LNAPL surface tension [dyne/cm]	25.000
LNAPL/Water surface tension [dyne/cm]	15.000
Porosity	0.400
Hydraulic Conductivity [ft/d]	5.000
Van Genuchten "N"	3.500
Van Genuchten "a" [ft-1]	2.000
Irreducible water saturation	0.250
Residual LNAPL saturation	0.100
Residual LNAPL f-factor	0.300

Figure 2.7—Data Input Window for a 1 Layer Model

## 2.4 MENU ITEMS

Access to most model options is achieved through use of the main menu and selection of menu items. The File menu (Figure 2.8) contains standard items for control of files, including creation

of a New simulation file, Open an existing simulation file, file Save, and Exit the application. The user is prompted to save an existing file if Exit is selected.

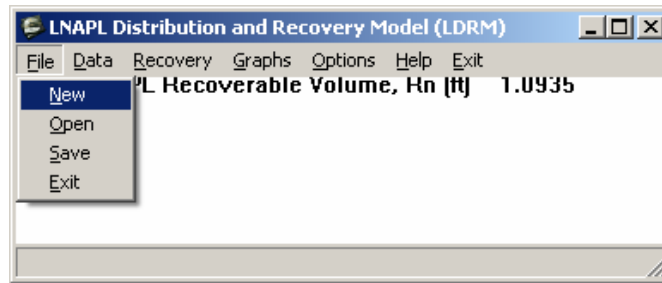


Figure 2.8—Standard File Menu Items

The Data menu contains three items, as shown in Figure 2.9. The first of these is to call the Edit the basic input data for the simulation, and the standard Data Input window (Figure 2.7) is opened. One may change input parameters during a simulation. The second menu item allows the user to Add field data to the graphs that are generated by the application. Such input field data is also added to the output data file. The detailed procedure for adding field data is presented in Section 2.4.1. The third item allows the user to Remove all field data from output graphs and from the output file.

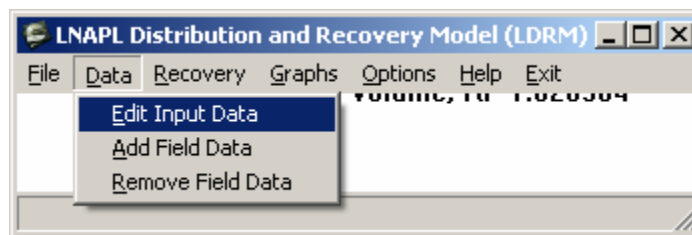


Figure 2.9—Data Menu Items

The Recovery menu (Figure 2.10) allows the user to select the LNAPL recovery technology and its characteristics for use during the simulation. Wells includes single and dual pump wells, vacuum-enhanced wells, and skimmer wells. If the well water discharge and vacuum are specified as 0, then the model assumes that a skimmer well is being used. A trench may also be specified. The model input for wells or a trench are discussed in Section 2.4.2.

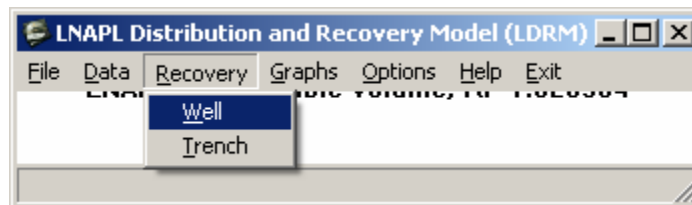


Figure 2.10—Recovery Menu Items

The Graphs menu (shown in Figure 2.11) has the available graphs listed as items. A total of 7 different graphs are available. However, graphs providing output on LNAPL recovery are active only after the recovery option (Recovery menu item) has been selected and executed. The menu shown in Figure 2.11 has the Saturation Profiles, Specific Volume, and LNAPL Distribution



graphs active. The Thickness, Drawdown, Rate and Volume graphs become active once the recovery has been calculated. The specific graph output is described in detail in Section 2.4.3.

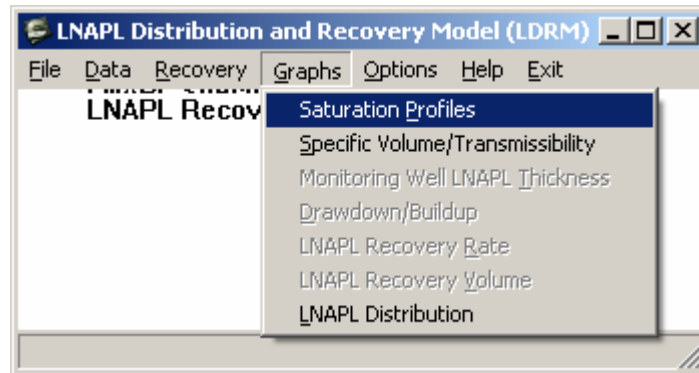


Figure 2.11—Graphs Menu Items

The Options menu (shown in Figure 2.12) provides access to two options that control calculation of important model features. The first option allows the user to change between different models for specifying the residual LNAPL saturation. These different models are explained in detail in Section 2.4.4. The second option, Pick Break Points: *bn1*, *bn2* (Alt-b), allows the user to specify the piecewise linear segment breakpoint values of LNAPL thickness for the LNAPL specific storage and transmissibility functions.

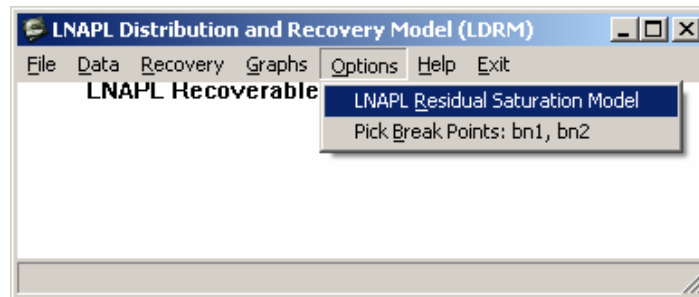


Figure 2.12—Options Menu Items

The Help menu (shown in Figure 2.13) provides limited help and model information for the user. The Soil Parameters item refers to API documents and programs that are useful in selection of model parameters relating to soil characteristics. The Rel. Perm. Models item is a warning that for a specific soil, the van Genuchten soil characteristic parameters  $\alpha$  and  $N$  will differ with selection of the Burdine or Mualem relative permeability models. The other two items provide information on model development and acknowledgements for model support.

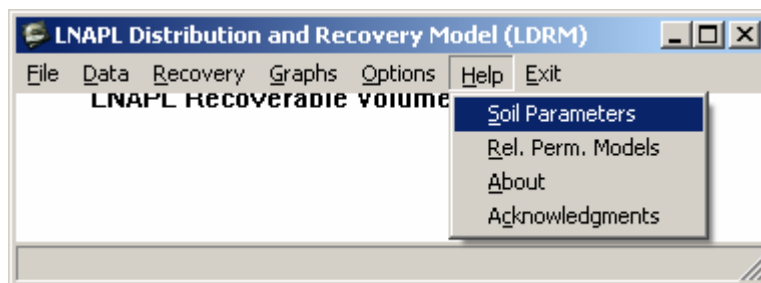


Figure 2.13—Help Menu Items

The Exit menu provides direct access to model termination with a message box that inquires whether the user wishes to save current work.

### 2.4.1 Add Field Data

The following field data values may be entered and displayed on the graphical output from model simulations:

- LNAPL saturation ( $S_n$ ),
- LNAPL monitoring well thickness ( $b_n$ ),
- LNAPL cumulative recovery volume ( $V_n$ ), and
- LNAPL recovery rate ( $Q_n$ ).

Field data is entered through use of a spreadsheet. The spreadsheet is automatically formatted for input. Field data is copied from another spreadsheet or text (ASCII) file. Upon saving and closing the spreadsheet, the entered data is copied to the simulation model and will be displayed when a figure is opened. All data is saved on the output file from a simulation.

To add field data select the Data → Add Field Data (Alt-d → Alt-a) item from the menu. The options message box shown in Figure 2.14 will be displayed. Select the data-type for entry and click OK. Two things then happen. First, the dialog shown in Figure 2.15 is displayed. Do not click OK on this dialog until after the data has been entered and saved. The second thing that happens is that a spreadsheet file *field\_data.csv* is created in the folder from which the application was launched (not the data folder if this is different), as shown in Figure 2.16. Open this spreadsheet and enter the data (which may be copied and pasted from another data spreadsheet). Once the data are entered, as shown in Figure 2.17, save *field\_data.csv*, click Yes on the “features” message box, close *field\_data.csv*, and click No on the “save” message box. One may now click OK on the dialog shown in Figure 2.15, and the data is copied to the simulation application file.

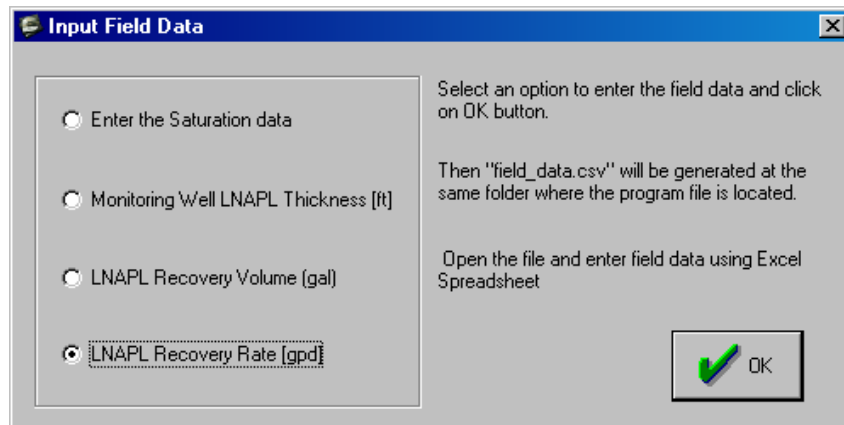


Figure 2.14—Input Field Data Options Message Window

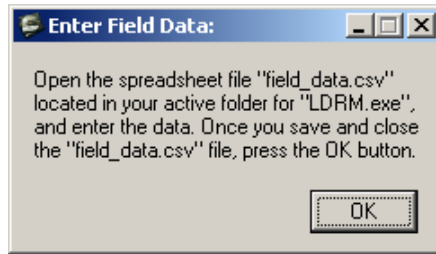


Figure 2.15—Data Transfer Control Message Box

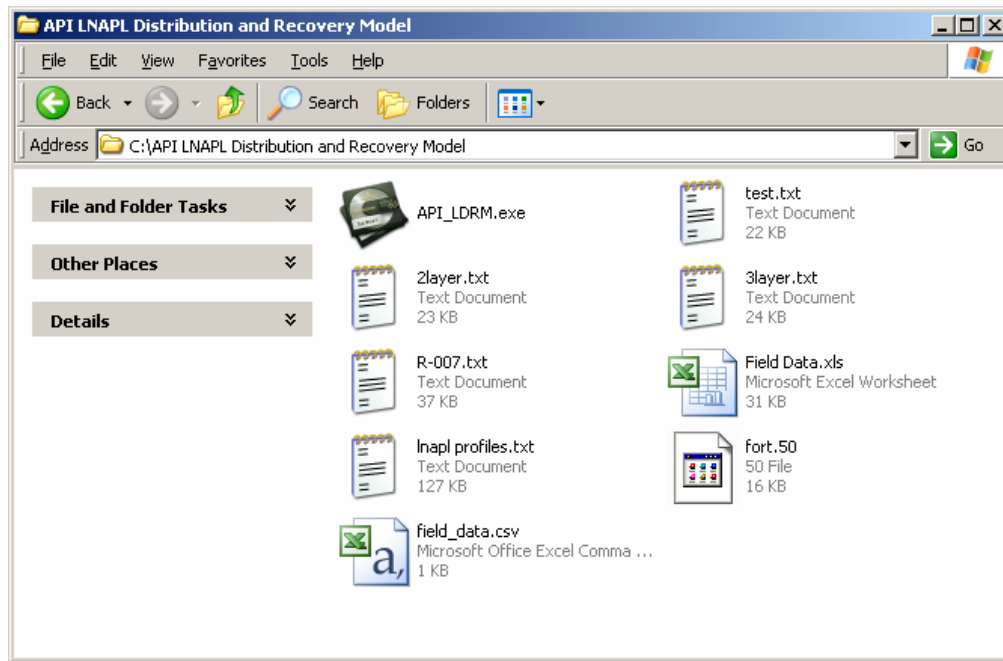


Figure 2.16—Application Folder with "field\_data.csv" Spreadsheet

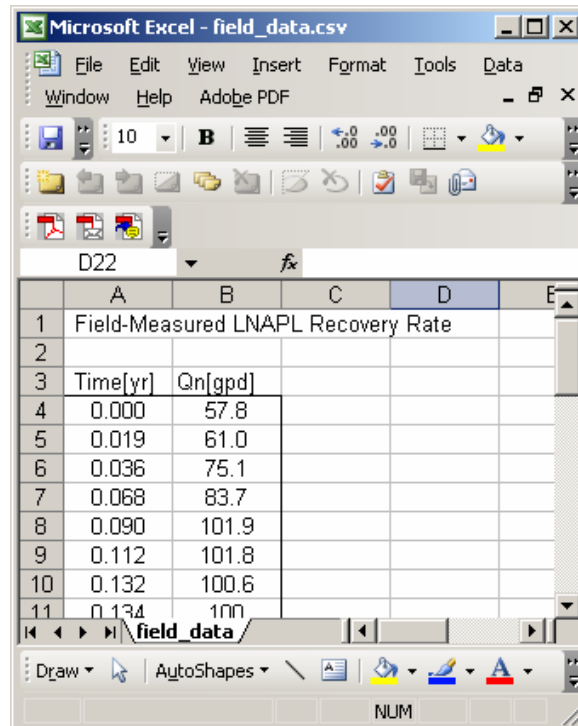


Figure 2.17—"field\_data.csv" Spreadsheet with Data

## 2.4.2 LNAPL Recovery

Once the basic input data (Section 2.3) has been entered, the user may select a recovery technology using the menu Recovery (Alt-r) item. Two options are available, as shown in Figure 2.10. If the user selects the Well (Alt-w) item, then the *Well Recovery Systems* data entry window shown in Figure 2.18 is displayed. The following parameters may be entered.

*Recovery time (T)* – time duration for simulated recovery

*Radius of Pumping Well (L)* – production or suction well effective radius

*Radius of Recovery (L)* – radius of capture (see discussion in Section 4.1 of Volume 1) of groundwater-enhanced or skimmer well

*Radius of Influence (L)* – radial distance with significant water-table drawdown associated with groundwater production

*Water production rate ( $L^3/T$ )* – groundwater pumping discharge from single- or dual-pump well

*Water saturated thickness (L)* – effective aquifer thickness of active flow towards the groundwater pumping well. This may be approximated by the well screened interval below the water table

*Suction Pressure* (fraction of atmospheric pressure) – well-suction applied for vacuum-enhanced recovery. Entered as a positive number

*Screen length (L)* – length of the well screened interval above the water table

*Air Radius of Capture (L)* – effective radial distance of influence for air flow

Parameter	Value
Recovery time [yr]	1.000
Radius of Pumping Well [ft]	0.500
Radius of Recovery [ft]	85.000
Radius of Influence [ft]	200.000
Water production rate [gpm]	9.700
Water Saturated thickness [ft]	30.000
(-)Suction Pressure [atm]	0.000
Screen Length [ft]	0.000
Air Radius of Capture [ft]	0.000

Figure 2.18—Well Recovery Systems Data Entry Window

#### Discussion:

1. If both the *Water production rate* and the *Suction Pressure* are zero (0.0) then a skimmer well is assumed. Further, if the downward hydraulic gradient within the upper soil layer exceeds the critical value for LNAPL displacement (see Volume 1, Section 3.2.2), then only residual LNAPL is assumed to exist in the upper layer and the model for recovery of LNAPL beneath fine-grain zones using skimmer wells (see Volume 1, Section 3.3.6) is assumed.
2. When a recovery well has both groundwater production and vacuum enhancement, then the *Radius of Recovery* and *Air Radius of Capture* can differ, and the water table drawdown/buildup is calculated using superposition.
3. The default *Air Radius of Capture* is calculated using equation (3.49) from Volume 1, though the user can enter a different value that will be used in calculations.

If the user selects the Trench (Alt-t) item from the Recovery menu, then the *Interceptor Trenches* data entry window shown in Figure 2.19 is displayed. The following parameters may be entered.

*Recovery time (T)* – time duration for simulated recovery

$Q_w$  ( $L^3/T$ ) – groundwater production rate that is used to enhance the natural hydraulic gradient

$J_w$  (-) – natural hydraulic gradient towards the trench

*Trench length (L)* – length of the trench or width of the LNAPL plume transverse to the hydraulic gradient, whichever is smallest

*Lens width (L)* – longitudinal extent of the LNAPL plume in the flow direction

*Screen depth (L)* – effective depth of the trench beneath the water table. This is used in conjunction with the *Trench length* and  $Q_w$  to determine the additional hydraulic gradient causing LNAPL migration to the trench (see equation 3.61 from Volume 1)

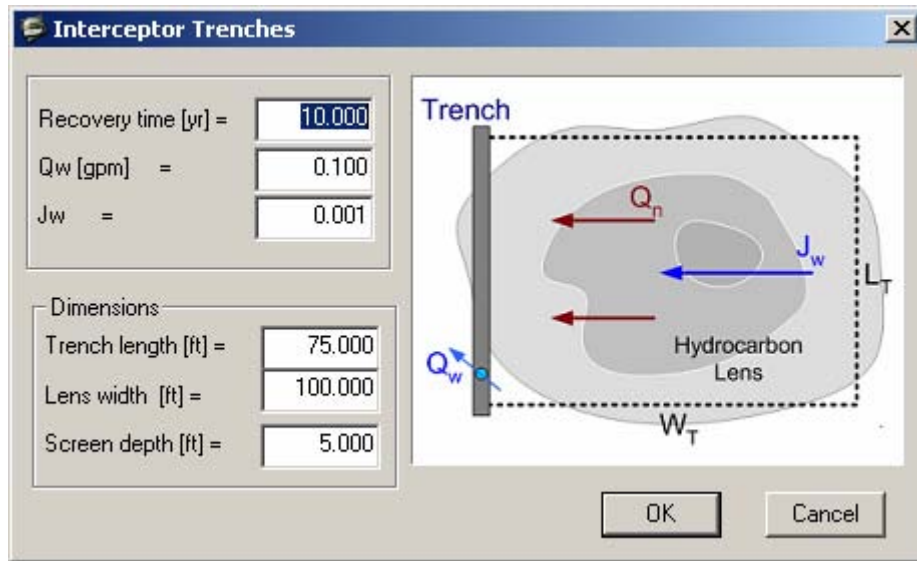


Figure 2.19—Interceptor Trench Data Entry Window

### 2.4.3 Graphs Output

As shown in Figure 2.11, seven different graphs may be displayed to summarize simulation model output. All data that are used to generate these graphs are written to the output file, so that graphical generation can be easily re-produced using alternative software. The first two and last graph are available once the basic input data has been entered (*Data Input* window, Section 2.3). The remaining four graphs require that a recovery technology be selected (menu Recovery item, Section 2.4.2). The content of these graphs is described as follows.

The first graph, *Saturation Profiles* (Alt-p), shows the vertical distribution of LNAPL saturation (red), LNAPL residual saturation (red-dashed), water saturation (blue), and LNAPL relative permeability (grey). An example profile corresponding to the *Data Input* window of Figure 2.20 is shown in Figure 2.21. This represents a two-layer heterogeneous system with a low permeability unit overlying a unit of higher permeability. The ground surface is located at an elevation of 25 feet above the datum, while the water table is at an elevation of 22 feet. The vertical facies transition occurs at an elevation of 20 feet (5 feet BGS). The heavy black line drawn along the right border of the figure shows the 5-foot LNAPL thickness in the well (extending from an elevation of 18 feet to 23 feet). The residual LNAPL saturation values are calculated using the residual f-factor (see equation 2.2, Volume 1) and results in different constant LNAPL residual saturation values for each layer. The maximum LNAPL saturation occurs immediately below the facies interface. The largest LNAPL saturation in the upper unit occurs at the elevation of the air-LNAPL interface in the well (elevation 23 feet). Because of capillary forces, the LNAPL saturation remains above residual even at the ground surface. The

LNAPL relative permeability is calculated using the LNAPL and water saturation, with the Mualem model for the upper layer and the Burdine model for the lower layer.

**Data Input**

Thickness, Elevations, Vertical gradient

Maximum Monitoring Well LNAPL Thickness [ft] = 5.000

Ground Surface Elevation [ft] = 25.000

Water table Elevation [ft] = 22.000

Elevation of Soil Faces Interface [ft] = 20.000

Water Vertical gradient (+ for upward) = -0.050

Fluid Characteristics

LNAPL density [gm/cc] = 0.800

LNAPL viscosity [cp] = 2.000

Air/Water surface tension [dyne/cm] = 65.000

Air/LNAPL surface tension [dyne/cm] = 25.000

LNAPL/Water interfacial tension [dyne/cm] = 15.000

Relative Permeability Model (Burdine is default)

Use Mualem Model for Layer  Layer 1  Layer 2

Soil 1

Porosity = 0.400

Hydraulic conductivity [ft/d] = 0.200

Van Genuchten "N" = 1.300

Van Genuchten "a" [ft-1] = 0.600

Irreducible water saturation = 0.500

Residual LNAPL saturation = 0.070

Residual LNAPL f-factor = 0.400

Soil 2

Porosity = 0.380

Hydraulic conductivity [ft/d] = 5.000

Van Genuchten "N" = 3.500

Van Genuchten "a" [ft-1] = 2.000

Irreducible water saturation = 0.150

Residual LNAPL saturation = 0.185

Residual LNAPL f-factor = 0.250

OK Cancel

Figure 2.20—Data Input Window for Two-Layer Soil

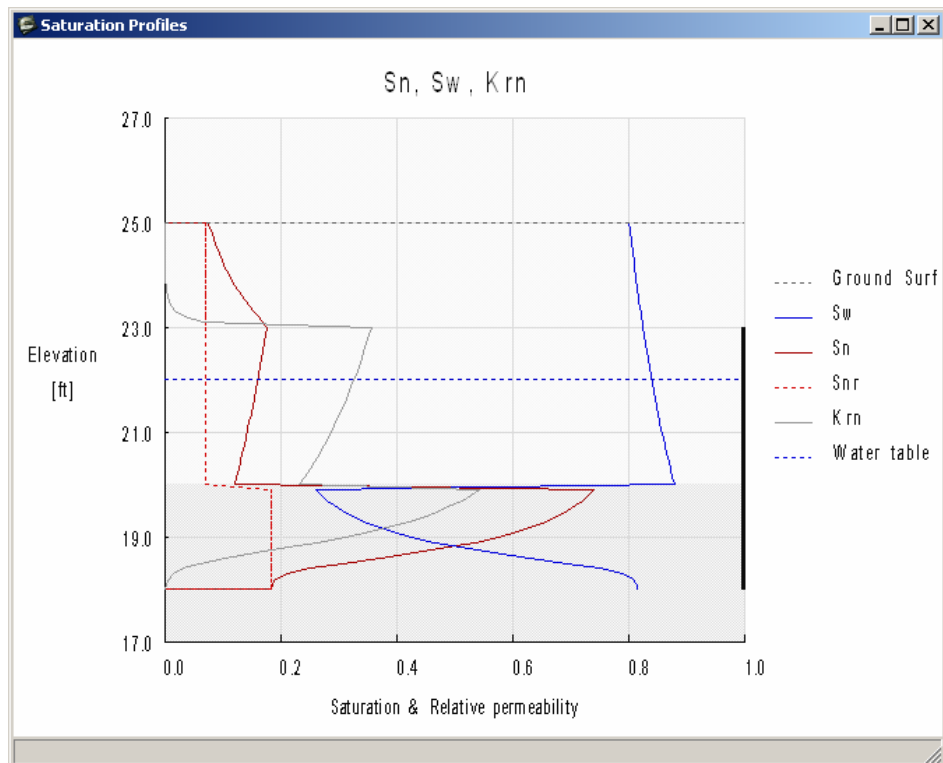


Figure 2.21—Saturation Profiles Graph Output

The second graph, *Specific Volume/Transmissibility* (Alt-s), is shown in Figure 2.22. The three curves present the specific volume functions  $D_n(b_n)$  and  $R_n(b_n)$  and the LNAPL transmissibility function  $T_n(b_n)$ . The solid red, blue and grey curves are developed as follows. For twenty evenly distributed values of  $b_n$  ranging from zero to the maximum value specified on the Data Input window, the functions are evaluated using equations (2.40), (2.41), and (3.31) from Volume 1. For each  $b_n$  value, the corresponding  $z_{nw}$  and  $z_{max}$  values are calculated using equations (2.20) and (2.38). Using the sets of  $(b_n, R_n)$  and  $(b_n, T_n)$  values, a difference algorithm is used to select two values ( $b_{n1}$  and  $b_{n2}$ ) to use at the breakpoints for the piecewise linear approximation models specified by equations (4.3) and (4.4). These values are used to plot the piecewise linear approximations (dashed segments) to  $R_n(b_n)$  and  $T_n(b_n)$  shown in Figure 2.22. As discussed in Section 2.4.5, the user may select alternative breakpoint values to use in the recovery model calculations.

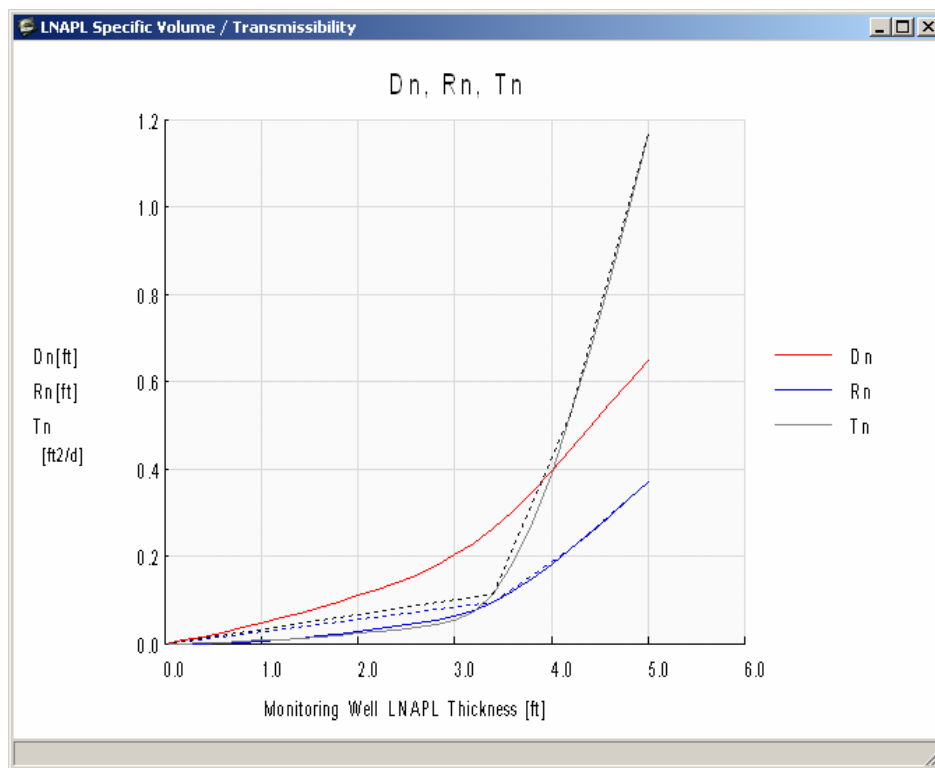


Figure 2.22—Specific Volume/Transmissibility Graph Output

The third graph, *Monitoring Well LNAPL Thickness* (Alt-t), is shown in Figure 2.23. This graph is available only after the recovery model has been run. This graph shows how the free product thickness ( $b_n$ ) varies with time during the recovery time interval. For the example shown in Figure 2.23, the LNAPL thickness decreases from 5 feet to about 3.7 feet over a time period of two years.



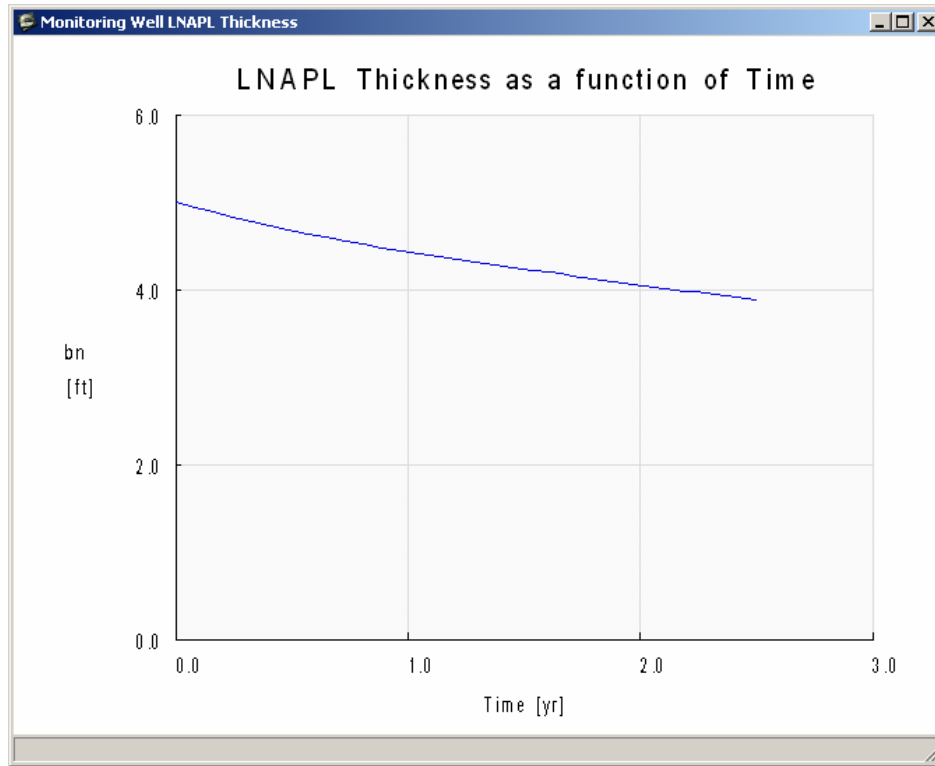


Figure 2.23—Free Product Thickness Graph Output

The fourth graph, *Drawdown/Buildup* (Alt-d), is shown in Figure 2.24. This graph is available only after the recovery model has been run, and only for groundwater or vacuum-enhanced wells. This graph shows the water table drawdown (due to groundwater pumping) and rise or buildup of the water table (due to an applied vacuum). Drawdown and buildup of the water table are added to calculate the net water table change, which is also plotted. Finally, the average drawdown/buildup within the radius of capture of the recovery well is shown. Drawdown and buildup are calculated using the Thiem equation (equation 3.34 and 3.52, respectively, from Volume 1). The average is a radial-distance weighted average. The example shown in Figure 2.24 corresponds to a radius of capture equal 60 feet (radius of influence equal 250 feet) and air radius of capture equal 20 feet. The groundwater production rate is 1 gallon per minute and the air-enhanced system suction pressure is 0.05 atmospheres. The average drawdown within the radius of capture is 0.88 feet for this example.

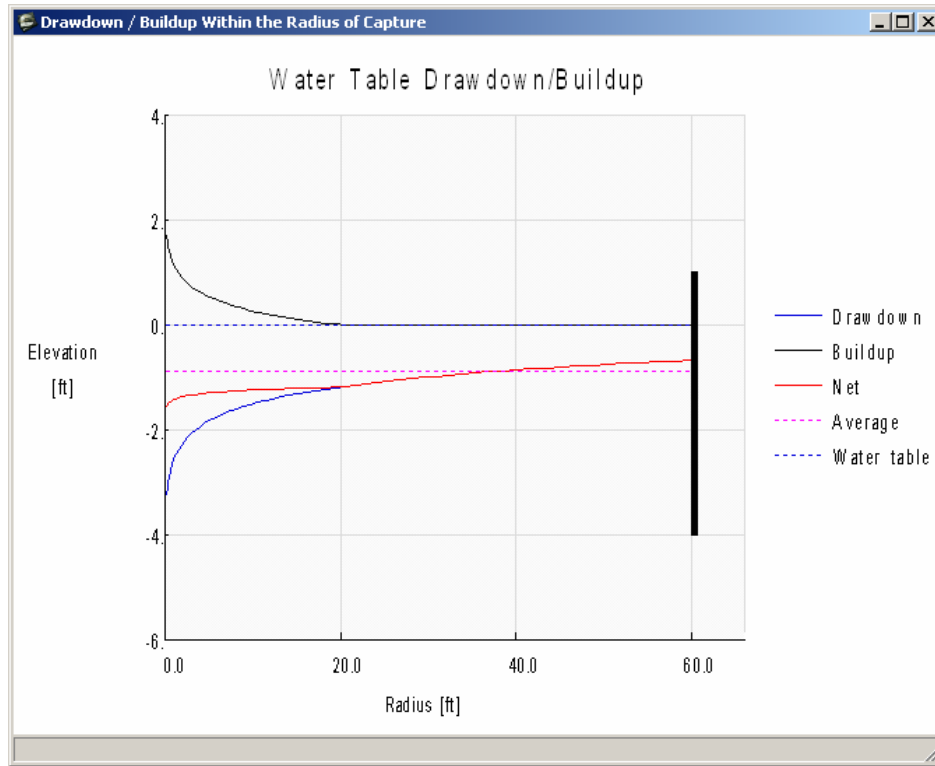


Figure 2.24—Drawdown/Buildup Graph Output

The fifth graph, *LNAPL Recovery Rate* (Alt-r), is shown in Figure 2.25. This graph is available only after the recovery model has been run. The LNAPL recovery rate,  $Q_n$ , is shown as a function of time during the recovery time period. For the example shown in this figure the recovery rate decreases from about 60 gallons per day (gpd) to about 10 gpd after two years. This corresponds directly to the nearly six-fold decrease in LNAPL transmissibility as the LNAPL thickness decreases from 5 to 3.7 feet (see Figures 2.22 and 2.23).

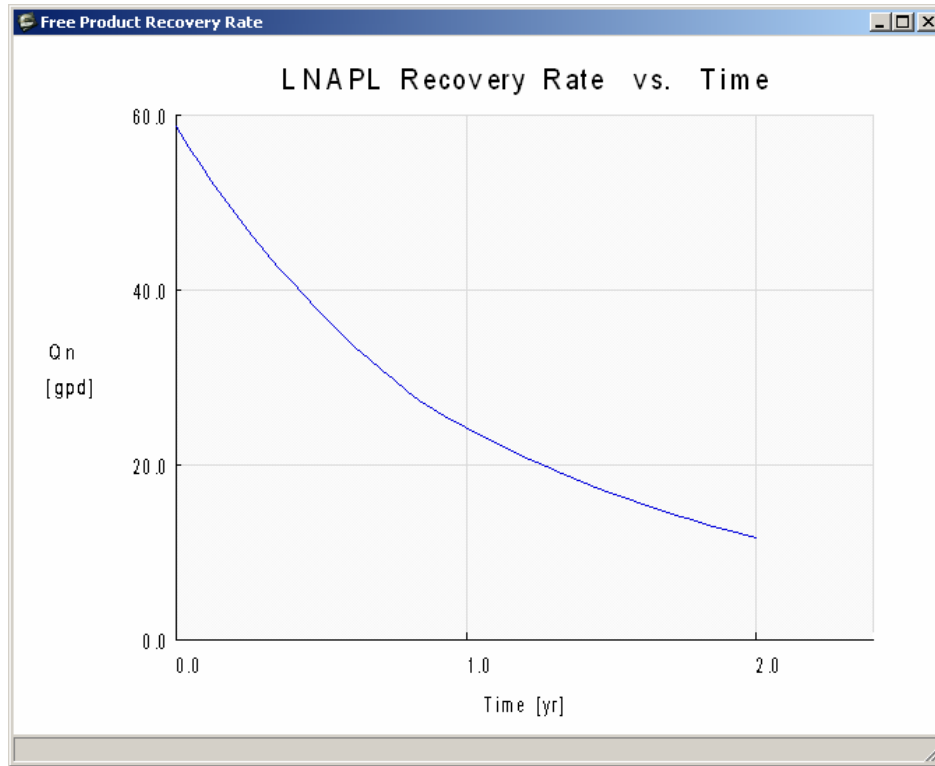


Figure 2.25—LNAPL Recovery Rate Graph Output

The sixth graph, *LNAPL Recovery Volume* (Alt-v), is shown in Figure 2.26. This graph is available only after the recovery model has been run. The cumulative LNAPL recovery volume,  $V_n$ , is shown as a function of time during the recovery period. In the example shown in this figure the recovery volume increases to approximately 20,000 gallons over two years. Also shown on this figure (blue dashed line) is the total LNAPL volume ( $A_c D_n(b_{nmax})$ ) within the area of capture  $A_c$ . The maximum recoverable LNAPL volume within the capture area is  $A_c R_n(b_{nmax})$ .

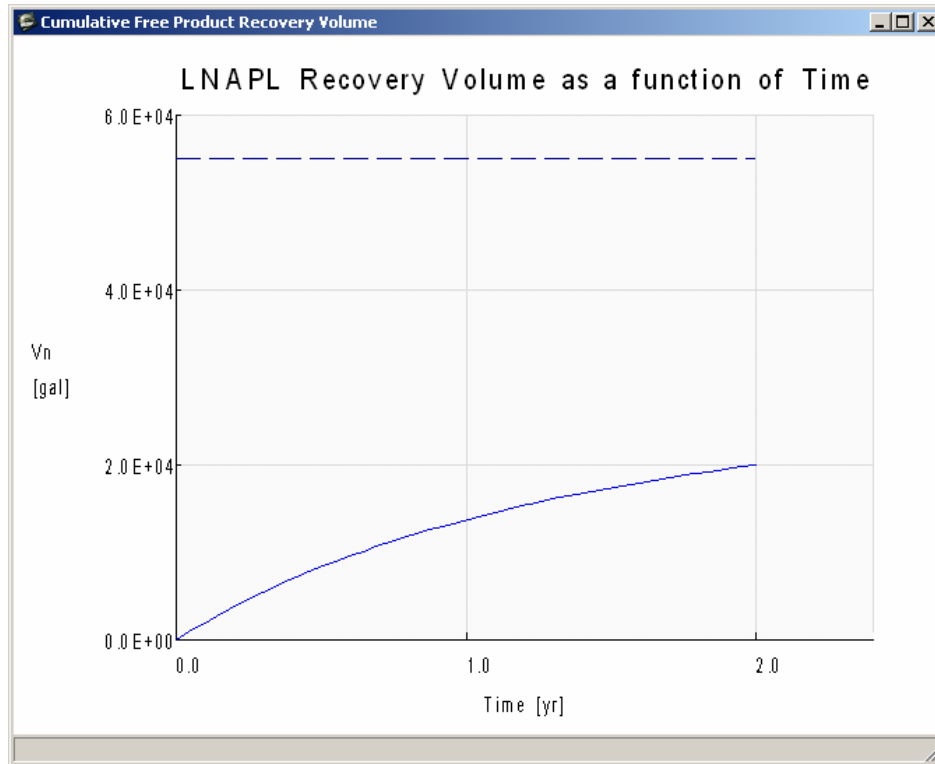


Figure 2.26—LNAPL Recovery Volume Graph Output

The seventh and final graph, *LNAPL Distribution* (Alt-1), shows the initial LNAPL and water saturation distribution and the distributions at a later time. The later-time distribution is based on a specified LNAPL thickness. If this graph is selected, then the dialog box in Figure 2.27 is shown. The user enters the LNAPL thickness corresponding to the later-time distribution, and then clicks OK. The saturation distribution graph is then display, such as shown in Figure 2.28. In this example the initial saturation distribution corresponds to LNAPL thickness equal 5 feet and the later-time distribution to 4-foot thickness. LNAPL thickness values are shown on the right boundary of the figure. There is a fairly uniform decrease in LNAPL saturation within the upper soil layer, but a large and nonuniform decrease in LNAPL saturation immediately below the facies interface.

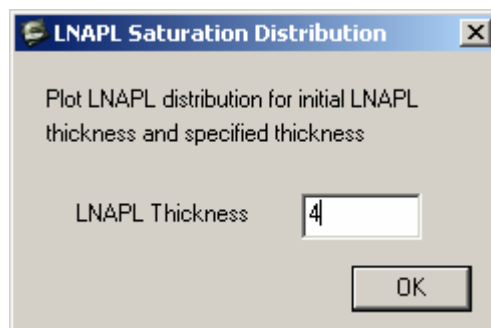


Figure 2.27—LNAPL Thickness Dialog Box for Later-Time Distributions

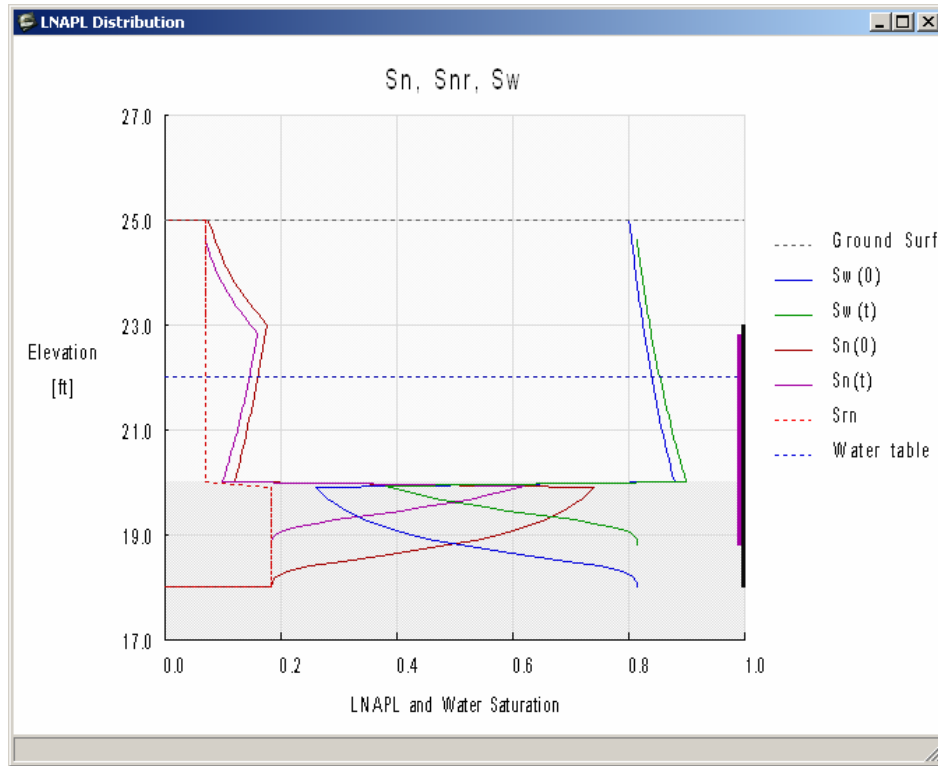


Figure 2.28—LNAPL Distribution Graph Output

#### 2.4.4 LNAPL Residual Saturation Models and Residual F-Factor Options

The *Options* (Alt-o) menu shown in Figure 2.12 allows the user to change the *LNAPL Residual Saturation Model* (Alt-r) that is used in the model calculations. Three different LNAPL residual saturation models are available, as shown in Figure 2.29. The user may specify constant residual LNAPL saturation values for each soil layer. The second choice also uses constant LNAPL residual saturation values for each soil layer, but with the values determined by the maximum initial LNAPL saturation in each layer and the f-factor  $f_r$  that is specified for each soil layer on the Data Input window (see Figure 2.20). For reference, see the discussion in Section 2.1.3 of Volume 1. This is the representation used in Figures 2.20 and 2.21. The third choice is to use LNAPL residual saturation that varies over the LNAPL thickness based on the initial LNAPL saturation that varies with elevation and the constant f-factor  $f_r$  for each soil layer. This is the representation used in Figure 2.30, which is the same as Figure 2.28 except that a variable LNAPL residual saturation model has been used. The values of the LNAPL residual f-factors for each layer can be changed using the Data Input window.

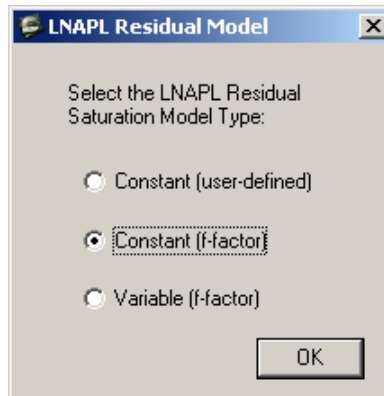


Figure 2.29—Three Different LNAPL Residual Saturation Model Representations

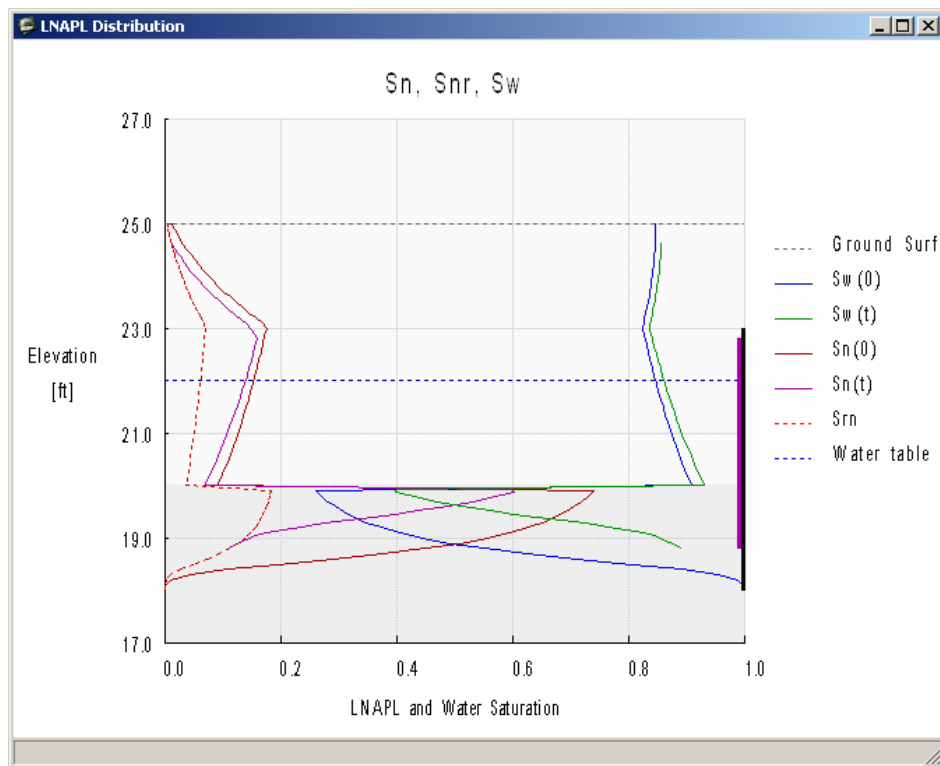


Figure 2.30—LNAPL Distribution Output Graph with Variable LNAPL Residual Saturation

### 2.4.5 Piecewise Linear Model Breakpoint Options

The basis of the LNAPL recovery model formulation is piecewise linear representation of the recoverable LNAPL specific volume and LNAPL transmissibility functions  $R_n(b_n)$  and  $T_n(b_n)$ . As discussed in association with Figure 2.22, these functions are evaluated for a range of LNAPL thickness values and a difference algorithm is used to select breakpoints  $b_{n1}$  and  $b_{n2}$  for the piecewise linear representation. These breakpoint values mark the terminal points of the interior linear segments (the exterior terminal points are  $b_n$  equal zero and  $b_{nmax}$ ). This algorithm often leads to adequate representation of the storage and mobility functions as judged by a close visual fit between the curves and piecewise linear segments shown in Figure 2.22. However, the user may desire to select alternative breakpoint values. The *Options* → *Pick Break Points: bn1, bn2* (Alt-o → Alt-b) menu item allows the user to select alternative points. If these options are

selected then the dialog of Figure 2.31 is shown. Based on visual inspection of the *Specific Volume/Transmissibility* graph, the user may select alternative  $b_n$  values for the segment breakpoints. The next lowest values from the calculated range of  $b_n$ -function values are then used as breakpoints in subsequent calculations. A number of trial points can be inspected. When the user is satisfied with the model fit, then the *Fix break points* box should be checked, which will fix the breakpoint values until the option dialog is opened again. Figure 2.32 shows the selected alternative piecewise linear model fit for the storage and mobility functions ( $R_n$  and  $T_n$ ). Figure 2.32 can be compared with Figure 2.22.

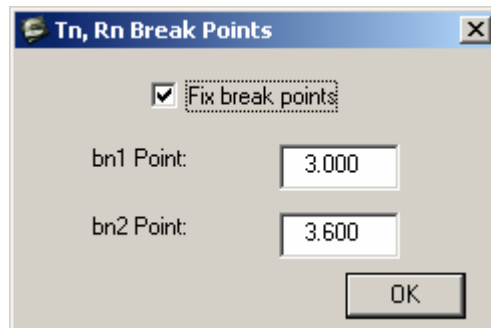


Figure 2.31. Pick Break Points:  $bn1$ ,  $bn2$  Message Box

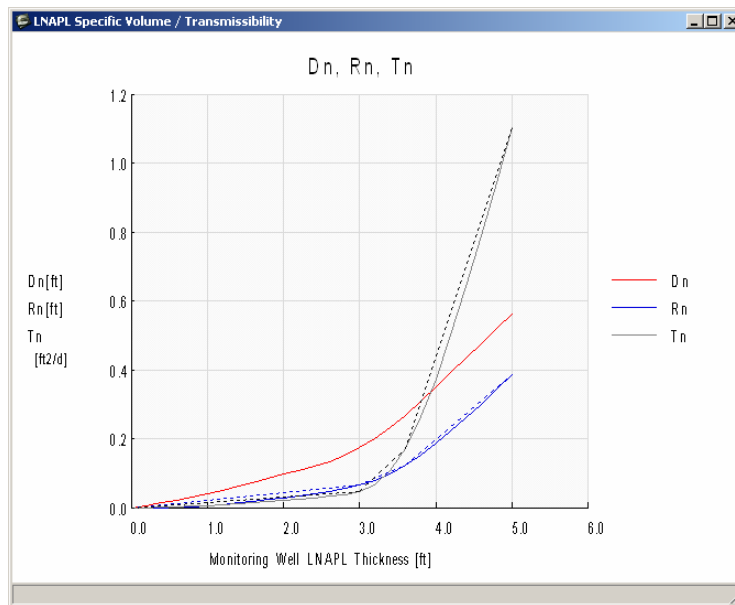


Figure 2.32—Piecewise Linear Model Representation with Alternative Breakpoints (Compare with Figure 2.22)

#### 2.4.6 Smear Correction Option

An option that is useful in some applications is to simulate the effect of LNAPL residual trapping above the water table associated with water table drawdown due to groundwater pumping. This “smearing” of the LNAPL above the water table results in a decrease in LNAPL specific volume during recovery operations, and the amount of LNAPL smearing increases with increasing groundwater pumping rate. The smearing simulation option may be invoked during project setup for a new project (see Figure 2.8). Alternatively, one may open an existing output file as a text

(ASCII) file and edit the project options. During the simulation, the initial LNAPL distribution and residual saturation are based on the conditions specified through the Data Input window. For example, Figure 2.33 shows the saturation distribution corresponding to an initial LNAPL thickness  $b_n = 2$  m with an initial water table elevation at depth 2 m below ground surface (bgs). The corresponding LNAPL specific volume is  $D_n(\text{initial}) = 0.246$  m.

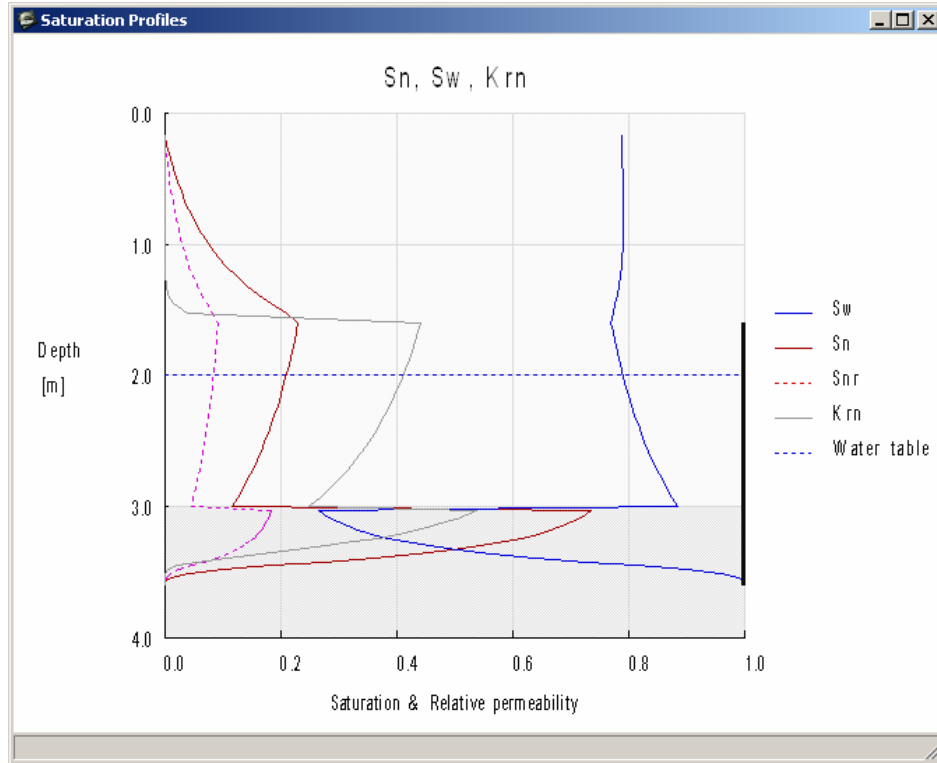


Figure 2.33—Initial LNAPL Saturation Distribution for Example with Smearing Option Selected

When LNAPL recovery using groundwater pumping wells is selected, the average drawdown within the radius of capture is calculated. For the new average water table elevation which is lowered because of groundwater pumping, the new LNAPL thickness is calculated so that the resulting LNAPL specific volume plus residual LNAPL volume in the region above the new LNAPL layer is equal to the initial LNAPL specific volume. At any elevation, the LNAPL residual saturation is specified as the maximum value based on the initial LNAPL thickness and water table elevation, and the final LNAPL thickness and water table elevation. Specifically, the new LNAPL thickness  $b_n(\text{new})$  is calculated from the following equation.

$$D_n(\text{initial}) = \int_{z_{\max}(b_n(\text{new}))}^{z_{\max}(\text{initial})} n S_{nri}(z) dz + \int_{z_{nw}(b_n(\text{new}))}^{z_{\max}(b_n(\text{new}))} n S_n(z) dz \quad (2.1)$$

In equation (2.1) the elevation of maximum capillary rise,  $z_{\max}(b_n(\text{new}))$ , and the elevation of the LNAPL-water interface in the well,  $z_{nw}(b_n(\text{new}))$ , both depend on the new LNAPL thickness,  $b_n(\text{new})$ . The initial LNAPL residual saturation above the new LNAPL layer,  $S_{nri}$ , is calculated from the initial LNAPL thickness the water table elevation. The LNAPL saturation distribution,  $S_n(z)$ , in the second integral of equation (2.1) is based on the new LNAPL thickness and water



table elevation. Equation (2.1) is solved by first bracketing the range and then applying a bisection algorithm to find the  $b_n(\text{new})$  value for which equation (2.1) is satisfied.

Figure 2.34 shows results from application of the smear correction algorithm for the initial distribution shown in Figure 2.33. Due to groundwater pumping (6 L/m for this example), the water table elevation decreases from 2 m to 2.85 m bgs. The new LNAPL specific volume is  $D_n(\text{new}) = 0.222$  m. The difference  $D_n(\text{initial}) - D_n(\text{new}) = 0.024$  m is associated with the LNAPL residual saturation remaining trapped above the new LNAPL layer. The new LNAPL layer thickness is  $b_n(\text{new}) = 1.19$  m. This is a significant decrease from the initial 2 m thickness, and it is associated with lowering the LNAPL layer elevation towards a soil layer with coarser-grain texture which has a greater capacity for storage and mobility of LNAPL.

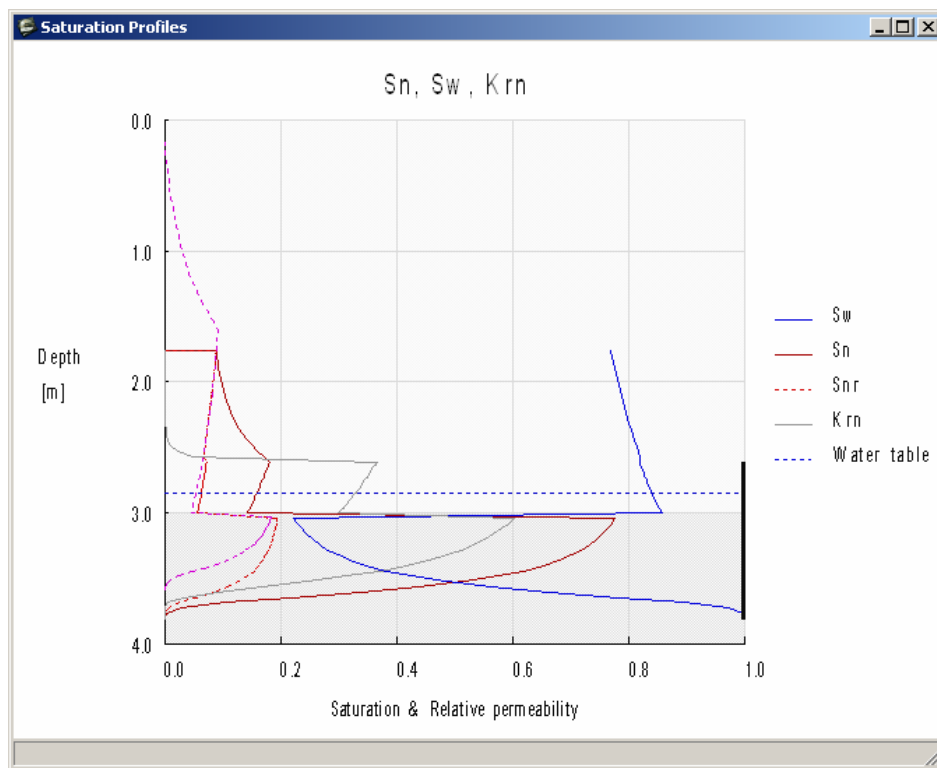


Figure 2.34—New LNAPL Layer Saturation Distribution Following Drawdown of the Water Table Using the Smear Correction Option

Within the new LNAPL layer shown in Figure 2.34, two LNAPL residual saturation curves are shown. These correspond to the initial and new LNAPL thickness values. The LNAPL residual saturation values increased due to water table drawdown and the adjusted soil layer distribution (relative to the new water table elevation). The larger values are used in calculation of the LNAPL saturation distribution.

## 2.5 MODEL OUTPUT OPTIONS

Output of model simulation results is provided in three different forms. First, summary graphical output is provided through the seven graphs described in Section 2.4.3. The second model of

output is through text information written to the main window of the LDRM application. The third method of output is detailed simulation data written to the output file that can be viewed and edited using most text processing applications. The latter two methods for output are described in this section.

### **2.5.1 Screen Output to the Main Application Window**

During application of the LDRM model it is useful for the user to have access to summary data concerning a simulation. Such data is written to the computer screen on the main window of the LDRM application. An example is shown in Figure 2.35. This figure shows the main window for the example described in Figures 2.33 and 2.34. When the Data Input window is first closed, only the first two lines are shown providing estimates of the LNAPL specific volume ( $D_n$ ) and recoverable volume ( $R_n$ ) corresponding to the initial water table elevation and LNAPL thickness. Once the Recovery Option is selected, the remaining variables are calculated and displayed. The drawdown is the average drawdown within the radius of capture. A new water table elevation is calculated and used only when the Smear Correction option has been selected. Similarly, the new LNAPL thickness and specific volumes are calculated and used only with the Smear Correction option. Otherwise, the original values are used. The initial and final LNAPL recovery rate ( $Q_n$ ) and final LNAPL thickness ( $b_n$ ) and LNAPL recovery volume ( $V_n$ ) are also presented. The percent recovery is based on the initial LNAPL volume [the initial LNAPL specific volume ( $D_n$ ) provided on the first line multiplied by the area of capture ( $A_c$ )].

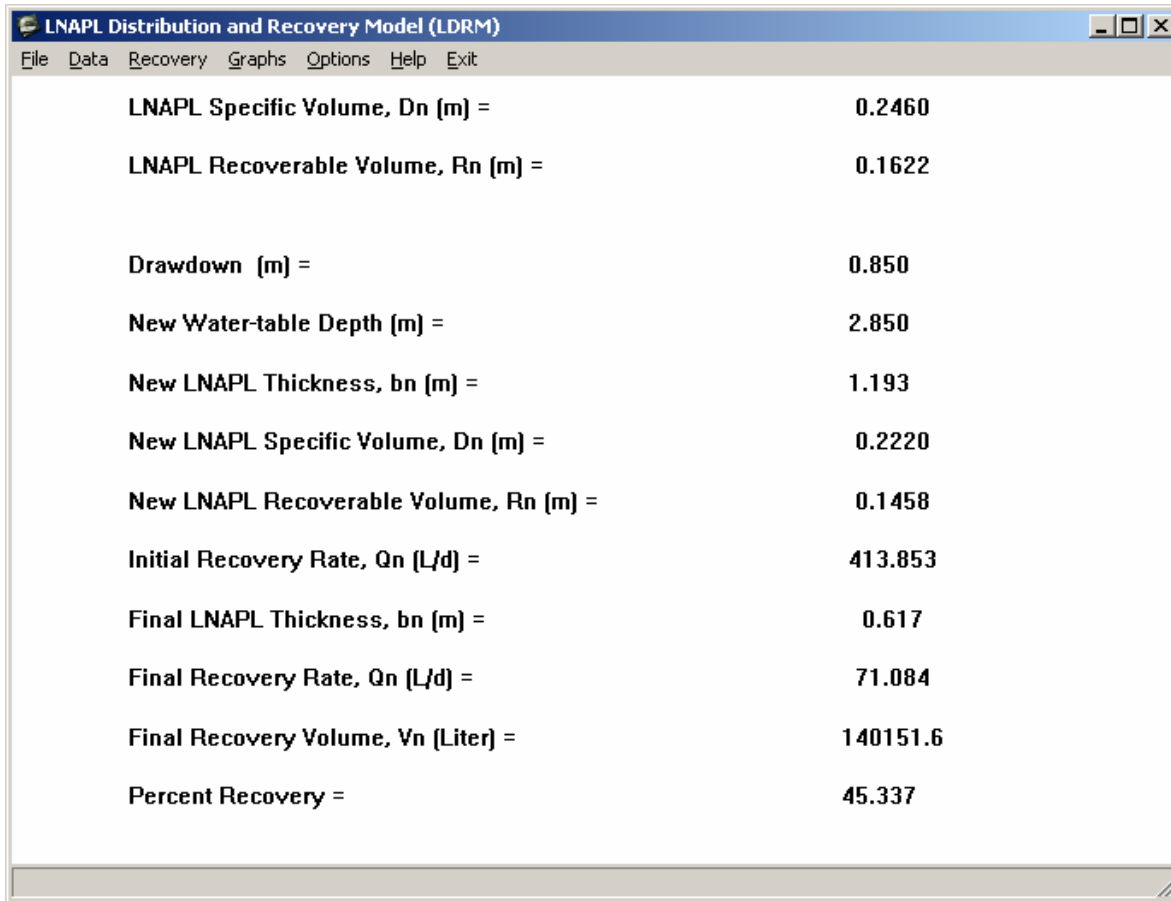


Figure 2.35—Summary Output Variables Written to the Main Window of the LDRM Application

## 2.5.2 File Output from LDRM Application

The user may save simulation results to an output text file that is expected to have “txt” as the file extension (the file name is \*.txt). All input and output data and variables are written to this file, as are data for generating all of the graphical output from the simulation and any field data that has been added for the simulation. Part of an example output file corresponding to Figures 2.33 through 2.35 is presented in Figure 2.36. Only the first part of the file has been copied. The selected options and input data are shown in this figure. One may edit the output file to change basic options; for example to invoke or cancel the Smear Correction option. The output file is read by the program to initiate a new simulation with the same basic data. Parts of the output file may also be copied to graphics programs (such as Excel) so that the user may create alternative graphical images of the output.

```

*****
*
* File Name = C:\LF9555\Work\API\2-layer (smear).txt
* Saved time = 17 : 19, 2006 . 5 . 18
*
*****

1. OPTIONS.

* Units = 2 (1: English Units, 2: SI Units)
* Soil Heterogeneity = 2 ( Number of Layers: 1, 2 or 3)
* Elevation = 2 (1: Elevation above datum, 2: depth BGS)
* FPR System Used = 1 (1: well, 2: trench, 0: Not used)
* Smear Correction = 1 (0: no adjustment, 1: smear correction)
* LNAPL Residual = 3 (1: const (user), 2: const (f), 3: variable)

2. INPUT PARAMETERS.

2.1 BASIC INPUT PARAMETERS.
Monitor. Well LNAPL thickness[m] = 2.000
Ground surface Depth [m] = 0.000
Groundwater Table Depth [m] = 2.000
Soil Layers Interface (z12) [m] = 3.000
Water vertical gradient(+up) = 0.000
LNAPL Density [g/cm3] = 0.800
LNAPL Viscosity [cp] = 2.000
Water Surface tension [dyne/cm] = 65.000
LNAPL Surface tension [dyne/cm] = 25.000
LNAPL/Water Interfacial tension = 15.000

2.1.1 SOIL PROPERTIES OF LAYER 1
Relative permeability model = 1 (Mualem)
Soil Porosity = 0.400
Hydraulic conductivity [m/d] = 0.050
van Genuchten "N" = 1.300
van Genuchten "alpha" [m-1] = 2.000
Swr1 = 0.500
Snr1 = Variable
LNAPL residual f-factor = 0.400

2.1.2 SOIL PROPERTIES OF LAYER 2
Relative permeability model = 0 (Burdine)
Soil Porosity = 0.380
Hydraulic conductivity [m/d] = 1.500
van Genuchten "N" = 3.500
van Genuchten "alpha" [m-1] = 6.500
Swr2 = 0.150
Snr2 = Variable
LNAPL residual f-factor = 0.250

2.2 INPUT DATA FOR THE RECOVERY WELL.
Design Recovery time [yr] = 2.000
Radius of pumping well [m] = 0.060
Radius of capture [m] = 20.000
Radius of influence [m] = 80.000
Water production rate [l/min] = 6.000
Groundwater thickness [m] = 3.000
Suction pressure [atm] = 0.000
Screen length for air flow [m] = 0.000

```

Figure 2.36—Leading Part of the LDRM Simulation Output File

### **3 PARAMETER SELECTION AND PROBLEM SOLVING GUIDE**

Section 3 of this User's Guide provides guidance for model conceptualization, parameter selection, and problem solving using the LDRM. The types of parameters required for the LDRM can be observed simply by opening the model, and by review of prior sections of this Guide. This section will cover several important background topics before working through four example problems. First, an overview of hydraulic oil recovery field experience is presented to provide a general overview and framework for interpreting model results. Next, an overview of parameter selection and bracketing techniques is provided to help the user frame problems and develop representative input parameter sets. As part of the discussion, an overview of the use of the API LNAPL Parameters Database will be provided to assist in parameter selection in cases when multiphase data are not available. The remainder of Section 3 will present four example problems to illustrate the implementation of scenario-based models for LNAPL recovery. The user is referred to Volume 1 of this document for background information and mathematical development of the model and Section 2 of this volume for instructions on how to operate the software.

#### **3.1 OBJECTIVES AND OVERVIEW**

The objectives of Section 3 are to ensure the user has adequate knowledge on the use of the LDRM in applied, scenario-based problem solving, including:

- Understanding the use of the LDRM for problem conceptualization and solving,
- Guidance on input parameter selection, and identification of parameter sensitivity and limitations,
- Understanding the basis of the LDRM and the limitations and simplifications therein,
- Recognizing conditions where the LDRM may be inapplicable

Clearly the most important steps in the modeling process, whether using the LDRM or others, is conceptualization of the problem and the selection of the appropriate corresponding input parameters. There is a meaningful difference between these two steps. Without a good selection of input parameters, answers will be non-representative, irrespective of the problem conceptualization. However, even with good parameter selection, poor conceptualization will also generate non-representative estimates. For instance, if a site is well constrained with respect to the input parameters, but the distribution of those parameters is not considered, the LDRM would not likely produce representative results, though they may still be instructive. Similarly, if hydraulic conditions are transiently variable, then the modeled system may not meet the key vertical equilibrium assumptions. It should be clear that the requirements of the LDRM approximations are not always met under real-world conditions, but in many cases are sufficiently approximated that valuable insight can be obtained from its application. However, in cases where any one of the approximations is poorly suited, one can expect results that at a minimum require significant interpretation, and at worst, may be unrepresentative.

The importance of applying this or other models with sufficient thought and care is that the process generally results in a refined or better understood conceptual site model (CSM). Multiphase calculations and estimates are themselves an aid in CSM development and understanding, as that problem solving requires constraining interrelated parameters, hydraulic

conditions, and other aspects of the problem being considered. For instance, do the model results compare well with recovery data, but not with saturation data? If so, the results cannot be correct. Do field measured LNAPL transmissivity values agree reasonably with the range predicted by the model? If not, then the “answer” should be self-evident; the model is not representative of the inputs and/or conceptualization specified by the user. Diligent and thorough thought, as well as experience and professional judgment are required to produce useful results in site-specific applications.

The following sections provide the user with the background needed to develop a sound model conceptualization and provide guidance on parameter selection, with an emphasis on methods to constrain parameter uncertainty where limited data exist. Before describing these approaches, an overview of hydraulic oil recovery field experience is presented to provide a general overview and framework for interpreting the LDRM results (Section 3.2) and several important parameter limitations are presented to remind the user of key considerations in model conceptualization and parameter selection (Section 3.3).

### **3.2 OIL RECOVERY EXPERIENCES: OILFIELD PRODUCTION VERSUS LNAPL RECOVERY**

It is illustrative to consider oil field and environmental experiences in context with the physics of LNAPL recovery presented in this users guide. These experiences and data clearly indicate the limits to the complete recovery of NAPL from geologic formations. Once in place, a fraction of the oil tenaciously holds onto its pore space. The magnitude of this residual fraction and its physical and chemical characteristics are key to site-specific risk.

In the oil industry there is economic incentive to optimize oil recovery efficiency. Consequently, many field and laboratory investigations of the controls on oil mobility and recovery have been undertaken that are relevant to environmental LNAPL recoverability. When oil displacement is carried out by flooding the reservoir with water, air, or steam, capillary forces are responsible for trapping some fraction of the oil initially in place. Studies of oil reservoir rocks have shown that the residual oil left behind at the conclusion of water flooding typically ranges from 25 to 50% of the pore volume (e.g., Chatzis et al., 1988; Melrose and Brandner, 1974). Pore structure and wettability are two properties that strongly influence residual oil saturation. A tendency has been observed for residual oil saturation to be greater where porosity is lower and the pore size (or grain size) distribution is wider. As a reminder, the environmental case is one where water is normally the wetting phase, except within certain types of geologic deposits. The same is not true in oil reservoirs, where the wettability sequence depends on the specifics of each reservoir setting.

Oil left behind in reservoirs can exist either as an immobile residual or as an unrecovered mobile fraction. Unrecovered mobile oil in large, well-managed reservoirs can range from just 20 and up to 70% of the initial mobile oil in place (Tyler and Finley, 1991). Unrecovered mobile oil exists because of heterogeneities in the reservoir and the limitations of well recovery efficiency. In comparing oil reservoirs to environmental conditions, it is important to consider that oil reservoirs typically have greater initial oil saturations and mobility than observed in environmental release conditions. Further, oil reservoirs are typically under confined conditions allowing more effective application of standard pumping and enhanced recovery techniques such as heating, water flooding, and chemical treatment methods. Offsetting factors are that crude oils

have viscosities that are typically higher than refined products (reducing flow), and reservoirs often have intrinsic permeabilities that are smaller than unconsolidated alluvial sediments prevalent in the environmental case. Thus, the reservoir comparison is for illustrative purposes more than as a refined quantitative comparison. In general, the hydraulics of recovery and initial oil conductivity are far better in reservoirs than for small volume LNAPL spills in unconfined, unconsolidated sediments. However, other factors limit total recovery in reservoirs that may be less restrictive under environmental release conditions.

Field and laboratory observations of environmental LNAPL recovery are different viewpoints of the same multiphase phenomena observed in petroleum production. However, measuring detailed subsurface LNAPL responses with respect to time and distance over the life of a remediation project is rare for typical environmental operations. The cost is high and interpretation of results is often difficult. Still, a few well-documented LNAPL remediation examples are available in literature. In summary, for most of the hydraulic recovery cases evaluated from literature and otherwise available to the authors, the total LNAPL recovery was less than 30% of the original volume in-place with the upper end being as high as 60%. A few other case studies are summarized by the EPA and others and are consistent with the theory and examples above. The implication is that for most sites, hydraulic recovery of more than 30% of the LNAPL in-place would be the exception rather than the rule. In finer-grained materials, hydraulic recovery of more than 15% of the LNAPL in place would be unusual. These generalizations are for overview purposes and certainly should not be arbitrarily applied to specific sites. However, it is useful to remember these ranges to assist interpreting the LDRM calculations.

### 3.3 PARAMETER LIMITATIONS

Before discussing the parameter selection process, it is useful to recognize some of the limitations that may be associated with input parameters. While this discussion is not comprehensive, it should caution the user regarding several important category limitations that should be considered both in the model conceptualization process and during parameter selection. The following categories are presented in no particular order, because the relative importance is ultimately site-specific.

- Data density limitations: The importance of multiphase conditions (parameters, boundary conditions, etc.) has only recently been recognized as important to environmental concerns. As a result, it is common for sites to have no multiphase data (e.g., capillarity, interfacial tensions, relative permeability, and others), and even where available, those data are generally sparse. The API LNAPL parameters database helps to bridge that gap, but it is a reference database that may or may not have site-specific applicability (an overview of the API LNAPL parameters database is presented in Section 3.5.2 and an example of its use is provided in Section 3.6.3.1).
- Sample scale limitations: Unlike many other hydrogeologic parameters, most multiphase parameters cannot be measured using field-scale testing (e.g., capillarity, interfacial tensions, relative permeability, and others). One can use the modeling to estimate these factors, but the solutions are non-unique (several unknowns resulting in a single solution). As a result, lab-scale testing is used, resulting in an unavoidable issue with

potential scale applicability. Lab-scale parameters are typically measured on small volume core samples that may suffer from sampling disturbance. These factors can result in challenges in the direct application of lab-test results. For instance, it is quite common to observe lab-scale hydraulic conductivity values that are smaller than field-scale values. Unfortunately, without field-scale tests for many of the important multiphase parameters (such as capillarity), it is difficult to know whether or not scale issues exist. In summary, measured multiphase parameters are useful, but are perhaps best viewed as a reasonable starting point that may require interpretive adjustment by the user to better represent observed field conditions.

- Lab testing conditions: Separate from scale and sampling issues, lab-testing methods are often performed under conditions that are unlikely to be present in the field (high pressures, high saturations, etc.). An important and common problem is encountered with lab measurement of LNAPL residual saturation values. Measured lab residuals are often larger than the LNAPL saturations observed in the field. This condition results because testing conditions are often run at higher initial LNAPL pressures and saturations than present in the field. As a result, lab residual saturation values are often not applicable to site LNAPL release and recovery conditions simulated by the LDRM (see Section 2.1.3; Figure 2.5). In other words, one cannot always simply “plug-in” a lab result and get a correct answer. Another important consideration is tested sample orientation. Most lab samples are vertical while most field problems are dominated by radial horizontal flow. A vertical orientation tends to bias the sample toward lower permeability horizons that may be present in the core. This can result, for instance, in lower hydraulic conductivity values, or higher capillarity than might be present in the lateral dimension.
- Distribution of heterogeneity: Most earth scientists and engineers recognize that earth systems are predominantly heterogeneous. The scale and distribution of that heterogeneity strongly affects multiphase modeling and estimates, more so than other forms of modeling. If the site is strongly heterogeneous, then one can expect that the LDRM modeling (or other methods) to be limited to interpretive scenario building.
- Vertical equilibrium conditions: The LDRM assumes vertical equilibrium conditions (see Section 2.4). The constraints of those assumptions need to be met for useful application of the model. It is often unknown whether the site is in vertical equilibrium, and in those instances, it is equally unclear if the model calculations will be representative. For instance, if one assumes that a well thickness of LNAPL represents the full vertical interval of hydrocarbons, but the site has experienced significant variability in water table levels, the vertical equilibrium assumption is possibly violated and the model results may not be representative, even if the other model constraints are met. In other words, one needs sufficient information about site conditions before applying the LDRM. In summary, the user is cautioned in applying this or other models without sufficient historical plume context and reasonable bracketing of potential hydraulic conditions through time.



### 3.4 MODEL CONCEPTUALIZATION

The model conceptualization and parameter selection procedure is a simple guidance that may assist the user, but is clearly not the only possible approach. The end result of suitable site conceptualization and parameter selection process is a model that reasonably represents the conditions of interest. Any process achieving that result is useful, with the converse also being unfortunately true. Therefore, the recommendations herein are best viewed as a starting point; other learning and methods may be useful to the problem-solver as they see fit.

The first step is to review the available geologic, hydrogeologic, and LNAPL data. One should first inspect existing information for site-specific parameter availability. Next, one should find secondary information that may be used to correlate the rest of the parameters necessary to execute the LDRM. Perhaps there are nearby sites in public domain files with measured parameters. Maybe local labs have experience in an area. In any case, it is convenient to divide the site information and parameters into five general categories of information of interest for users of the LDRM.

- Physical properties of the aquifer materials (parameter inputs),
- Physical properties of the LNAPL (parameter inputs),
- The nature of the lateral and vertical extent of LNAPL, including saturations (LCSM),
- The hydrogeologic and fluid level history (LCSM),
- Existing historic LNAPL recovery data (LCSM)

Typically, this compilation is then reviewed for parameter availability, or other descriptive features that may relate to those specific parameters (like soil texture, grain-size distribution, bedding descriptions, LNAPL characteristics, etc.). There can be a range of values for each physical parameter of the soil, LNAPL, or system geometry. It is generally useful to look at how the range of variability of these parameters affects LDRM results; i.e., their sensitivity to the particular set of calculations.

Following this compilation and review stage, it is useful to create hydrogeologic cross-sections or other mapping showing the factors of interest (e.g., Figures 3.1 and 3.2). Other mapping might include observable LNAPL thickness distribution through time, hydraulic conductivity and gradient mapping, vadose zone thickness mapping, etc. The purpose of mapping is to enhance the interpretive assessment of the LCSM. The level of mapping and its detail of course depends on the site setting, complexity, risk/receptor pathways, and other considerations.

From this exercise, one would typically identify one or more “type” areas that are representative of the broader site and encompass key facets for which LDRM estimates will be made. This “type area” concept is analogous to that of classical geology: “[it] serves as an objective standard to which spatially separated parts may be compared and preferably shows the maximally exposed strata” (adapted from AGI, 1984). For this purpose, the analogy means an LNAPL type area represents (to an adequate degree) the soil, LNAPL, and hydraulic conditions such that inferences from this type area and associated modeling results can be used elsewhere across the site. The concept also recognizes that data collection efforts often have a bias toward key areas of interest (i.e., type areas), and applications of these concepts are necessary to make the most out of the evaluation effort. While there may be more than one type area for a given

site, a general need is for a type area in or around the release location and at off-site plume locations (as applicable).

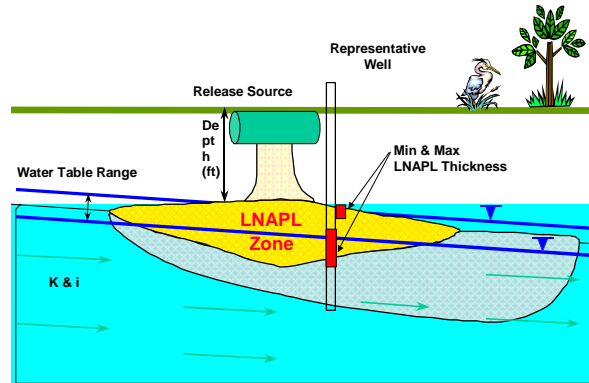


Figure 3.1—Simple Conceptual Site Model

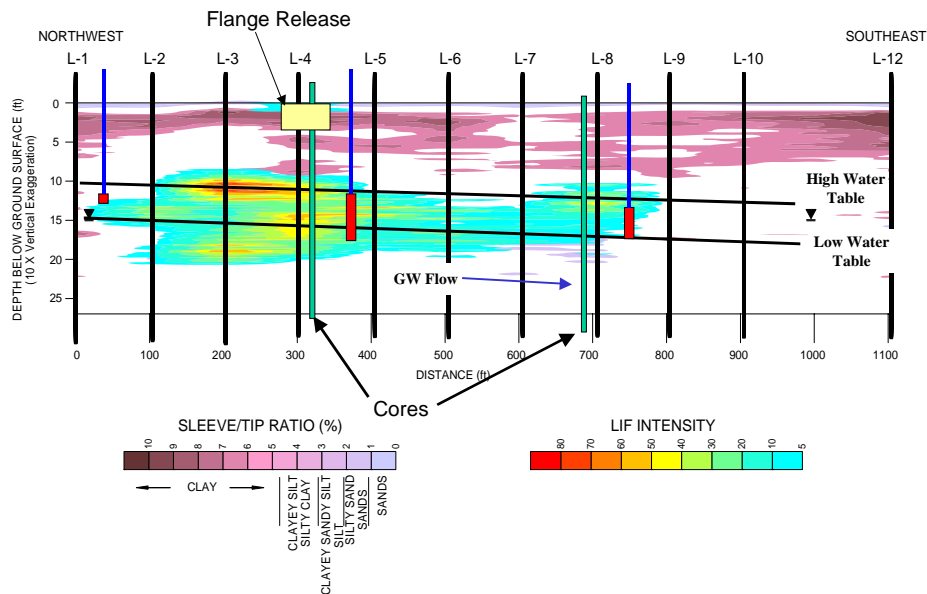


Figure 3.2—Complex Cross-Section Showing Heterogeneity (Based on Combined Coring and Geophysics), Along with the Water Table Elevation Range and Site Investigation Locations

Once the site has been conceptualized, the LCSM needs to be inspected for consistency with the LDRM constraining assumptions. Recall that this is a critical step in the application of this or any model. If the site conditions do not meet the LDRM constraints, then a more complex model (typically numerical methods) is required, or an alternate solution like field-pilot demonstrations may be necessary to derive the desired understanding. Assuming the LDRM is sufficient and useful for the expected LCSM, the next step is definition of the inputs needed to run the model.

### 3.5 MULTIPHASE PARAMETER SELECTION

For obvious reasons, site-specific multiphase parameters are preferred for model input. Parameters should be measured for the range of soil types in the LNAPL plume, and the range of parameters is then used to bracket possible recovery outcomes using the LDRM. The parameter ranges should then be refined by tuning the model to data from a variety of related field

information. This may include comparing to LNAPL transmissivity, saturation, and recovery data. Where such field data are not available, a bandwidth of LDRM results encompassing the full range of measured parameters should be considered, and results from specific runs should not be looked upon with a high degree of certainty.

The LDRM input parameters are not always available at sites when the calculations are to be performed. A typical situation is where the capillary properties of the soils and LNAPL within the LNAPL body have not been measured. The following sections describe resources for multiphase parameter selection and suggested approaches for parameterization where site-specific data are not available.

### **3.5.1 Background to Multiphase Parameter Databases**

A typical approach for determining inputs when limited data are available is to consult a published reference for guidance on parameter ranges to consider. There are several available multiphase parameter databases in published literature that may be consulted for this purpose. The following discussion focuses on those databases that have seen the most use in environmental multiphase field problem solving.

One of the most commonly quoted parameter databases is that of Carsel and Parish (1988). This database was derived from a wide number of soil samples from across the United States that were analyzed using grain-size distribution relationships to estimate capillary and other soil properties. There are two limitations of this dataset. First, there are no direct parametric measurements (i.e., lab tests) to verify the parameter values. Second, the samples are not representative of typical *in situ* environmental conditions due to the grain-size basis for the estimations. As a result, many researchers have found that the values in this database generally do a poor job of representing *in situ* environmental conditions, despite the quality of this reference for other purposes.

Mualem (1976a) compiled a soil catalogue that contains measured capillary pressure, saturation data, and some other unsaturated properties for a wide range of soils. Mualem also did significant study in unsaturated mechanics and modeling, and one of the relative permeability models used in LDRM comes from this related work (Mualem, 1976b). While the soil catalogue is useful, it has two limitations for environmental application. First, these are generally agricultural materials, and not *in situ* native soils. Second, as a practical matter, just the raw laboratory data are provided, and one must fit capillary curves to these data and then attempt to apply the results without a significant body of comparative petrophysical information. In other words, one can generate a large amount of multiphase properties, but it is difficult to cross correlate this data to site-specific environmental conditions.

Another literature database was prepared by the U.S. Salinity Lab for the distribution of general USDA soil types (M.G. Schaap, U.S. Salinity Lab, 1999). Like the first database discussed, these properties are based on empirical functions that translate physical and pedogenic properties of the soil into predicted multiphase parameters. This database is more advanced than those previously discussed, and may serve as a reasonable starting point for parameter selections, as shown below in Table 3.1.

Texture Class	N	-- $\theta_r$ --		-- $\theta_s$ --		-- $\log(\alpha)$ --		-- $\log(n)$ --		-- $K_s$ --	
		cm <sup>3</sup> /cm <sup>3</sup>		cm <sup>3</sup> /cm <sup>3</sup>		log(1/cm)		log <sub>10</sub>		log(cm/day)	
Clay	84	0.098	-0.107	0.459	-0.079	-1.825	-0.68	0.098	-0.07	1.169	-0.92
C loam	140	0.079	-0.076	0.442	-0.079	-1.801	-0.69	0.151	-0.12	0.913	-1.09
Loam	242	0.061	-0.073	0.399	-0.098	-1.954	-0.73	0.168	-0.13	1.081	-0.92
L Sand	201	0.049	-0.042	0.39	-0.07	-1.459	-0.47	0.242	-0.16	2.022	-0.64
Sand	308	0.053	-0.029	0.375	-0.055	-1.453	-0.25	0.502	-0.18	2.808	-0.59
S Clay	11	0.117	-0.114	0.385	-0.046	-1.476	-0.57	0.082	-0.06	1.055	-0.89
S C L	87	0.063	-0.078	0.384	-0.061	-1.676	-0.71	0.124	-0.12	1.12	-0.85
S loam	476	0.039	-0.054	0.387	-0.085	-1.574	-0.56	0.161	-0.11	1.583	-0.66
Silt	6	0.05	-0.041	0.489	-0.078	-2.182	-0.3	0.225	-0.13	1.641	-0.27
Si Clay	28	0.111	-0.119	0.481	-0.08	-1.79	-0.64	0.121	-0.1	0.983	-0.57
Si C L	172	0.09	-0.082	0.482	-0.086	-2.076	-0.59	0.182	-0.13	1.046	-0.76
Si Loam	330	0.065	-0.073	0.439	-0.093	-2.296	-0.57	0.221	-0.14	1.261	-0.74

Table 3.1—USDA Soil Types and Multiphase Parameters (from M.G. Schaap, U.S. Salinity Lab, 1999). Where:  $N$  is the number of samples;  $\theta_r$  is the residual volumetric moisture content;  $\theta_s$  is the saturated volumetric moisture content (total porosity);  $\log(\alpha)$  is the log of the van Genuchten model  $\alpha$  parameter;  $\log(n)$  is the log of the van Genuchten model  $N$  parameter; and  $K_s$  is the log of the saturated hydraulic conductivity. Abbreviations: S = sand; C = clay; L = loam; Si = silt.

To address the limitations of the databases discussed above, the API compiled the LNAPL Parameters Database (2003, 2006). This database is comprised of lab measurements of hydraulic and multiphase properties for the corresponding media of interest from environmental samples collected from in situ site locations. Where the other databases correlate a general soil-type description with the parameters, the LNAPL Parameters Database allows the user to query and cross-compare ranges for a variety of measured parameters. For example, a common situation is in which the user has petrophysical properties such as grain size and/or hydraulic conductivity data but is lacking capillary properties. The user could use the database to define a range of potentially representative van Genuchten parameters based on comparison to the measured parameters. The use of LNAPL Parameters Database will be discussed in the following report section and an example of its use is provided in Section 3.6.3.1. The current version of the LNAPL Parameters Database, updated and extended with additional datasets in 2006, is available at: [www.api.org/lnapl](http://www.api.org/lnapl).

### 3.5.2 Introduction to the API LNAPL Parameters Database

The following discussion provides a brief introduction to the API LNAPL Parameters Database. Additional discussion is provided in the User's Guide for the database, available from the referenced API website ([www.api.org/lnapl](http://www.api.org/lnapl)).

The API LNAPL Parameters database is a collection of information about samples with measured capillary parameters, as well as other physical parameters. The capillary data availability is key for inclusion in the database since these data are measured far less often than other petrophysical properties. Furthermore, capillary properties are sensitive within the LDRM and other multiphase calculations. The data come from a variety of sites, from service stations to refineries, all having related LNAPL issues requiring data and analyses. The data that have been included in this database were not collected for the purpose of populating a database. They were collected by site technical teams to answer specific questions and to aid in the mitigation and remediation of site-specific problems. Given these facts, it is not surprising that the range of tests performed on each sample and the testing procedures used during the tests differ significantly. Nevertheless, this is currently the most complete set of laboratory measurements of samples

whose properties have been analyzed for the purpose of understanding LNAPL remediation in near-surface aquifers.

The API LNAPL database contains the following types of information:

- Sample capillary parameters for the van Genuchten and Brooks-Corey capillary functions, and the raw data from which they were derived. This information is available for nearly all samples in the database.
- Petrophysical data including density (bulk/grain), porosity, permeability, conductivity, water and hydrocarbon saturations, as available.
- Raw grain size distribution data (weight fraction vs. grain size)
- Grain size at various percentages of the cumulative sample weight (i.e. the grain size at the 10<sup>th</sup>, 50<sup>th</sup>, and 90<sup>th</sup> percentiles).
- Grain size distribution statistics (mean, median, standard deviation).
- Fraction of the sample in various grain size classifications (%sand, %silt, etc.). Typically, if the full raw grain size distribution is available, then all of the summary parameters are also available. For some samples, only summary data are available, while others have no data available.
- Fluid properties (viscosity, density, interfacial tensions). Typically, fluid properties samples are not taken from the same samples where rock properties are measured. Fluid properties samples are provided as a form of site characterization, rather than for direct comparison with other samples within the site.

In many cases, the process of measuring one set of sample properties (grain size) makes the sample useless for measuring other properties (porosity). In general, the collection of measurements attributed to a single sample are collected from slices of a single core not separated by more than 6 vertical inches from the slice where the sample capillarity was determined.

The first step in use is opening the database with Microsoft Access 2000<sup>™</sup>. Next, one would typically go to the “Forms” menu, and select “Query Forms.” From this screen, one can explore the multiphase parameters associated with samples based on the category options shown. The first 3 or 4 general soil or parameter range queries are the most useful for initiating most parameter searches. The remainder become sample-specific, which is useful after an initial survey of parameter ranges has been made.

The API LNAPL Parameters database is used to develop a range of parameter values when one or more soil properties have not been measured. As is the case where measured parameters are available, a range of parameters should be used to bracket possible recovery outcomes using the LDRM. The parameter ranges should then be refined by tuning the model to LNAPL saturation, transmissivity, and recovery data from field (as available). Where field LNAPL data are not available, a bandwidth of results encompassing the full range of measured parameters should be considered and results from specific runs should not be held with a high degree of certainty.

For parameters that are absent in the site data, the first step is to identify other available site data that are in one or more ways related to the missing parameters in question. For instance, grain-size distribution may be correlated to permeability and capillarity, and grain-size data can be

used to query the API LNAPL Parameters database for other parameters. More specific queries are desirable, where possible. For instance, if soil parameters are needed and grain-size distribution data are available, one could query the parameters database by those specific grain-size characteristics. Similarly, hydraulic conductivity could be another query factor that has direct hydrogeologic applicability. The least specific query is through soil type description for sites having only boring logs with USCS, USDA, Folk or other common soil designations. While least specific, these are sometimes the only available site data to start from. Since the USCS, USDA, and other soil description systems were developed primarily for purposes other than environmental hydrogeologic applications, these soil designations are not always well correlated to the hydrogeologic parameters of interest.

A high level of detail is not always a requirement because final parameter tuning will depend on comparison of the LDRM predictions to site LNAPL data (recovery, saturation, transmissivity, etc.). Therefore, one can perhaps expect that a detailed evaluation will provide a better starting point for parameterization, but any method of querying the database should eventually be tuned to site observations. In other words, the variations in methods to select the first range of selected inputs are really just fine points that may not in the end make any difference to the final parameter set selected. In any case, whether the database query is highly refined or not, the steps of testing the resultant outcomes against site data will help to narrow potential ranges of parameter input. Application of the database is exemplified in example problem #3 (Section 3.6.3).

### **3.6 EXAMPLE PROBLEMS**

When solving problems using the LDRM (or others, for that matter), it is important to retain an active understanding of the assumptions and limitations of the model. Several key assumptions are critical in the LDRM, as detailed below. There are also other potential limitations stemming from unconsidered site specifics or general unknowns in current scientific knowledge. Technical considerations have been discussed in context with the mathematical development of the LDRM in prior sections. Keeping these limitations in mind while using the LDRM will help generate better answers.

The assumptions listed below are ordered in relative importance, based on experience and scientific opinion, but the hierarchy at a particular site may be different. Further, certain limitations apply only when specific evaluation conditions are selected in the LDRM. The key assumptions are:

- Uniform radial distribution and subsequent uniform drainage (recovery) of the LNAPL within the radius of recovery (analogous to piston drainage),
- All LNAPL within the radius of recovery will be captured at some point in time; using too large a capture radius will result in unrealistically high recovery results,
- Recovery is estimated by steady-state radial or 1-D flow equations,
- Heterogeneity of earth materials or LNAPL properties is not considered (except for simple uniformly layered soil horizons),
- The background groundwater gradient is implicitly flat (zero), and has no affect on the solution; capture is fully radial and equal in all directions (for recovery wells),

- Groundwater drawdown will mathematically exceed the aquifer thickness when the pumping rates are larger than the capacity of the aquifer as defined by the hydraulic conductivity and thickness terms,
- The groundwater and LNAPL gradients caused by recovery pumping are averaged across the recovery domain,
- LNAPL conductivity is averaged across the vertical saturation profile, which itself is radially uniform across the zone of recovery,
- LNAPL conditions are at all times under vertical equilibrium,
- LNAPL is assumed to have been in-place for some time, and that the LNAPL saturations estimated are additive to a residual saturation profile already in place,
- Homogeneous or uniformly layered soil conditions, and homogeneous fluid and chemical conditions,
- Only a single recovery center is considered and interaction or interference of multiple recovery centers is not considered,
- Hysteresis is not explicitly considered, but a variable residual saturation is considered with the “f-factor” approach described elsewhere in this Guide,
- Hydraulic well efficiency is assumed to be 100%.

Given these assumptions, one can generate realistic and useful estimates from the LDRM simply by making sound assumptions and consistent comparisons to available field information for all pertinent aspects. The following list suggests some items that may be helpful in tuning the model estimates to field conditions (known or expected).

- Does the LNAPL saturation profile predicted by the LDRM reasonably match saturations observed in the field (note, one may convert total petroleum hydrocarbon (TPH) values to saturation). If predicted saturations are too large, one must change either the initial thickness assumption, and/or the capillary properties of the soil.
- Does the drawdown predicted by LDRM match that observed or expected in the field? If the drawdown is too large, one must reduce the ground water pumping rate or increase the hydraulic conductivity.
- Do the predicted LNAPL recovery rates match those observed in the field?
- Are the total specific and recoverable LNAPL volumes consistent with those observed in the field and/or measured through other testing methods?

Based on the preceding discussion, one can quickly understand the importance of sound judgment and critical thought in using the LDRM or other estimation codes. Multiphase modeling is non-unique, and therefore only through a critical thought process may one generate reasonable and useful results. Simply “pushing buttons” will not suffice, nor generate useful answers. Comparison of model results with field data is of paramount importance. With these caveats, proceed to the example problems below.

### **3.6.1 Problem #1: Simple Skimming Recovery Evaluation**

This problem is designed to introduce the user to the LDRM and problem solving sequence. All necessary parameter inputs will be given and the problem will be used to compare solutions evaluating the skimming of LNAPL using different residual saturation assumptions; for these

purposes, skimming means pumping of LNAPL with no groundwater pumping. For the conditions given (discussed below), the following questions will be considered:

- How much LNAPL is present in the formation? How much would be present if the initial observed thickness were doubled?
- How much LNAPL is recoverable? In total gallons? As a percentage of the total initially in-place?
- How long does it take to recover 95% of the recoverable fraction?
- How does changing the residual saturation assumptions in the model change these values?

### 3.6.1.1 Parameter Selection

This initial problem setup will be a simple, single-layer homogeneous dune sand setting, with diesel fuel as the LNAPL type. For the base case, it is assumed that the hydrogeologic and oil properties are all known and homogeneous. The properties and conditions necessary to execute the problem are given in the following screen shots from the LDRM. To start, double click the LDRM icon or execute the LDRM from the Windows™ “Run” menu, then select the “Start a New Simulation File”, as shown below.

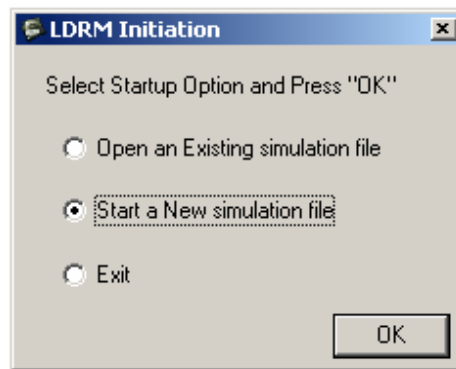


Figure 3.3—Startup Box, with Selection Shown

Next, an options box is given that sets up the basic problem conditions, units of measurement, and other aspects, as shown below. Ensure that the same selections as shown as those in Figure 3.4.



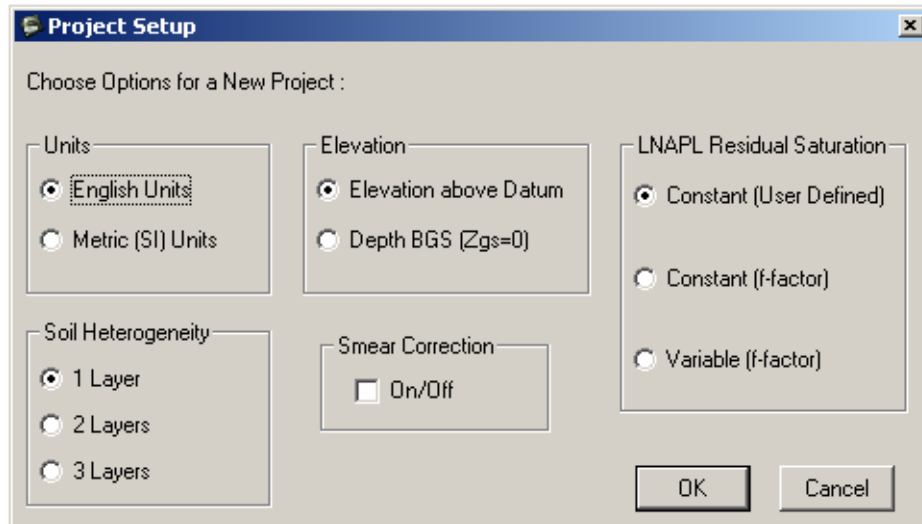


Figure 3.4—Startup Box, with Selection Shown

### 3.6.1.2 Example Problem #1 Execution

Once “OK” is selected on the screen above, the screen shown in Figure 3.5 will appear. Again, the parameters shown are given for this particular simple problem. The capillary parameters are sensitive, and must be carefully selected and evaluated during a comprehensive problem solving exercise.

After the inputs have been provided to the “Data Input” screen shown in Figure 3.5, click “OK”, and the program will execute the LNAPL distribution component of the problem, and a summary results screen will appear with the following values:

LNAPL Specific Volume,  $D_n$  (ft) = 0.2588

LNAPL Recoverable Volume,  $R_n$  (ft) = 0.1051

Note that although the units of specific and recoverable volume reduce to length, the real meaning of the terms is volume per area ( $\text{ft}^3/\text{ft}^2$ ;  $\text{m}^3/\text{m}^2$ ; etc.). This is not a thickness exaggeration term, nor is it a “length” term in the vertical direction. This is a volumetric term, not to be confused with a linear measurement.

With the specific volume, one can integrate over an area represented by the observed thickness and other parameters to estimate a total LNAPL volume. For instance, if this 2-ft thickness contour represented a 50-ft radius around the point of measurement, the area would be  $7,854 \text{ ft}^2$  ( $\pi r^2$ ), and the corresponding LNAPL volume would be  $2033 \text{ ft}^3$ , or equivalently, 15,205 gallons.

**Data Input**

**Thickness, Elevations, Vertical gradient**

Maximum Monitoring Well LNAPL Thickness [ft] = 2.000

Ground Surface Elevation [ft] = 25.000

Water table Elevation [ft] = 10.000

Water Vertical gradient (+ for upward) = 0.000

**Fluid Characteristics**

LNAPL density [gm/cc] = 0.820

LNAPL viscosity [cp] = 2.000

Air/Water surface tension [dyne/cm] = 70.000

Air/LNAPL surface tension [dyne/cm] = 25.000

LNAPL/Water surface tension [dyne/cm] = 25.000

**Soil Characteristics**

Porosity = 0.400

Hydraulic Conductivity [ft/d] = 50.000

Van Genuchten "N" = 3.250

Van Genuchten "a" [ft-1] = 1.220

Irreducible water saturation = 0.100

Residual LNAPL saturation = 0.150

Residual LNAPL f-factor = 0.300

**Relative Permeability Model (Burdine is default)**

Use Mualem Model for Layer  Layer 1

OK Cancel

Figure 3.5—Input Parameters Controlling the LNAPL Distribution at Vertical Equilibrium. Recall that the LNAPL thickness is that observed, at vertical equilibrium, in a monitoring well, which is then used to define the capillary pressure as a function of elevation above the LNAPL/water interface. The capillary properties control the associated saturations of water, LNAPL, and air. The viscosity and hydraulic conductivity will influence the later recovery calculations. Note that the default relative permeability model (Burdine) is selected.

From this first part of the problem, the first two questions on the problem list can be answered. To perform the second part of the first question, simply go to the “File” menu, save the original problem, then go to the “Data” menu and choose the “Edit Input Data” option. Change the “Maximum Monitoring Well Thickness” to 4 ft (twice the original). Hit “OK”, and the problem will run again, this time outputting the following answers:

$$\text{LNAPL Specific Volume, } D_n \text{ (ft)} = 0.8034$$

$$\text{LNAPL Recoverable Volume, } R_n \text{ (ft)} = 0.4959$$

All other things being equal, doubling the thickness results in a specific volume that is 3.10 times greater than the original volume. The recoverable volume increases from about 41% to 62%. These changes result from the non-linearity of the capillary expressions. The contrast would be more pronounced when comparing very small well LNAPL thicknesses to larger thicknesses, or when soil capillarity is greater (tighter pore space, finer-grained).

Using the results for a 2-ft initial thickness and framing above, about 825ft<sup>3</sup>, or 6,175 gallons are potentially recoverable under the idealized conditions of the model. That is, the theoretical endpoint of recovery is about 41% of the total LNAPL in-place (notice that the recovery model

does not need to be run to estimate this factor). Recall that many complicating factors affecting hydraulic recovery are not considered by the model, and these values can be considered as an ideal best-case endpoint that is not likely to be achieved in the field.

To find the answers to the remainder of the questions, the recovery aspects related to skimming for the given problem need to be calculated. First, go to the “File” menu and open the problem file that was saved in the steps above. It should have exactly the same inputs as were shown in Figure 3.5. Verify those values and then hit the “OK” button. The distribution calculation will be repeated, showing the same output as before.

The next step, prior to executing the recovery problem, is to inspect the output graphs, particularly the “Specific Volumes/Transmissibility” chart found under the “Graphs” menu. That chart is shown in Figure 3.6. On that chart is a “linearized fit” of the LNAPL transmissivity. Notice that the default fit is not all that good. A good fit is needed before solving the recovery problem because the solution is taken, in part, from this piecewise linear fit of transmissivity. To better the fit, go to the “Options” menu and select “Pick Break Points:  $bn1$ ,  $bn2$ ”. A submenu appears and allows the user to select better-fit points. Perhaps 0.9 and 1.4 are better fits (try those, and select the “fix break points” option to have the program accept the changes). Inspection of the new output graph should show a better fit.

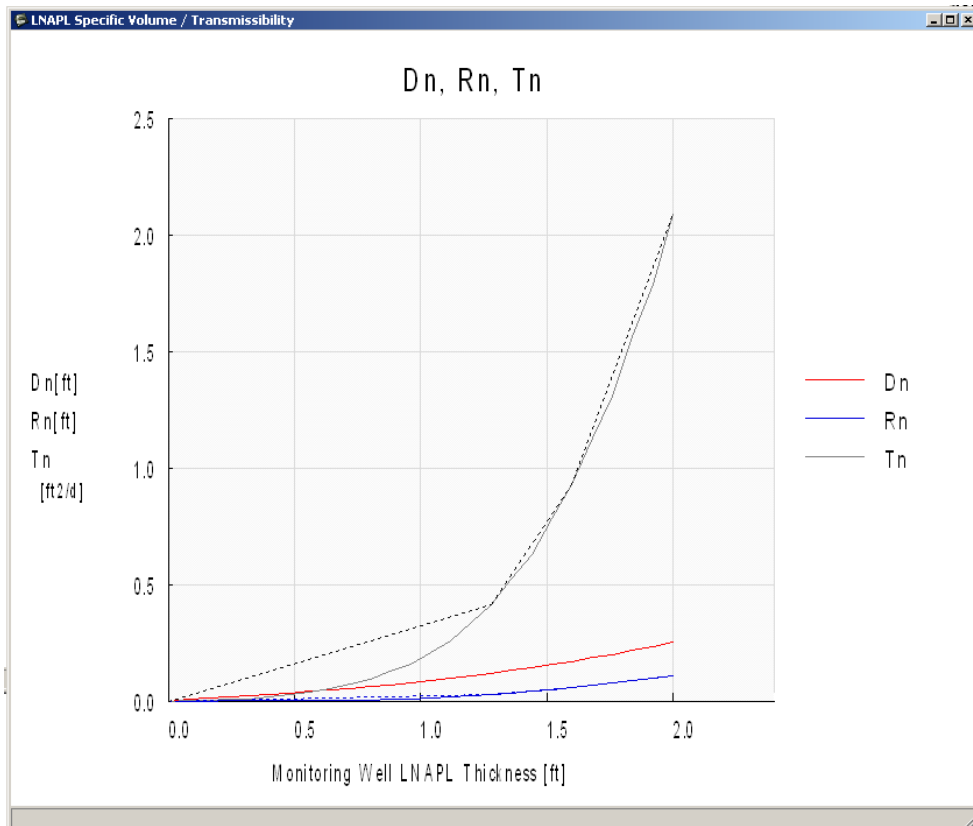


Figure 3.6—Results Chart of Specific Volumes/Transmissibility for the Given Problem. Recall that  $D_n$  is the Specific Volume, and  $R_n$  is the Recoverable Volume.  $T_n$  is the LNAPL Transmissivity. Paralleling that is a Linearized “fit” that can be Tuned by the User as Discussed in the Text.

The recovery model (part 2 of the problem) is now ready to be executed. Go to the “Recovery” menu, and select “Well”. A screen will appear (as shown in Figure 3.7), and all parameters selected should be the same as shown below. Notice that the groundwater production rate is set to zero for skimming and that there is no air-phase pressure drop to induce air movement. Since one of the objectives is to determine how long it will take to recover 95% of the theoretically recoverable LNAPL ( $R_r$ ), a simulation time of 100 years is selected.

The screenshot shows a dialog box titled "Well Recovery Systems" with a close button (X) in the top right corner. The dialog is divided into two main sections: "Water Enhanced system" and "Air Enhanced system".

**Water Enhanced system:**

- Water production rate [gpm] = 0.000
- Water Saturated thickness [ft] = 15.000

**Air Enhanced system:**

- (-)Suction Pressure [atm] = 0.000
- Screen Length [ft] = 0.000
- Air Radius of Capture [ft] = 0.000

**General Parameters (left side):**

- Recovery time [yr] = 100.000
- Radius of Pumping Well [ft] = 0.250
- Radius of Recovery [ft] = 50.000
- Radius of Influence [ft] = 50.000

At the bottom right of the dialog are "OK" and "Cancel" buttons.

Figure 3.7—Input Parameters for Skimming Recovery Portion of Problem #1

When “OK” is selected, the skimming recovery problem will execute, and results will appear on the screen, as shown in Figure 3.8. Notice that the first two outputs are the same as those given in Part 1 of the problem (a way of verifying that inputs have not changed). The remainder of the outputs are summaries for the end of the modeled timeframe (100 yrs). There are no meaningful changes to the initial LNAPL thickness or water table in this simulation because skimming does not use groundwater drawdown and LNAPL redistribution.

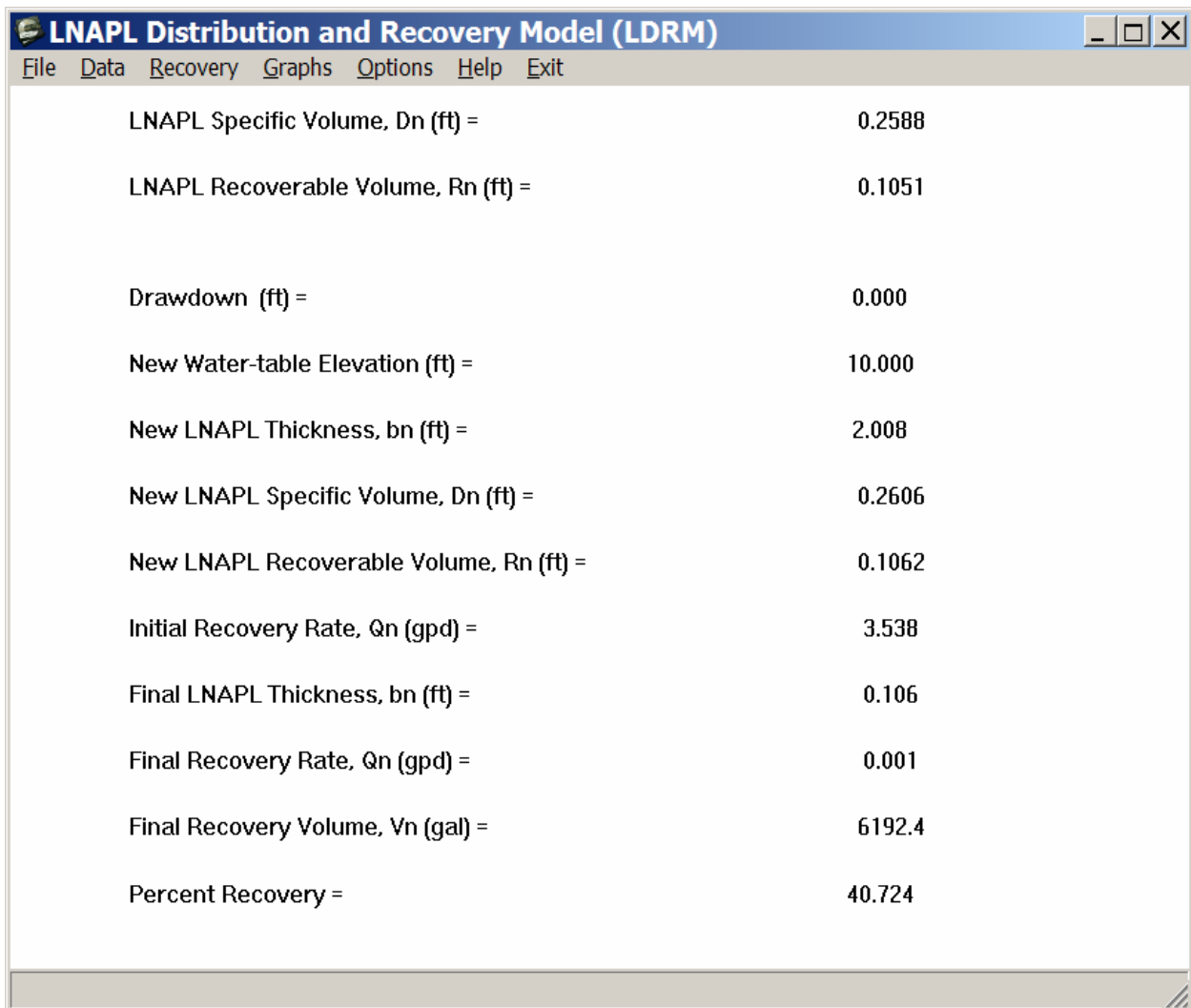


Figure 3.8—Summary Output for Skimming Recovery Using the Constant Residual Saturation Option (Original Problem Definition)

The total percent recovery of about 41% at 100 years is more than the target of 95% of the recoverable fraction; 95% of the recoverable volume is 38.7% of the total volume (Figure 3-8 above). By going to the “Graphs” menu and selecting “LNAPL recovery volume”, one can inspect the asymptotic recovery curve that was generated by the inputs and see that the recovery target is achieved on the order of 20 - 30 years. Iteratively running the calculation and selecting smaller runtimes until the target is achieved can further refine this number. Doing so results in a 95% recovery target time of 25 years (by iteratively re-running the problem while changing the time of recovery).

To answer the fourth question, change the residual saturation portion of the model to “Constant (f-factors)”. To do this, one can either start a new problem, or change the residual saturation model in the “Options” menu (recall Figure 2.12). After selecting the “Residual LNAPL Saturation Model” and “Constant (f-factor)”, hit “OK”, and the “Data Input Box” will appear (Figure 3.5). Make sure the “Residual LNAPL f-factor” is set to 0.3. Notice that the LNAPL

residual saturation values are now determined by the factors found during the referenced research in the LDRM User's Guide. The summary results for LNAPL distribution are shown below in Figure 3.9. As seen, the potentially recoverable fraction is estimated to increase to 47% (from 41% previously), but the specific volume is smaller under the new model.

LNAPL Specific Volume,  $D_n$  (ft) = 0.2331

LNAPL Recoverable Volume,  $R_n$  (ft) = 0.1092

The results shown in Figure 3.9 demonstrate a greater net recoverable volume under these particular residual saturation assumptions. Re-iterating the steps above, it is found to require about 14 years to reach 95% of the recoverable fraction. The user may choose to inspect recovery and saturation graphs to review differences between the two simulation assumptions.

The screenshot shows a window titled "LNAPL Distribution and Recovery Model (LDRM)" with a menu bar containing "File", "Data", "Recovery", "Graphs", "Options", "Help", and "Exit". The main area displays a list of simulation parameters and their values:

LNAPL Specific Volume, $D_n$ (ft) =	0.2588
LNAPL Recoverable Volume, $R_n$ (ft) =	0.1051
Drawdown (ft) =	0.000
New Water-table Elevation (ft) =	10.000
New LNAPL Thickness, $b_n$ (ft) =	2.094
New LNAPL Specific Volume, $D_n$ (ft) =	0.2595
New LNAPL Recoverable Volume, $R_n$ (ft) =	0.1224
Initial Recovery Rate, $Q_n$ (gpd) =	3.826
Final LNAPL Thickness, $b_n$ (ft) =	0.147
Final Recovery Rate, $Q_n$ (gpd) =	0.002
Final Recovery Volume, $V_n$ (gal) =	7121.2
Percent Recovery =	46.832

Figure 3.9—Summary Output for the F-factor Residual Saturation Conditions, with Other Parameters Being the Basic Skimming Simulation

### 3.6.2 Problem #2: Optimizing Remedial Options

Problem #2 will use the properties given in Problem #1, and expand the analyses to address issues pertaining to achieving remedial goals. For the conditions given in Problem #1, the following questions are considered:

- How can the remedial system be changed to achieve 90% recovery of the recoverable fraction in 2 years? Will skimming alone reach the goal? If not, how much groundwater pumping is needed?
- How does applying a vacuum of 20 and 75 inches of water column affect results of the first skimming calculations? Can the goal be reached without producing groundwater?
- How does turning on the “smear zone correction” affect results of dual pumping at 1 and 10 gpm in terms of the total recoverable volume?

#### 3.6.2.1 Parameter Selection

While still the simple, single-layer homogeneous dune sand setting as in Problem #1, this problem asks questions related to remedial optimization of LNAPL source removal through hydraulic and vacuum-assisted cleanup approaches. Costing and other aspects of optimization are not covered, but clearly changing the recovery options to increase recovery rates has a corresponding affect on the cost of cleanup. Since the basic conditions for this problem are the same as those given in Problem 1, begin by opening the file that was saved for the first set of conditions. Rerunning the LNAPL distribution portion of the problem should result in the following values that were generated in the first problem. If that does not occur, the original problem was not saved correctly, and that will need to be replicated.

LNAPL Specific Volume,  $D_n$  (ft) = 0.2588

LNAPL Recoverable Volume,  $R_n$  (ft) = 0.1051

Now, for the first question in Problem #2, how can the remedial system be changed to achieve 90% recovery of the recoverable fraction in 2 years? The 90% recoverable volume is  $0.0946 \text{ ft}^3/\text{ft}^2$  ( $0.9 * 0.1051$ ), and as a percentage of the total, that would equate to about 36.5%. To solve the problem as given, the recovery time is set to 2 years as shown in Figure 3.10 below, and then several remedial options are iteratively run to find out which will achieve the 2 year cleanup goal.

Starting with the skimming example shown, 12.8% of the LNAPL is recovered in 2 years, so obviously the gradients need to be increased. During this exercise, it may be useful to maintain a separate spreadsheet with the remedial inputs variables and the key results. Iterating using dual pumping (groundwater and LNAPL pumping), it is demonstrated that as 3-gpm groundwater production is approached, 31.4% of the LNAPL has been recovered. Tuning further, 4.97 gpm groundwater production results in the goal of 36.5% total recovery, as shown in Table 3.2 below. Note, in this example the radius of recovery has not been adjusted with changes in pumping rate; consideration of the radius of recovery is covered in subsequent problems.

Figure 3.10—Data Input Screen for a Recovery Time of 2 Years

Simulation Number	Description	Water Production Rate (gpm)	Suction (atm)	% of Total LNAPL Recovered	% of Recoverable LNAPL
1	Skimming	0.00	0	12.84%	32%
2	Dual-Pump	1.00	0	18.29%	45%
3	Dual-Pump	3.00	0	31.43%	77%
4	Dual-Pump	4.97	0	36.50%	90%

Table 3.2—Results of Initial Optimization Simulations

The 2-year, 90% recovery goal (90% of the recoverable fraction) has been achieved by using groundwater pumping to increase the recovery gradient. The second question in the problem was how the initial skimming scenario is affected by putting a vacuum on the recovery well; 20 and 75 inches water column, or equivalently, 0.049 and 0.184 atm (gauge). To put a vacuum in the recovery calculation, one simply enters the given gauge suction into the “Air Enhanced System” section of the “Well Recovery Systems input box” shown in Figure 3.10; for this case, assume a screen length of 10 ft, and an air radius of capture of 40-ft. After entering the given vacuums for skimming only, observe that the vacuum enhances recovery, and that the recovery goal is reached in 2 years with skimming and an applied vacuum of 0.023 atm (9.4 inches of water column; extended results are in Table 3.3). These results suggest that it may not be necessary to produce water in this case to reach the stated goals; vacuum application may suffice instead. Note also that the percent recoverable for the higher vacuums is greater than 100% of the initial estimate because the remediation calculation itself results in a “new recoverable volume” term (recall Figures 3.8 and 3.9).

Simulation Number	Description	Water Production Rate (gpm)	Suction (atm)	% LNAPL Recovered	% of Recoverable
5	Vac-assist skimming	0.00	0.049	41.97%	>100%
6	Vac-assist skimming	0.00	0.184	47.74%	>100%
7	Vac-assist skimming	0.00	0.0236	36.54%	90%

Table 3.3—Results for Vacuum-Assisted Skimming



The 3<sup>rd</sup> part of the problem asks how the smear correction affects the recoverable fractions for two different groundwater-pumping rates (1 and 10 gpm). Recall that the smear correction accounts for LNAPL lost to residual storage as a function of drawdown. Therefore, the expectation might be that there will be less recoverable volume at the higher pumping rates because of the larger associated drawdown. To run the problem, start a new problem to access the “Project Setup Input” screen with the “Smear Correction” turned on (shown below in Figure 3.11). Then proceed to re-enter the inputs from Problem 1 and verify through the  $D_n$  and  $R_n$  terms, as done above.

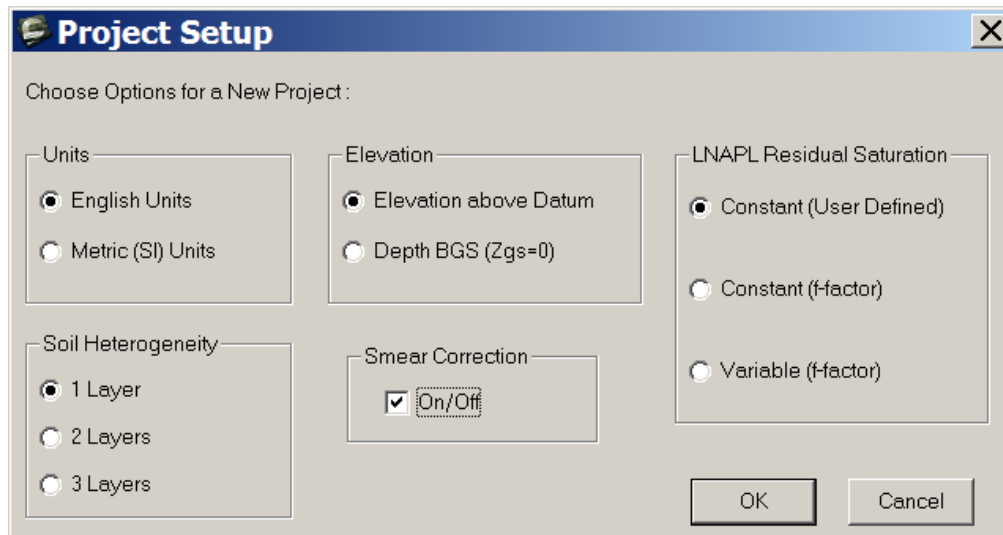


Figure 3.11—Results for Vacuum-Assisted Skimming

Following the LNAPL distribution calculation, run the well recovery model at 1 and 10 gpm for the same inputs as used above. With the increased pumping rate, a small amount of available and recoverable specific volume is lost (Table 3.4 results). Of course, if the residual saturation were greater, even more of the LNAPL would be lost to residual storage.

Simulation Number	Description	Water Production Rate (gpm)	Specific Volume ( $D_n$ )	Recoverable Volume ( $R_n$ )	% LNAPL Recovered
1	Skimming	0	0.261	0.106	12.8%
8	Dual-pump; smear correction	1	0.255	0.103	17.6%
9	Dual-pump; smear correction	10	0.245	0.096	37.1%

Table 3.4—Results of the Smear Zone Correction Problem

For the purposes of this simple but expanded problem, the implications of other factors used in the recovery specification have not been discussed. Through experimentation, one will find that the radius of influence term is not highly sensitive in the calculations, but clearly would increase in the real world as the pumping rate increased. If desired, one could simply run the Theis equation for late time to analytically determine the radius of influence term for a given conductivity and pumping rate. However, the “Radius of Recovery” term is very important in the calculations because it makes an explicit assumption about the zone over which recovery is occurring, and therefore an implicit assumption about the volume in-place and the time to recover that volume.

In reviewing the mathematical development, one will also recognize that the model will eventually recover all recoverable LNAPL in the assumed “Radius of Recovery”; it will simply take a longer time for larger radii and associated LNAPL volumes. Further, as with groundwater capture zones, the capture function is not radial around a pumping well, drawdown is radial and that is superimposed on the regional fluid gradients for both groundwater and LNAPL. Since the “Radius of Recovery” is in effect a judgment term, one must be careful in selecting and evaluating this factor. Despite all the sound technical work to produce the given estimates, the complex hydraulics that occur for both groundwater and LNAPL flow under pumping conditions cannot be accounted for in a simple radial flow model. The answers one generates are going to be highly affected by the “Radius of Recovery” assumptions used in the estimates. The “Radius of Recovery” term is examined further in Problem 4 where the model is fit against a well-characterized facility where LNAPL recovery has been closely tracked over time.

### **3.6.3 Problem #3: Parameter Bracketing Problem**

The third problem is designed to demonstrate the use of LDRM to evaluate the cost-benefit of multiple LNAPL recovery methods. There are three technical objectives of this example problem. First, the use of the API LNAPL Parameters database for initial selection of multiphase parameters is demonstrated. Secondly, the concept of parameter bracketing is illustrated. Lastly, the problem will illustrate the importance of tuning the model to field data.

For this problem, the example site is an active truck stop and fueling station. During a recent station reconstruction, it was discovered that fresh gasoline had been released to the subsurface, resulting in an LNAPL body that occupies approximately 1250 m<sup>2</sup> near the former underground storage tanks. The core of the LNAPL body occupies approximately 900 m<sup>2</sup> where 1 m of free product is present in the monitoring wells. The observed free product thickness declines rapidly with distance away from the core of the LNAPL body. The site is located in a non-beneficial use groundwater aquifer and there are no complete risk pathways to other receptors. As such, the only regulatory mandate is to recover LNAPL to the extent practicable. The regulatory authority agreed that the remediation endpoint for the cleanup would be removal of 90% of the recoverable LNAPL in the core of the plume.

Naturally, the site owner would like to minimize the cost of the LNAPL recovery efforts. To achieve the site owner’s goals, the following questions must be answered:

- How much LNAPL is present in the formation?
- How much LNAPL is recoverable?
- What is the most cost effective method for LNAPL recovery and how long will it take?

Multiple site investigations have been conducted to assess the lateral extent of LNAPL and dissolved-phase impacts. Pilot testing of multiple LNAPL recovery methods has also been performed. Data generated during these investigations are summarized in the following paragraphs.

The soils beneath the site are fairly homogeneous and consist of well-graded, medium-grained sands. These soils would be described in the Unified Soil Classification System (USCS) as SW materials (well-graded sand with less than 5% fines). The grain size distribution of two aquifer samples has been measured. Slug tests were conducted at the site, resulting in field-based

hydraulic conductivity estimates that range from about  $1.7 \times 10^{-3}$  to  $1.5 \times 10^{-2}$  centimeters per second (cm/sec) (approximately 1.5 to 13 meters per day (m/day)).

During the investigations, soil and fluid samples were collected for laboratory analysis. Soil samples were submitted for chemical analysis of total petroleum hydrocarbons and volatile constituents. Based on analyses of soil samples collected near wells with comparatively thin product accumulations, the field residual LNAPL saturation is estimated to be approximately 15% in the capillary fringe and water table region. Test results in the vadose zone suggest a much lower residual LNAPL saturation of approximately 7.5% or less. Test results in the core of the LNAPL plume suggest peak saturations of approximately 40%-42%. The site fluids have been analyzed to determine the physical properties of the LNAPL and water.

Monitoring wells have been installed within and outside of the LNAPL body to monitor fluid levels and dissolved-phase plume transport. Fluid level monitoring has indicated that the water table at the site has not fluctuated more than approximately 0.1 to 0.2 m during two years of monitoring. This suggests that vertical equilibrium may be a satisfactory assumption for this site. Wells in the core of the LNAPL body contain approximately 1 meter of hydrocarbons.

Short-term pilot testing of LNAPL recovery was performed to determine potential LNAPL recovery rates. Skimming was conducted on several wells and recovery rates of approximately 1 liter per day (l/day) were observed. Dual-phase recovery was also tested by adding water production of approximately 1 gallon per minute (3.8 liters per minute (l/min)), resulting in recovery rates of approximately 600 l/day. Vacuum-enhanced product recovery was attempted, but air leakage from the surface prevented significant enhancement of the recovery gradient.

Review of the required input parameters for the LDRM reveals that soil capillary properties, residual (irreducible) water saturation, and porosity are missing. The following section describes a method for estimating these parameters using the API LNAPL Parameters database. After the parameters are estimated, the LDRM will be executed and the parameters will be bracketed and tuned through a comparison to field recovery data. Then the site owner's questions can be answered.

### **3.6.3.1 Parameter Selection Using the API LNAPL Parameter Database**

For this example site, it is known that the soils are well-graded, medium-grained sands that are logged as SW soils under the USCS (Table 3.5; Figures 3.12 and 3.13). The hydraulic conductivity of the soils is known from field measurements to be approximately between  $1.7 \times 10^{-3}$  to  $1.5 \times 10^{-2}$  cm/sec.

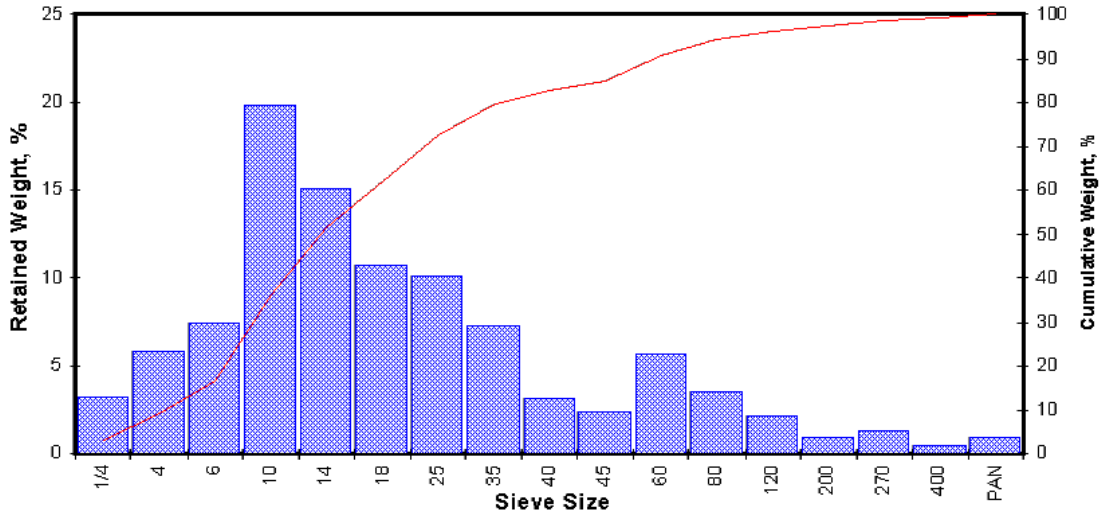


Figure 3.12—Site-Specific Grain Size Data—Sample 1

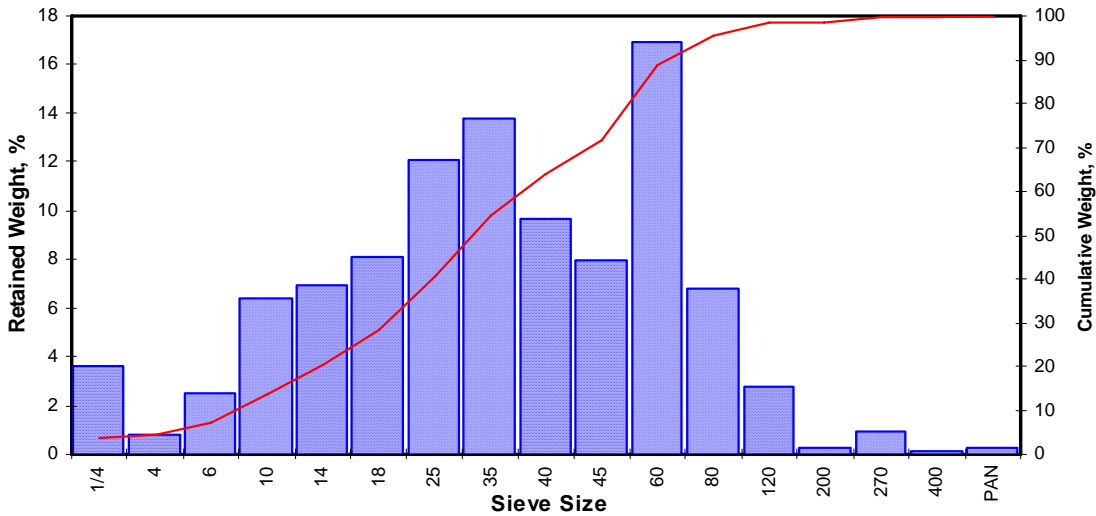


Figure 3.13—Site-Specific Grain Size Data—Sample 2

Sample ID	Depth (ft)	Grain Size Description (1)	Median Grain Size (mm)	Particle Size Distribution (wt%)					Silt & Clay	
				Gravel	Coarse	Medium	Fine	Silt		Clay
Sample 1	14.8	Med. Sand	1.461	9.01	27.30	46.37	14.67	NA	NA	2.66
Sample 2	15.9	Med. Sand	0.556	4.46	8.95	50.47	34.71	NA	NA	1.41
Seive Opening (mm)				4.757	2.000	0.420	0.074	0.053		

Table 3.5—Site-Specific Grain Size Data

In the API database, initially query by the corresponding soil type for a first cut. Using the “Query by Soil Type” option, the result is 7 matching samples. Given the measured field-testing results for the site, query the database for soils with hydraulic conductivity ranging from  $1.7 \times 10^{-3}$  to  $1.5 \times 10^{-2}$  cm/sec. Using the “Query by Conductivity Range” option, the result is 10 matching samples.

When the user selects the “Report: Samples and Stats” tab in the query options, the following tables are returned for each of the queries:

**USCS Symbol: SW**  
**well graded sand (fines<5%, coarse>50%, sand>gravel)**

Sample Id	230			
Van Genuchten Alpha <cm-1>	4.47E-03	Brooks-Corey Bubbling Pressure (Pd) <cm>		1.64E+02
Van Genuchten Beta (N)	2.20E+00	Brooks-Corey Lambda		1.12
Van Genuchten Fit R-squared	0.992	Brooks-Corey Fit R-squared		0.968
Residual Water	6.0%			
Sample Id	234			
Van Genuchten Alpha <cm-1>	3.74E-03	Brooks-Corey Bubbling Pressure (Pd) <cm>		1.55E+02
Van Genuchten Beta (N)	1.95E+00	Brooks-Corey Lambda		0.70
Van Genuchten Fit R-squared	0.990	Brooks-Corey Fit R-squared		0.938
Residual Water	2.0%			
Sample Id	235			
Van Genuchten Alpha <cm-1>	3.12E-03	Brooks-Corey Bubbling Pressure (Pd) <cm>		1.99E+02
Van Genuchten Beta (N)	3.50E+00	Brooks-Corey Lambda		1.70
Van Genuchten Fit R-squared	0.987	Brooks-Corey Fit R-squared		0.888
Residual Water	23.0%			
Sample Id	162			
Van Genuchten Alpha <cm-1>	7.83E-02	Brooks-Corey Bubbling Pressure (Pd) <cm>		5.82E+00
Van Genuchten Beta (N)	1.55E+00	Brooks-Corey Lambda		0.44
Van Genuchten Fit R-squared	0.975	Brooks-Corey Fit R-squared		0.992
Residual Water	29.0%			
Sample Id	106			
Van Genuchten Alpha <cm-1>	4.00E-02	Brooks-Corey Bubbling Pressure (Pd) <cm>		3.04E+00
Van Genuchten Beta (N)	4.06E+00	Brooks-Corey Lambda		1.13
Van Genuchten Fit R-squared	1.000	Brooks-Corey Fit R-squared		0.918
Residual Water	3.8%			
Sample Id	107			
Van Genuchten Alpha <cm-1>	3.10E-02	Brooks-Corey Bubbling Pressure (Pd) <cm>		6.37E+00
Van Genuchten Beta (N)	5.54E+00	Brooks-Corey Lambda		1.96
Van Genuchten Fit R-squared	1.000	Brooks-Corey Fit R-squared		0.919
Residual Water	4.3%			
Sample Id	108			
Van Genuchten Alpha <cm-1>	4.00E-02	Brooks-Corey Bubbling Pressure (Pd) <cm>		1.67E+01
Van Genuchten Beta (N)	4.05E+00	Brooks-Corey Lambda		5.82
Van Genuchten Fit R-squared	0.998	Brooks-Corey Fit R-squared		0.988
Residual Water	12.0%			

**USCS Symbol: SW**  
**well graded sand (fines<5%, coarse>50%, sand>gravel)**

Statistical summary of query results		Records: 7		
Parameter	Average	Minimum	Maximum	Std Deviation
VG - alpha (cm-1)	2.87E-02	3.12E-03	7.83E-02	2.76E-02
VG - Beta (N)	3.26E+00	1.55E+00	5.54E+00	1.43E+00
VG - Res. Water	11.4%	2.0%	29.0%	10.6%
BC Pd (cm)	7.85E+01	3.04E+00	1.99E+02	8.90E+01
BC lambda	1.84	0.44	0.44	1.83

Figure 3.14—Capillary Fit Parameters for Samples with Soil Description

Sample Id	1	Conductivity	0.00249
Van Genuchen Alpha <cm-1>	1.82E-02	Brooks-Corey Bubbling Pressure (Pd) <cm>	4.44E+01
Van Genuchen Beta (N)	1.78E+00	Brooks-Corey Lambda	0.73
Van Genuchen Fit R-squared	0.997	Brooks-Corey Fit R-squared	0.999
Residual Water	8.0%		
Sample Id	11	Conductivity	0.0145
Van Genuchen Alpha <cm-1>	1.80E-02	Brooks-Corey Bubbling Pressure (Pd) <cm>	2.02E+01
Van Genuchen Beta (N)	1.20E+00	Brooks-Corey Lambda	0.14
Van Genuchen Fit R-squared	0.987	Brooks-Corey Fit R-squared	0.954
Residual Water	45.0%		
Sample Id	14	Conductivity	0.00437
Van Genuchen Alpha <cm-1>	2.74E-02	Brooks-Corey Bubbling Pressure (Pd) <cm>	2.70E+01
Van Genuchen Beta (N)	2.20E+00	Brooks-Corey Lambda	1.01
Van Genuchen Fit R-squared	0.992	Brooks-Corey Fit R-squared	0.983
Residual Water	15.0%		
Sample Id	133	Conductivity	0.00172
Van Genuchen Alpha <cm-1>	2.71E-02	Brooks-Corey Bubbling Pressure (Pd) <cm>	2.22E+01
Van Genuchen Beta (N)	2.25E+00	Brooks-Corey Lambda	0.77
Van Genuchen Fit R-squared	0.977	Brooks-Corey Fit R-squared	0.978
Residual Water	13.0%		
Sample Id	98	Conductivity	0.0121
Van Genuchen Alpha <cm-1>	1.30E-02	Brooks-Corey Bubbling Pressure (Pd) <cm>	2.12E+01
Van Genuchen Beta (N)	1.91E+00	Brooks-Corey Lambda	0.88
Van Genuchen Fit R-squared	0.998	Brooks-Corey Fit R-squared	0.996
Residual Water	28.0%		
Sample Id	99	Conductivity	0.00657
Van Genuchen Alpha <cm-1>	1.20E-02	Brooks-Corey Bubbling Pressure (Pd) <cm>	1.90E+01
Van Genuchen Beta (N)	2.33E+00	Brooks-Corey Lambda	1.05
Van Genuchen Fit R-squared	0.999	Brooks-Corey Fit R-squared	0.990
Residual Water	28.0%		
Sample Id	104	Conductivity	0.00257
Van Genuchen Alpha <cm-1>	2.50E-02	Brooks-Corey Bubbling Pressure (Pd) <cm>	1.10E+01
Van Genuchen Beta (N)	1.24E+00	Brooks-Corey Lambda	0.18
Van Genuchen Fit R-squared	0.998	Brooks-Corey Fit R-squared	0.972
Residual Water	24.2%		
Sample Id	119	Conductivity	0.00235
Van Genuchen Alpha <cm-1>	1.25E-02	Brooks-Corey Bubbling Pressure (Pd) <cm>	4.21E+01
Van Genuchen Beta (N)	1.74E+00	Brooks-Corey Lambda	0.54
Van Genuchen Fit R-squared	0.998	Brooks-Corey Fit R-squared	0.990
Residual Water	31.9%		

### Capillary Fit Parameters For Given Conductivity Range

Sample Id	118	Conductivity	0.00244	
Van Genuchen Alpha <cm-1>	8.70E-03	Brooks-Corey Bubbling Pressure (Pd) <cm>	4.85E+01	
Van Genuchen Beta (N)	2.72E+00	Brooks-Corey Lambda	1.02	
Van Genuchen Fit R-squared	0.997	Brooks-Corey Fit R-squared	0.987	
Residual Water	24.9%			
Sample Id	127	Conductivity	0.00238	
Van Genuchen Alpha <cm-1>	1.30E-02	Brooks-Corey Bubbling Pressure (Pd) <cm>	5.31E+01	
Van Genuchen Beta (N)	2.25E+00	Brooks-Corey Lambda	0.72	
Van Genuchen Fit R-squared	0.998	Brooks-Corey Fit R-squared	0.928	
Residual Water	13.0%			
Statistical summary of query results		Records:	10	
Parameter	Average	Minimum	Maximum	Std Deviation
VG - alpha (cm-1)	1.75E-02	8.70E-03	2.74E-02	6.84E-03
VG - Beta (N)	1.96E+00	1.20E+00	2.72E+00	4.85E-01
VG - Res. Water	23.1%	8.0%	45.0%	11.1%
BC Pd (cm)	3.09E+01	1.10E+01	5.31E+01	1.47E+01
BC lambda	0.71	0.14	0.14	0.33

Figure 3.15—Capillary Fit Parameters for Given Conductivity Range

Statistics of the capillary values are found at the bottom of both query reports. It can be seen that the average capillary “ $\alpha$ ” value for the van Genuchten function are  $2.87 \times 10^{-2}$  and  $1.75 \times 10^{-2}$  1/cm, respectively, with corresponding “ $N$ ” values of 3.26 and 1.96. These values are probably a reasonable starting point for LDRM calculations. However, because there is grain-size data, it is also possible to review these data for potential similarities to the site-specific soils. In so doing, only one database well-graded sand sample reasonably matches the grain-size distribution in the site samples, Sample 162 (Figure 3.16-a). Similarly, an inspection of the grain size distribution of the samples in the measured conductivity range reveals that most of the samples are much finer-grained than the site soils (Figure 3.16-b). Although they are slightly more fine-grained, database samples 11, 14, and 133 are similar to site sample #2 (Figure 3.16-b). Based on the foregoing, the initial parameter estimates for the model can now be developed.



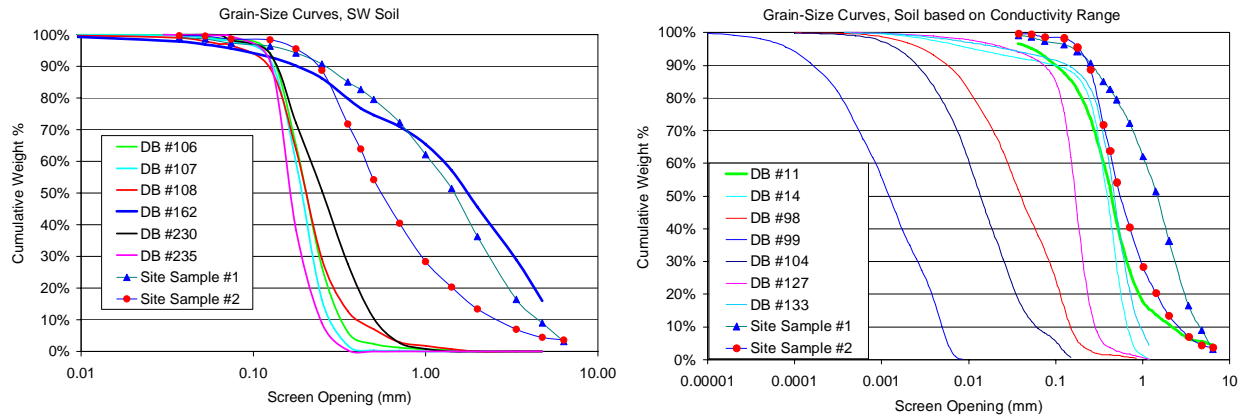


Figure 3.16-a and 3.16-b—Grain Size Curves, Site Samples versus Database Samples

Referring to the summary reports above, a range of property values based on samples 11, 14, 133, and 162 can be derived. The van Genuchten “ $\alpha$ ” of the samples range from  $1.80 \times 10^{-2}$  and  $7.83 \times 10^{-2}$  1/cm with “ $N$ ” values ranging between 1.2 and 2.25. The residual water saturation for the samples ranges from 13% to 45%. The result for sample 11 (45%) appears to be somewhat high compared to the expected range for sands, so that value will be eliminated from consideration, leaving a range of 13% to 29%. Since the residual water saturation is not as sensitive as the other capillary properties, the mid-point of the range (21%) will be selected for the model input. There is now a range of capillary property inputs for the problem. The porosity must now be estimated.

The porosity of samples can be found by re-running the above queries for the petrophysical properties. Running these queries results in a porosity range of 33%-49% for SW soils and 22%-50% for the selected hydraulic conductivity range. The overall range is, therefore, 22%-50%. The low-end porosity results likely reflect samples that contain a comparatively higher fraction of coarse sand and/or gravels. Similarly, the high-end porosity results are probably for samples that contain fines. By focusing on that samples that most closely matched the site soils in the queries above, it can be seen that the porosity ranges from 32% and 46%. The mid-point of the range (39%) is selected for model input. Keep in mind that the porosity affects the total and recoverable specific LNAPL volumes. Where data are available to independently calculate the LNAPL volume, the specific volume can be checked against those calculations.

There is now a range of multiphase parameters for input to the LDRM, each of which will generate a different initial basic distribution of LNAPL under vertical equilibrium conditions and the variants offered in the LDRM.

### 3.6.3.2 Example Problem #3 Execution

The user is now ready to run the LDRM. First, the sensitive parameters need to be tuned based on field observations. Once the user is comfortable with the parameter bracketing, the site owner’s questions can then be answered.

The capillary properties are initially bracketed based on the saturations estimates from the field sampling results. A starting point is the two multiphase data sets derived in Section 3.6.3.1. Recalling that the peak saturations measured in the field were approximately 40% – 42%, the



user should look for the capillary values in this range that most closely match the observed peak LNAPL saturation. The user should start with the low end van Genuchten “ $\alpha$ ” and “ $N$ ”, as shown in the following input screen. Note that the Mualem permeability model has been selected. The van Genuchten “ $N$ ” values in the API LNAPL Parameter database are derived using the Mualem expression ( $M = 1 - 1/N$ ). Recalling from Section 3.1.3 that while there are subjective trends with grain-size, there is little published information to suggest which of the empirical relative permeability models should be used for a specific site. In practice, the User should inspect the effect of the different models and select the model that yields the most representative results. The measured fluid properties are included in the input screen and other parameters are as presented in the problem introduction.

Section	Parameter	Value
Thickness, Elevations, Vertical gradient	Maximum monitoring well LNAPL thickness [m]	1.000
	Ground surface elevation [m]	20.000
	Water table elevation [m]	15.000
	Water Vertical gradient (+ for upward)	0.000
Fluid Characteristics	LNAPL density [gm/cc]	0.730
	LNAPL viscosity [cp]	0.620
	Air/Water surface tension [dyne/cm]	70.000
	Air/LNAPL surface tension [dyne/cm]	24.000
	LNAPL/Water surface tension [dyne/cm]	52.000
Soil Characteristics	Porosity	0.390
	Hydraulic conductivity [m/d]	13.000
	Van Genuchten "N"	1.2
	van Genuchten "a" [m-1]	1.8
	Irreducible water saturation	0.210
	Residual LNAPL saturation	0.150
Residual LNAPL f-factor	None	
Relative Permeability Model (Burdine is default)	Use Mualem Model for Layer	<input checked="" type="checkbox"/> Layer 1

Figure 3.17—Initial Data Input Screen for Example Problem #3

After clicking “OK” and graphing the saturation profile, the following screen is displayed in Figure 3.1.8. Inspection of the profile reveals the predicted peak saturation is approximately 19%. This suggests that the van Genuchten “ $\alpha$ ” and/or “ $N$ ” require adjustment. At this point, the user would adjust the van Genuchten “ $\alpha$ ” and/or “ $N$ ” until peak saturations are approximately 40%-42%. Doing so reveals that multiple combinations of “ $\alpha$ ” and “ $N$ ” can generate the target peak saturations. In fact, all that can be done at this point is to establish the minimum expected “ $\alpha$ ” value for the given range of “ $N$ ” values. Doing so reveals that “ $\alpha$ ” must be greater than  $3.5 \times 10^{-2}$  1/cm. At this point, “ $\alpha$ ” and “ $N$ ” have been bracketed between two possible end member combinations ( $3.5 \times 10^{-2}$  1/cm, 2.25 and  $7.8 \times 10^{-2}$  1/cm, 1.50). The following screens show LNAPL saturation profiles for these end members.

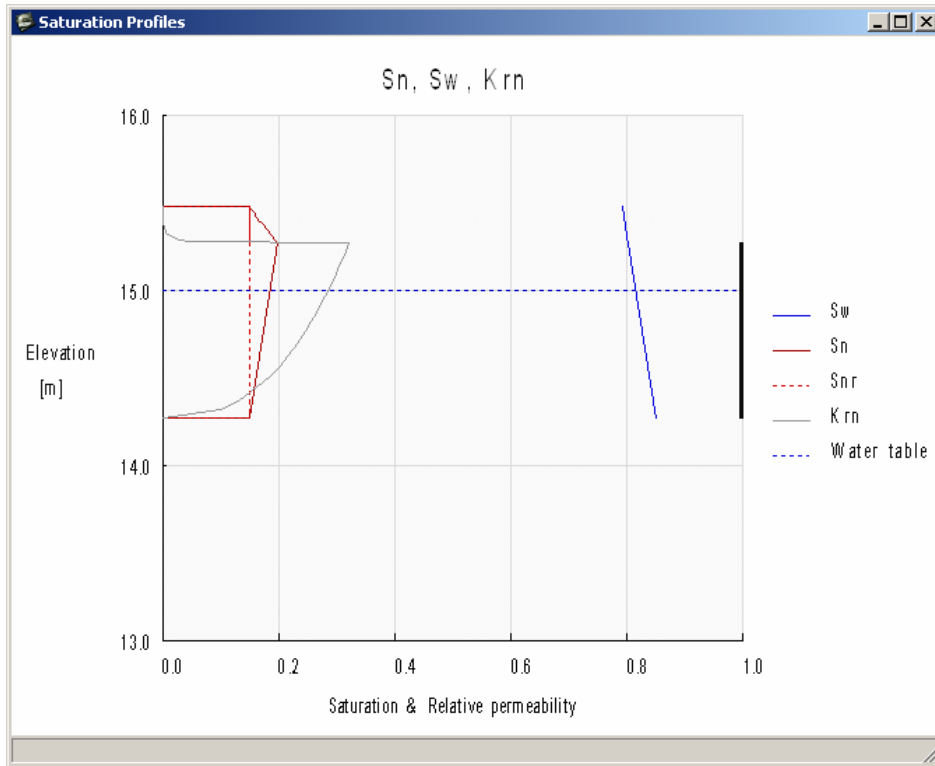


Figure 3.1.8—Saturation Profiles for Data Input in Figure 3.1.7

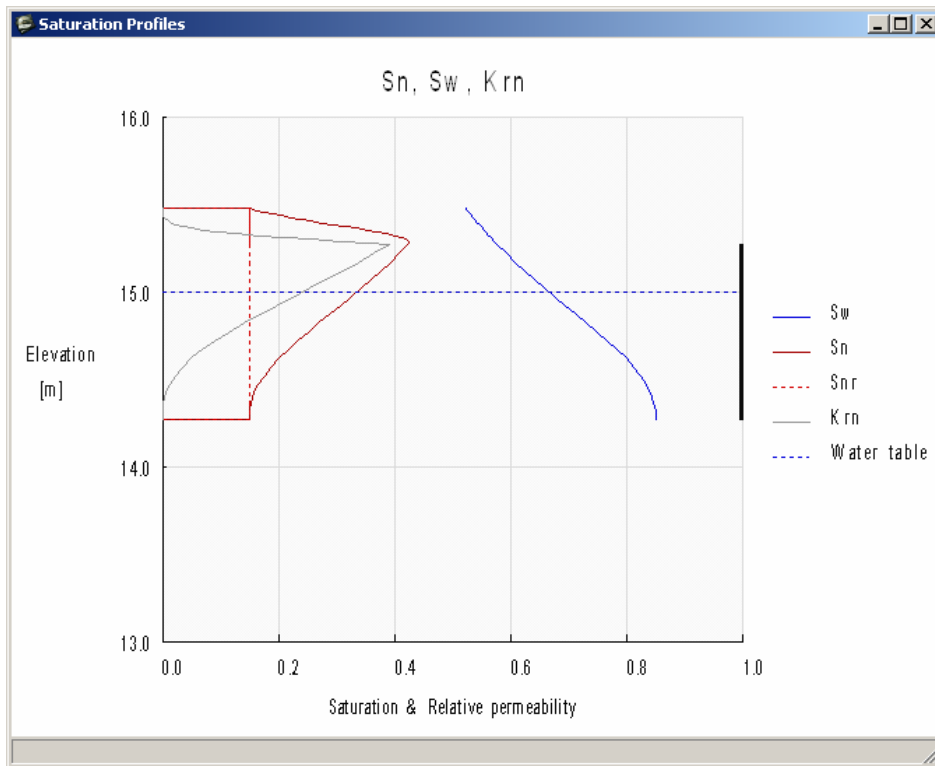


Figure 3.19—Saturation Profile for  $\alpha = 3.5 \times 10^{-2}$  1/cm and  $N = 2.25$ .

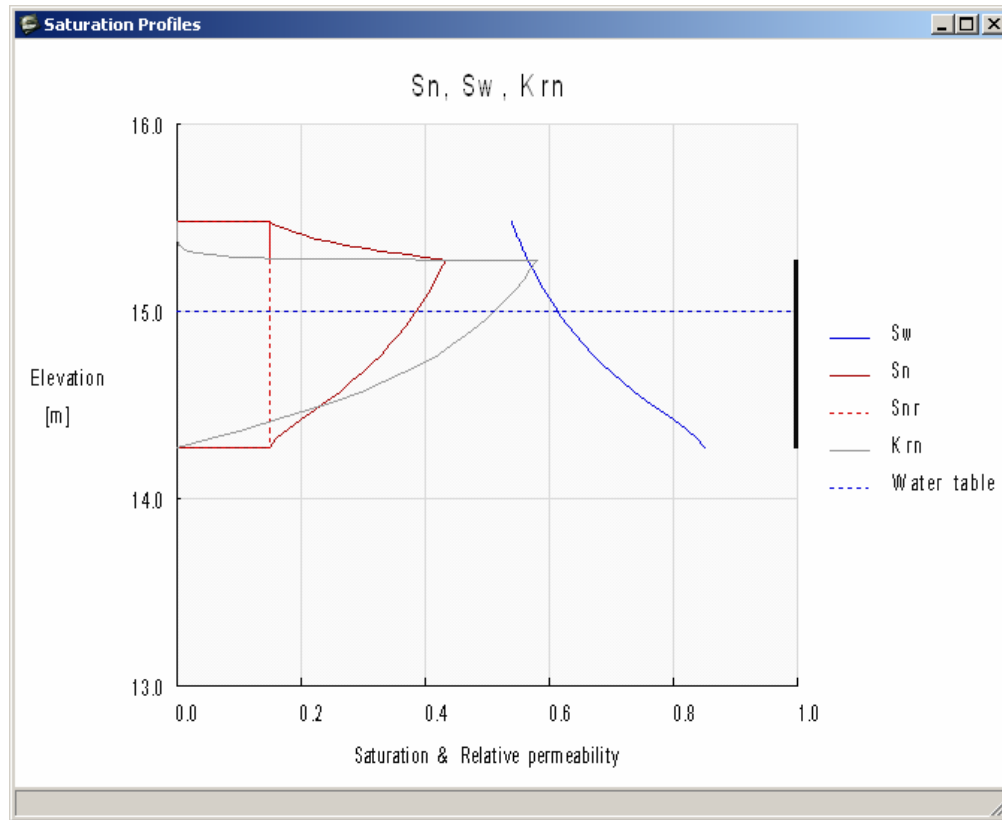


Figure 3.20—Saturation Profile for  $\alpha = 7.8 \times 10^{-2}$  1/cm and  $N = 1.50$ .

It is important to note that even though the saturation profiles are similar and have the same peak saturation, the LNAPL relative permeability profiles are markedly different. The peak relative permeability is almost 40% higher for the profile that uses the higher van Genuchten “ $\alpha$ ” and lower “ $N$ ” values. This is an important facet to consider because the LNAPL relative permeability exerts a strong control on the LNAPL transmissivity and resulting recovery, but is rarely measured. Where possible, hydrocarbon baildown tests or other data should be used to constrain the LNAPL transmissivity and indirectly the capillary properties.

The capillary properties are now further tuned based on initial recovery rates from short-term pilot tests of skimming and dual-phase recovery conducted at the site. This requires the user to also tune hydraulic conductivity at the same time. Before proceeding, it is important to note that when data are not available to constrain either hydraulic conductivity or the capillary properties independently, it is may not possible to obtain a reasonably unique parameter set, as both exert a strong control on the LNAPL transmissivity and resulting recovery.

The starting point is the range of capillary parameters from the previous bracketing work above and the full range of hydraulic conductivity values from the slug tests. The bracketed “ $\alpha$ ” and “ $N$ ” end member combinations are  $3.5 \times 10^{-2}$  1/cm, 2.25 and  $7.8 \times 10^{-2}$  1/cm, 1.50. Hydraulic conductivity ranges from approximately 1.5 to 13 m/day (note that the API LNAPL database gives the “ $\alpha$ ” units as 1/cm; these will need to be converted to 1/m to enter into the LDRM).

Start by attempting to eliminate parameter sets that produce recovery results that are too high. To do this, combine the end-member capillary data set that produced the large LNAPL relative

permeability with the low-end hydraulic conductivity ( $\alpha = 7.8$  1/m;  $N = 1.50$ ; and  $K = 1.5$  m/day). At this point, return to the data input screen and enter these parameters.

Next, run the skimming and dual-phase recovery calculations using the parameters set and compare the recovery estimates to the pilot test recovery rates. After clicking “OK”, go to the well recovery systems input and run the scenarios, starting with skimming. Only three parameters must be entered to run a skimming scenario (recovery time, well radius, and radius of recovery). Since only initial recovery rates are important in this step, enter any non-zero number for recovery time. The well radius is 0.06 m. The radius of recovery is not known. Use the low end of the recommended values in Section 1.2.1 of the user manual, i.e. 3 meters. All other parameters should be set to zero. Click “OK” and graph the LNAPL recovery rate. Note the initial recovery rate of approximately 1.45 l/day skimming. Now run the dual-phase recovery scenario. For dual-phase recovery, the saturated thickness, radius of influence, and pumping rate must also be input. The saturated well screens are 3 m long, so use this number for the saturated thickness parameter. Drawdown was not observed beyond approximately 30 m from the pumping well during pilot testing, so this value will be used for the radius of influence. The radius of recovery is not known, but must be less than the groundwater radius of influences, so 20 m is assumed. Lastly, the dual-phase pilot test was conducted with 1 gallon per minute (3.8 l/m) of groundwater production. Click “OK” and graph the LNAPL recovery rate. Note the initial recovery rate of approximately 1,100 l/day for dual-phase recovery.

After running the two scenarios above, it can be seen that the resulting initial recovery rates predicted by the model are greater than those observed in the field (1 l/day and 600 l/day for skimming and dual-phase recovery, respectively). At this point, one can conclude that the end-member capillary properties produce a LNAPL transmissivity that is too large, even with the lowest conductivity value.

The next step is to attempt to eliminate parameter sets that produce recovery results that are too low. To do this, combine the end member capillary data set that produced the small LNAPL relative permeability with the high-end hydraulic conductivity ( $\alpha = 3.5$  1/m;  $N = 2.25$ ; and  $K = 13$  m/day). At this point, return to the data input screen and enter these parameters and then re-run the skimming and dual-phase recovery scenarios. Doing this gives predicted initial recovery rates of 5.4 l/day and 480 l/day for skimming and dual-phase recovery, respectively. It can be seen that this parameter set results in a predicted skimmer rate that is greater than that observed in the field. Conversely, the predicted dual-phase recovery rate is less than that observed in the field.

At this point, the user might consider changing the hydraulic conductivity to see what affect this parameter has on the predicted recovery rates. Return to the data input screen and enter 2 m/day. After clicking “OK” and re-running the recovery scenarios, the predicted recovery rates are 0.83 l/day and 480 l/day for skimming and dual-phase recovery, respectively. It is important to note that the predicted recovery rate for dual-phase recovery did not change even though the hydraulic conductivity was reduced. At first this may not make intuitive sense. This occurs because the steady-state assumptions and mathematical development of this model dictate that for a given groundwater production rate, any change in conductivity results in offsetting changes in gradient and LNAPL transmissivity. The lesson here is that in order to tune dual-phase recovery

simulations, the user must be prepared to tune the model to groundwater drawdown and pumping rates.

The capillary parameters and hydraulic conductivity are not yet fully constrained. At this point, the model could be tuned by varying the capillary properties and conductivity. However, this may lead to multiple, non-unique solutions. As suggested above, one should first constrain the conductivity by looking at groundwater drawdown. During the dual-phase pilot test, it was noted that drawdown in the pumping well was approximately 1.8 m. It is known that the well efficiency is approximately 50% from a brief step test conducted as part of the overall pilot testing program. Given this, one would expect approximately 0.9 m of drawdown in the formation immediately adjacent to the well (i.e., at a radius of 0.06 m).

Next, the user should compare the predicted drawdown to the expected drawdown. This is accomplished by executing multiple dual-phase recovery scenarios using a range of conductivity values. After each run, the user can view the predicted drawdown by selecting the “Drawdown/Buildup” option from the graphing menu. In some cases, it may be difficult to estimate the exact drawdown from the graph, particularly as one gets closer to the target drawdown. In these instances, the model file can be saved after executing the recovery scenario and then opened using a text editor or other program to read the drawdown. After going through the above-described process, the model predicts 0.9 m of drawdown at a radius of 0.06 m when a conductivity of 2 m/day is input.

The model is now fine-tuned to hydraulic conductivity. The user should now re-visit the capillary properties and finish tuning them to the field recovery rates. This is accomplished by varying the capillary properties while holding the conductivity constant at 2.0 m/day. Again, the capillary properties used must be such that the paired “ $\alpha$ ” and “ $N$ ” generate the target peak saturations, as previously discussed. For this problem, some example pairs that satisfy this requirement are  $\alpha = 3.5$  1/m,  $N = 2.25$ ;  $\alpha = 4.0$  1/m,  $N = 2.0$ ;  $\alpha = 5.0$  1/m,  $N = 1.75$ ;  $\alpha = 6.0$  1/m,  $N = 1.6$ . After going through this process, the model predicts recovery rates for skimming and dual-phase recovery of 1.06 l/day and 610 l/day, respectively, when  $\alpha = 4.0$  1/m and  $N = 2.0$ .

At this point, the input parameters are constrained and the model is considered tuned to field data. For the purposes of concluding this example problem, assume that the model adequately represents field conditions. In reality, some level of uncertainty remains and it would be prudent to conduct a sensitivity analysis of those parameters that are least constrained. For example, changing the radius of capture from 3 m to 10 m changes the predicted initial recovery rate by approximately 20%. Also, the user may have noticed that the porosity and residual water content parameters have not been revisited. Porosity affects the total and recoverable specific LNAPL volumes but not LNAPL recoverability. Residual water saturation is inversely related to the LNAPL volumes and recoverability, but is less sensitive than the other parameters controlling these facets. These aspects will be left for the user to explore further.

### **3.6.3.3 Problem #3: Conclusion**

Now that the model is tuned to field conditions, the site owner’s questions can be answered. Again, the user is reminded that some level of uncertainty remains and it would be prudent to conduct a sensitivity analysis of those parameters that are least constrained. In the framework of

this problem, the parameters that control the LNAPL total and recoverable volumes might be looked at most closely since the remediation goal is defined by those volumes.

- How much LNAPL is present in the formation? Input the final parameter set in the data input screen and click OK. The LNAPL specific volume and recoverable volumes are displayed on the main screen. The specific volume is  $0.1312 \text{ m}^3/\text{m}^2$ . For the  $900 \text{ m}^2$  LNAPL body, this translates to approximately 118,080 liters of product.
- How much LNAPL is recoverable? The recoverable volume is  $.0606 \text{ m}^3/\text{m}^2$  or, approximately 46%. This translates to approximately 54,540 liters of recoverable product. Recalling that the regulatory mandate is to recover 90% of this volume, the target is 49,086 liters.
- What is the most cost effective method for LNAPL recovery and how long will it take? To answer this question, one must first determine the number of wells required and how long it will take to recover 90% of the recoverable LNAPL in the core area of the plume.

For dual-phase recovery, this question is relatively simple. The radius of recovery is 20 m, which corresponds to an area of  $1,250 \text{ m}^2$ . This area of recovery is greater than the release area of  $900 \text{ m}^2$ , which roughly takes the shape of a 30 m by 30 m square. Therefore, only one dual-phase well would be required. To determine the time required to recover 90% of the LNAPL, run the dual-phase scenario and save the model file. Open the model's file in a text editor and find the time needed to recover 49,086 liters. In this case, the time is approximately 4.4 months. Assuming a system installation cost of \$75,000, a total operation and maintenance cost of \$25,000, and \$20,000 in discharge fees, the total estimated cost for dual-phase recovery is \$120,000. In practice, a single well may not suffice. Field experience strongly suggests that the LDRM may over-predict LNAPL recovery from the distal portions of the recovery radius. Simply stated, the model assumes that all recoverable LNAPL is removed and that this recovery occurs uniformly across the recovery domain. In practice, the LNAPL saturation is typically observed to decline more quickly near the recovery well. This results in a reduction in the LNAPL relative permeability near the well, ultimately limiting the potential for recovery from more distal areas. As such, it might be practical to consider adding a second or third well. If this decision is made before the system is installed, the additional wells can be added for a small incremental cost.

For skimming, the radius of recovery is 3 m. To ensure that the entire core of the LNAPL body falls within the radius of recovery of a skimming well, there would need to be approximately seventy-seven wells and skimmers. To determine the time required to recover 90% of the LNAPL, run the skimmer scenario. The time required to recover 90% is approximately 21 years. Assuming a system installation cost of approximately \$100,000 and total operation and maintenance cost of \$100,000, the total estimated cost for skimming recovery is \$200,000. If the site owner can perform the operations and maintenance, the total cost might be reduced. Even if the cost for skimming was less than that for dual-phase recovery, there may be practical issues associated with the installation of seventy-seven wells in a 30 m x 30 m area. Furthermore, the operation and maintenance plan would need to address potential well interference issues.

Overall, dual-phase recovery appears to be more cost effective than skimming, primarily due to the larger number of skimmer wells required and the order-of-magnitude longer recovery period. If the site owner can perform the operations and maintenance of the skimmer system, the cost of the two alternatives might be similar. If that is the case, then time and the practical issues discussed above become important factors.

### **3.6.4 Problem #4: Case Study: LNAPL Recovery in Glacial Outwash Sands (Adapted from API Publication 4715)**

The fourth problem compares the LDRM to a real world dual-phase recovery project. For this example problem, the LDRM will be tuned using site-specific parameters and the recovery history from a dual-phase recovery well. This problem emphasizes the importance of comparing model results to field-based data and confirming that key model assumptions that form the basis for scenario-based models such as LDRM are not violated. This problem will show that violating two key model assumptions can lead to erroneous results if not realized and managed by the User during the modeling process. Similarly, when the limitations are recognized, the modeling effort can lead to additional insights and learning even when all the constraining assumptions are not met.

#### **3.6.4.1 Problem Overview**

A former refinery in the U.S. has been extensively studied because LNAPL has migrated over a significant area and potentially threatens a groundwater resource and an adjacent stream. Pumping large amounts of groundwater is required to achieve hydraulic control of the groundwater system to mitigate potential impacts at a stream. Soil saturation and petrophysical measurements, laser fluorescence, cone penetrometer, and hydraulic tests have been combined to produce a comprehensive data set. From these data, oil company scientists have estimated the original LNAPL volume to be approximately 36 million gallons in predominantly permeable outwash sand and gravel sediments. The high permeability outwash sands and gravels put this site in the upper percentiles of probable LNAPL recovery success.

Of the LNAPL in-place at the former refinery, about 4 million gallons have been recovered through aggressive groundwater and product pumping over 13 years. Approximately 90% of the LNAPL was recovered over the first 3.5 years of operation. The cost of the system installation and operation has been approximately \$8.5 million, for a current net cost of a slightly more than \$2 per gallon recovered. However, because product recovery has diminished through time, consistent with theory, the cost per gallon has increased from about \$1 over the initial recovery period to about \$50 currently. The future cost per gallon recovered is expected to increase as a greater percentage of costs are allocated to operation and water disposal per gallon of LNAPL recovered.

Despite the large volume of LNAPL recovered, the adjacent stream could still potentially be impacted by the LNAPL beneath the site during certain hydrologic events (e.g., a low water table stand). Consequently, containment and alternate recovery strategies are being considered since product recovery has not completely addressed the key impacts and potential risks of concern. Thus we are reminded that limits to LNAPL recovery can sometimes preclude risk mitigation goals even in permeable materials.

Early in the remediation history, between 1986 and 1989, three large-diameter, dual-phase LNAPL recovery wells operated and accounted for approximately 75% of the LNAPL recovered to date. Despite the addition of 10 recovery wells after the initial recovery period, LNAPL recovery rates were strongly diminished, particularly during average to wet years. However, during dry years, significant LNAPL recovery was still possible, with some years experiencing as much as 4% of the LNAPL recovered to date.

#### **3.6.4.2 Data Summary**

As mentioned above, the former refinery has been extensively studied. The soil and fluid properties that will be used in the calculations that follow are summarized in the following paragraphs.

The soils beneath the site consist of high permeability outwash sands, gravels, and cobbles that are most frequently described using the USCS as SP, SW, and GW materials. Numerous vadose and aquifer zone samples have been sieved to determine gradation. Overall, the percentage of fines is less than 10%, with most samples containing less than 5%. In sandy intervals, the gravel percentage is generally in the 20-40% range. Highly conductive gravel zones containing as much as 70% gravel and larger clasts are present starting at approximately 15 feet below the water table or about 50 feet below ground surface. These zones are generally 5 to 10 feet thick and are encountered below the LNAPL body. The significance of the above-described heterogeneity will bear itself out during model calibration.

Numerous aquifer tests have been conducted at the site. Based on these tests, the field-based transmissivity ranges from about 20,000 to 100,000 square feet per day (sq ft/day). Given an average aquifer thickness of approximately 50 feet, these results translate to an average hydraulic conductivity of 400 to 2,000 feet per day (ft/day). The prolific nature of the aquifer is further evidenced by the specific capacity of the recovery wells, which ranges up to 500 gallons per minute per foot drawdown (gpm/ft). As discussed above, the highly conductive gravel zones are located beneath the LNAPL body. The conductivity of the shallow portion of the aquifer where the LNAPL body is found has been estimated to be 300-600 ft/day based on tests conducted on partially penetrating wells. The hydraulic conductivity of the aquifer below the LNAPL body may be as high as 2,500 ft/day. The User should recall that a key model assumption for this initial problem setup is that the aquifer is homogeneous with regard to groundwater pumping. Where a layered system is selected, the layer-thickness weighted transmissivity controls the groundwater pumping, and is therefore weighted to the thickest layers of greatest conductivity. Therefore, the User should make a “mental note” regarding the above-described hydraulic conductivity contrast and be prepared to compare the model results with field data to determine if this condition significantly affects the calculations.

Soil samples have been collected for petrophysical and capillary properties. The porosity of fifty soil samples was measured and ranges from 22% to 42%, with an average and standard deviation of 33% and 5%, respectively. Capillary tests were performed on two soil samples. The predicted van Genuchten “ $\alpha$ ” parameters for the two samples are both rather large ( $6.95 \times 10^{-2}$  and  $7.50 \times 10^{-2}$  1/cm (2.1 to 2.3 1/ft)). The van Genuchten “N” parameters for the samples are nearly identical at 1.68 and 1.70. The predicted residual water saturation of the two samples is also very similar 13% and 14%.



The site fluids were analyzed to determine the physical properties of the LNAPL and water. The product density is 0.82 grams per cubic centimeter. The viscosity of the product is approximately 1.4 centipoise. Lastly, the interfacial tension pairs are as follows: Air/Water: 58 dynes/cm; LNAPL/Air: 25 dynes/cm; and LNAPL/Water: 13.6 dynes/cm.

Fluid levels at the former refinery have been gauged since 1985, with LNAPL recovery beginning in 1986. Prior to hydraulic recovery, the observed LNAPL well thickness near the recovery well ranged from 0.13 to 0.96-foot and averaged 0.60-foot. Water levels fluctuate seasonally as much as ten feet between spring and late fall. Since the early 1990s, a relatively consistent relationship has been noted between water levels and free product appearance in wells. In summary, there is a fairly well established water level altitude above which LNAPL does not appear in wells. When the water table declines below this elevation, free product accumulates in the monitoring wells in approximate proportion to the depth below the threshold elevation. Based on these fluid level observations and the extensive laser-induced fluorescence and soil coring work, the project team has concluded that a portion of the remaining LNAPL body is “stranded” beneath the water table threshold elevation at saturations below the two-phase residual saturation. When the water table falls below the threshold elevation, the LNAPL becomes mobile due to the much lower residual saturation under three-phase conditions.

Extensive efforts have been undertaken to estimate the distribution and volume of LNAPL in the subsurface beneath the former refinery. The morphology of the LNAPL body was first characterized using standard investigation techniques and this understanding has been more recently enhanced through the use of direct push laser-induced fluorescence techniques. The LNAPL saturation distribution and volume has been studied through standard characterization methods, LNAPL partitioning interwell tracer tests (PITT), and numerical multiphase modeling efforts. In total, there is an estimated 32 million gallons of LNAPL remaining beneath the approximately 175-acre plume footprint, corresponding to a specific volume of approximately 4.2 gallons per cubic foot ( $\text{gal}/\text{ft}^3$ ), or approximately  $0.56 \text{ ft}^3/\text{ft}^2$ . These estimates are based on conditions present in the middle to late 1990s and, therefore, reflect a partially recovered and smeared plume condition. The original volume would include the 4 million gallons recovered and the original specific volume estimate is increased to  $4.7 \text{ gal}/\text{ft}^3$  or, approximately  $0.63 \text{ ft}^3/\text{ft}^2$ . Peak LNAPL saturations have been estimated to be approximately 33%. Residual saturation under three-phase conditions (air/NAPL/water) is estimated to be 2-4%. Under two-phase conditions (NAPL/water), the residual saturation is much higher, approximately 20%.

The User should recall that the LDRM was not formulated to simulate field sites where water table fluctuations are significant, regardless of whether conditions of vertical equilibrium exist. The LDRM model-scenario formulation is based on an initial LNAPL distribution that is calculated from the LNAPL thickness specified in the Data Input window, along with the water table elevation and soil layer configuration. Even when the ‘smear correction’ option is selected, the total LNAPL specific volume is determined by the initial LNAPL thickness; it is assumed that there is no residual LNAPL initially present below or above the initial LNAPL layer. Therefore, the User should make a “mental note” regarding the preceding discussion of water table fluctuations and 2-phase to 3-phase transient drainage events. The User should be prepared to compare the model results with field data to determine if this condition significantly affects the calculations.

### **3.6.4.3 Model Conceptualization Summary**

Recalling the discussion in Section 3.4, the key facets of the model conceptualization are:

- Assess parameter availability,
- Bracket parameter ranges and inspect for parameter variability,
- Identify one or more “type” areas that are representative of the broader site,
- Inspect the LCSM for consistency with the LDRM constraining assumptions.

In essence, the first two items are already complete. By reviewing the data summary in Section 3.6.4.2, it is seen that all input parameters are available from site-specific measurements or modeling. The parameters are bracketed by multiple measurements and are mostly of low variability. A notable exception is hydraulic conductivity, which ranges from 400 to 2,000 ft/day. Drawdown data can be used to constrain the hydraulic conductivity in the area of pumping. The type area (the third item) is defined in the framing of this example problem. That is, the predicted recovery trend is being compared to that of one site recovery well.

The fourth item requires additional thought before proceeding. As discussed above, review of the supporting field data has revealed that two key model assumptions should be carefully considered. First, the soil descriptions and aquifer test results suggest a significant contrast in hydraulic conductivity between the smear zone and the underlying aquifer materials. Because the recovery wells at this site are fully penetrating, we should expect either the LNAPL recovery rates and/or the drawdown to be incorrect if a single value of hydraulic conductivity value is used in a single-layer simulation. The second key assumption concerns the significance of water table fluctuations. As discussed above, there is a seasonal water table fluctuation of up to ten feet at this facility. This fluctuation is by itself enough to suspect time periods with vertical disequilibrium, where hydrostatic conditions do not exist. However, vertical equilibrium conditions are expected to exist for most time periods, but the LDRM formulation is not able to account for residual LNAPL trapped beneath the fluctuating water table. The well-established relationship between product thickness and water table elevation has been observed since the early 1990s and the residual LNAPL saturation is known to be significantly different under 2-phase versus 3-phase conditions. To proceed, it must be assumed that vertical equilibrium conditions were approximated during the early recovery period (1986 – 1989). One must be vigilant during the model-tuning process to verify that this assumption makes sense; otherwise the results may be erroneous.

### **3.6.4.4 Example Problem #4 Execution**

To begin model execution, enter the parameters presented in Section 3.6.4.2, as shown in the following input screen.

**Data Input**

Thickness, Elevations, Vertical gradient

Maximum Monitoring Well LNAPL Thickness [ft] = 0.6

Ground Surface Elevation [ft] = 100

Water table Elevation [ft] = 65

Water Vertical gradient (+ for upward) = 0

Fluid Characteristics

LNAPL density [gm/cc] = 0.82

LNAPL viscosity [cp] = 1.4

Air/Water surface tension [dyne/cm] = 58

Air/LNAPL surface tension [dyne/cm] = 25

LNAPL/Water surface tension [dyne/cm] = 13.6

Soil Characteristics

Porosity = 0.33

Hydraulic Conductivity [ft/d] = 450

Van Genuchten "N" = 1.69

Van Genuchten "a" [ft-1] = 2.2

Irreducible water saturation = 0.13

Residual LNAPL saturation = 0.2

Residual LNAPL f-factor = None

Relative Permeability Model (Burdine is default)

Use Mualem Model for Layer  Layer 1

OK Cancel

Figure 3.21—Data Input Screen for Example Problem #4

The user should note that average porosity, van Genuchten “ $\alpha$ ”, hydraulic conductivity, and LNAPL well thickness were used. The porosity directly affects the LNAPL specific volume and less dramatically affects recovery rates, whereas “ $\alpha$ ” and hydraulic conductivity significantly affect the recovery rates. The LNAPL well thickness affects both volume and recovery.

After clicking “OK”, the LNAPL specific volume is displayed as  $0.0928 \text{ ft}^3/\text{ft}^2$ . Plot the saturation profile by selecting “Saturation Profiles” from the Graphs menu. The following screen should appear:

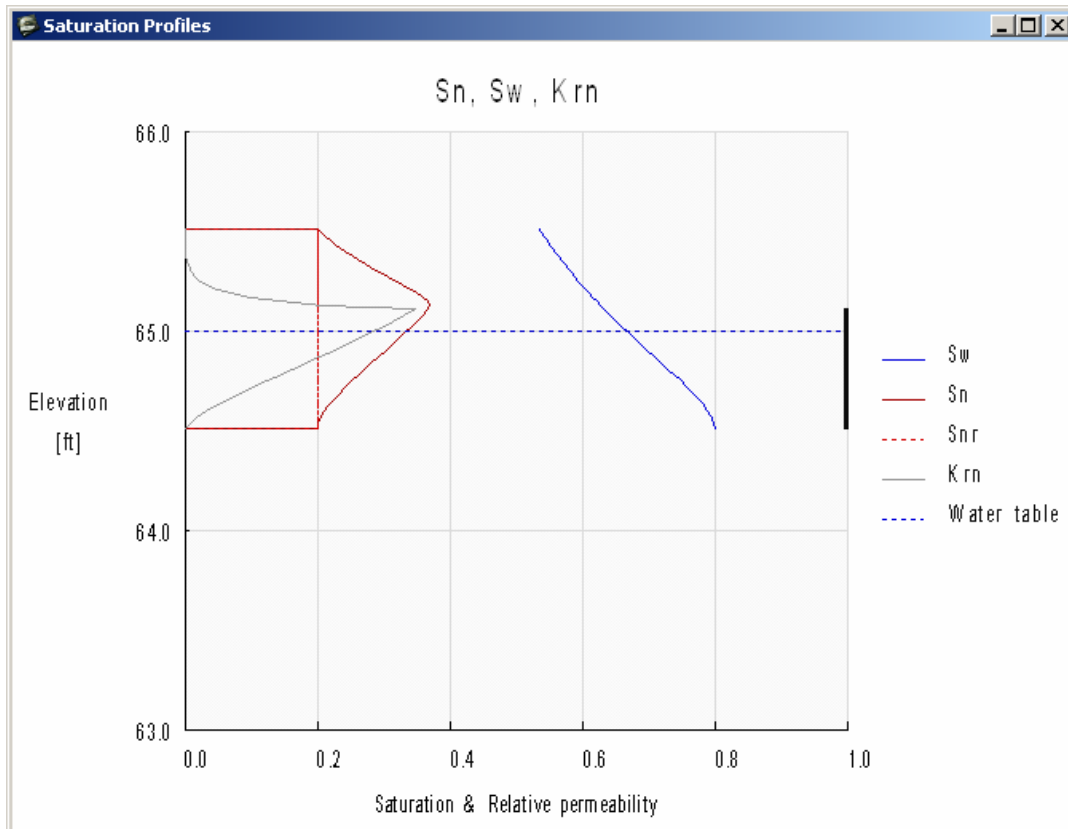


Figure 3.22—Saturation Profile for Example Problem #4 Input Data

At this point, the peak LNAPL saturations are approximately 35%, which is reasonably close the peak saturations observed in the field (~33%). However, the predicted specific volume is almost an order-of-magnitude lower than that estimated from field data and other modeling. This is the first clue that water table fluctuations and trapping of residual LNAPL beneath the water table play a significant role. In fact, the user must enter a well thickness of approximately 3 feet to approach the specific volume estimated from field data. However, when doing so, the peak saturations are over double those observed in the field. A similar conclusion can be reached if the user were to vary the capillary properties. Even increasing the porosity along with the well thickness and/or capillary properties does not help. In essence, this situation is irreconcilable. That is, the field-measured specific volume cannot be approached without changing the well thickness or capillary properties far beyond their expected range and without obtaining peak LNAPL saturations that greatly exceed field measurements. For now, assume that the field-measured specific volume is higher than that predicted by the model because of LNAPL smearing by the fluctuating water table. Move forward by assuming that the mobile fraction of LNAPL (that observed in the wells) was in vertical equilibrium during the recovery period and is adequately represented by the model.

Now compare the predicted drawdown to that observed in the field. At this point, proceed to the well recovery systems input screen and input the following parameters:

Well Recovery Systems

Recovery time [yr] = 5.000

Radius of Pumping Well [ft] = 0.750

Radius of Recovery [ft] = 700.000

Radius of Influence [ft] = 3000.000

Water Enhanced system

Water production rate [gpm] = 800.000

Water Saturated thickness [ft] = 50.000

Air Enhanced system

(-)Suction Pressure [atm] = 0.000

Screen Length [ft] = 0.000

Air Radius of Capture [ft] = 0.000

OK Cancel

Figure 3.23—Recovery Input Data for Example Problem #4

After clicking “OK” and plotting the Drawdown/Buildup, the user should see the following screen:

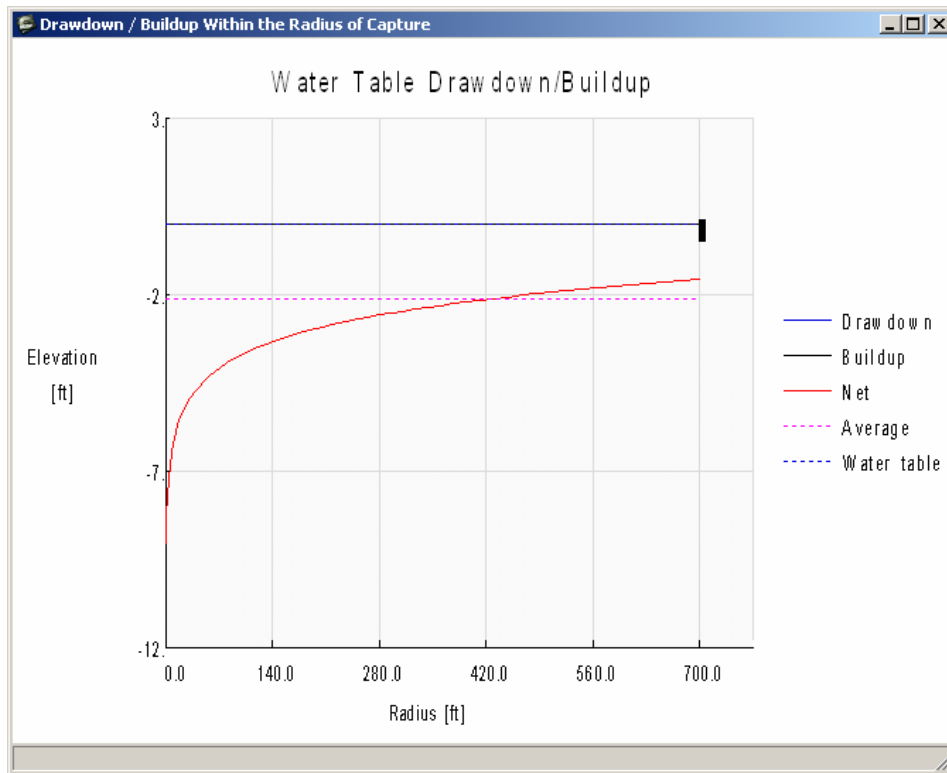


Figure 3.24—Drawdown/Buildup Screen for Example Problem #4

The predicted drawdown at the recovery well is approximately 9 feet. This well’s efficiency is known to be 80% and the field-measured drawdown in the pumping well at 800 gpm is 4.25 feet. Accounting for well inefficiency, the actual drawdown adjacent to the well is approximately 3.4 feet under field conditions. Therefore, the model is over-predicting drawdown by approximately 5.6 feet.

At this point, the User could try increasing the hydraulic conductivity until the model predicts the correct drawdown. Doing so reveals that the hydraulic conductivity must be increased to 1,200 ft/day. Although this value falls within the overall range of hydraulic conductivity measured at the facility, recall that the hydraulic conductivity of the upper portion of the aquifer, where the LNAPL is located, is only 300-600 ft/day. Accurate recovery results cannot be obtained using 1,200 ft/day because the model also uses this parameter to calculate the LNAPL transmissivity. Clearly, recovery will be over predicted by using a hydraulic conductivity that is larger than that of the materials through which the LNAPL is moving. At this point, the user should conclude that the heterogeneity of the aquifer must be accounted for if reasonable simulation results are to be made.

At this point, the user has two options. First, the hydraulic conductivity of the upper zone could be used along with a lower groundwater production rate that generates the correct drawdown. The other option would be to start over and build a two-layer model. For this example, the latter option will be used.

Start a new simulation, select two layers and input the parameters shown on the following screen:

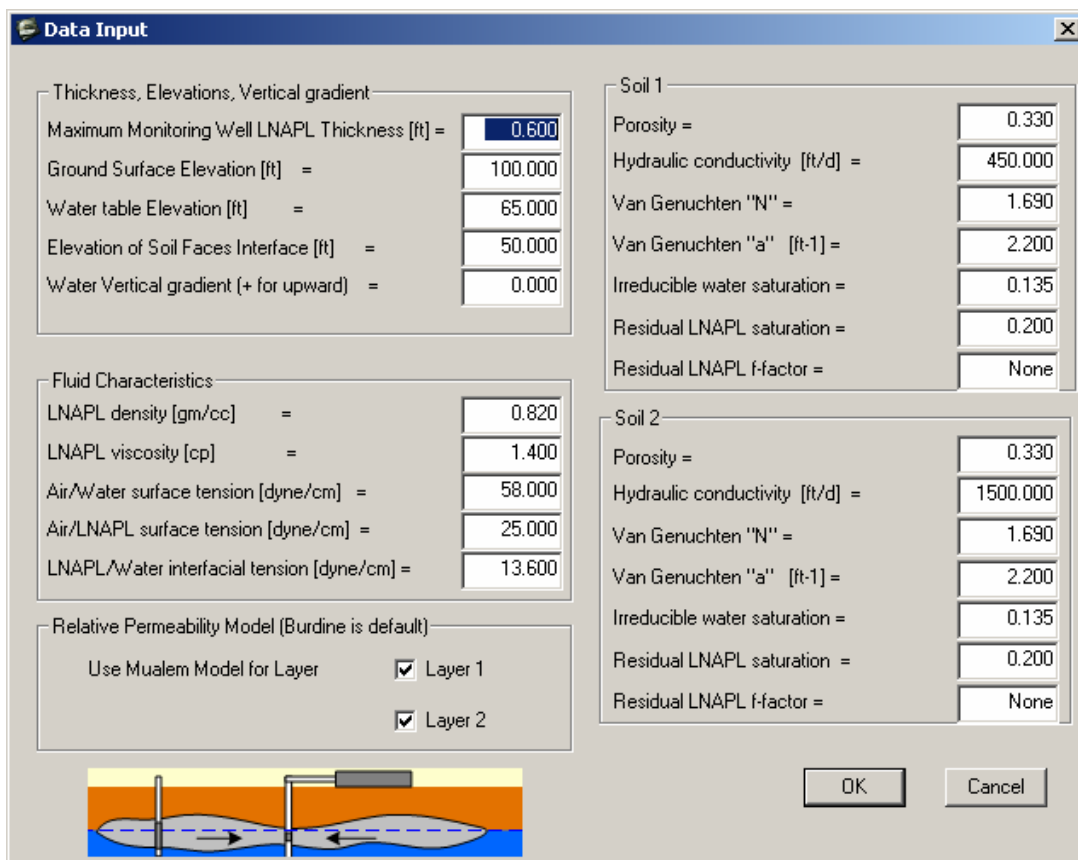


Figure 3.25—Data Input for Model with Two Layers

Click “OK” and re-run the dual-phase recovery scenario and plot the Drawdown/Buildup. The following screen should appear.

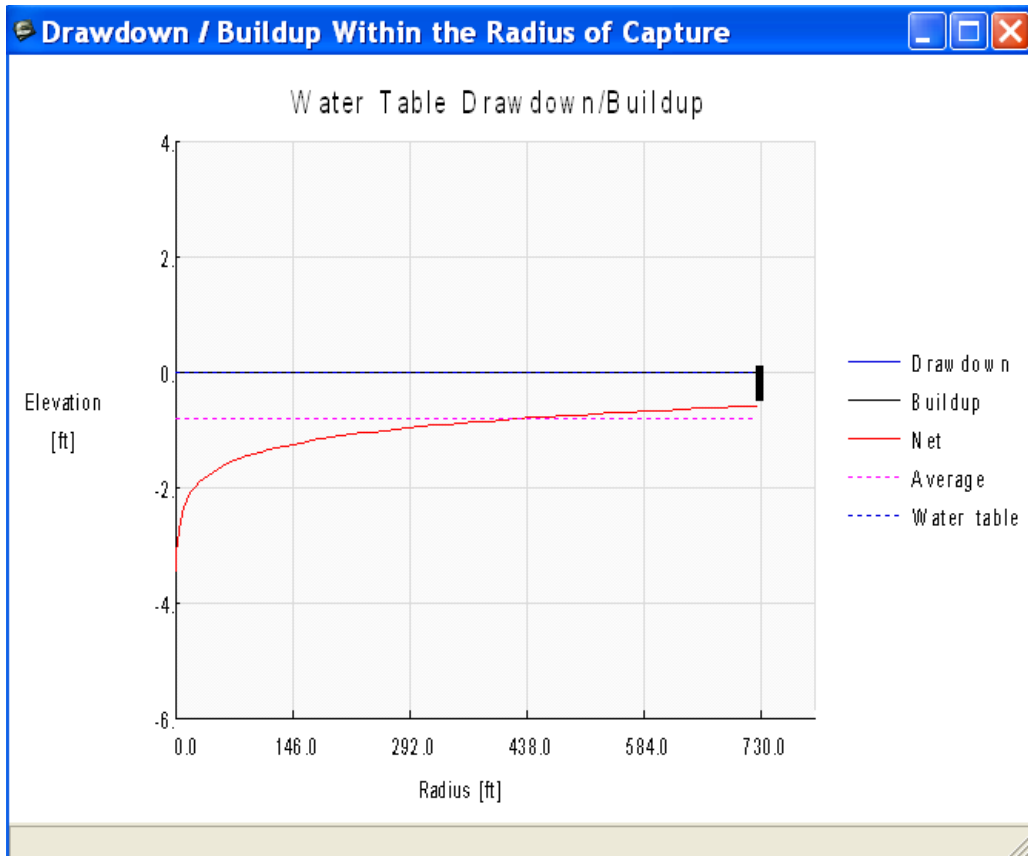


Figure 3.26—Drawdown/Buildup for 2-Layer Model

The drawdown at the recovery well is approximately 3.4 feet, which is the expected value. Note that the correct hydraulic conductivities were provided in an effort to save time. In reality, these values will need to be varied until a reasonable match to drawdown is achieved. The user should also recognize that this answer is non-unique. That is, other combinations of hydraulic conductivity values could have resulted in 3.4 feet of drawdown.

Now that the hydraulic conductivity has been tuned to field data, look at recovery rates and volumes over time. If it is available, import field recovery rates and volumes into the LDRM by following the procedures in Section 2.4.1 of this User’s Guide. For demonstration purposes, field data from this site have been added and appear in the following figures.

Next, adjust the breakpoints for the transmissivity curves and then re-run the recovery scenarios. The user might want to vary the radius of capture until it generates a total LNAPL volume that matches the asymptotic endpoint of the field recovery curve. For this problem, this condition is met with a radius of recovery of 1,350 feet. This is only one approach to estimating the radius of capture. A better method of setting the radius of capture would be to estimate it from measurements of LNAPL drawdown in the field, when available.

Using a radius of capture of 1350 feet, the model should generate the following recovery rates and volumes over time:

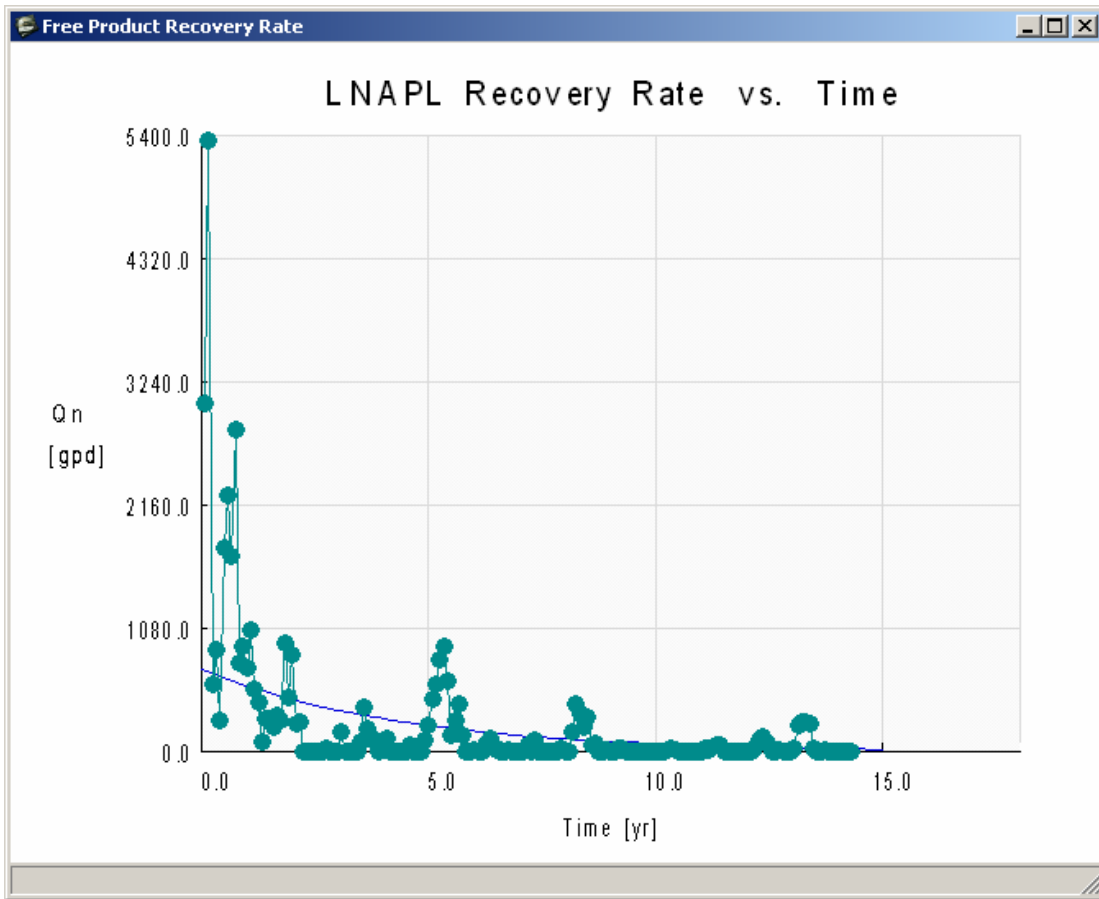


Figure 3.27—LNAPL Recovery Rate Versus Time



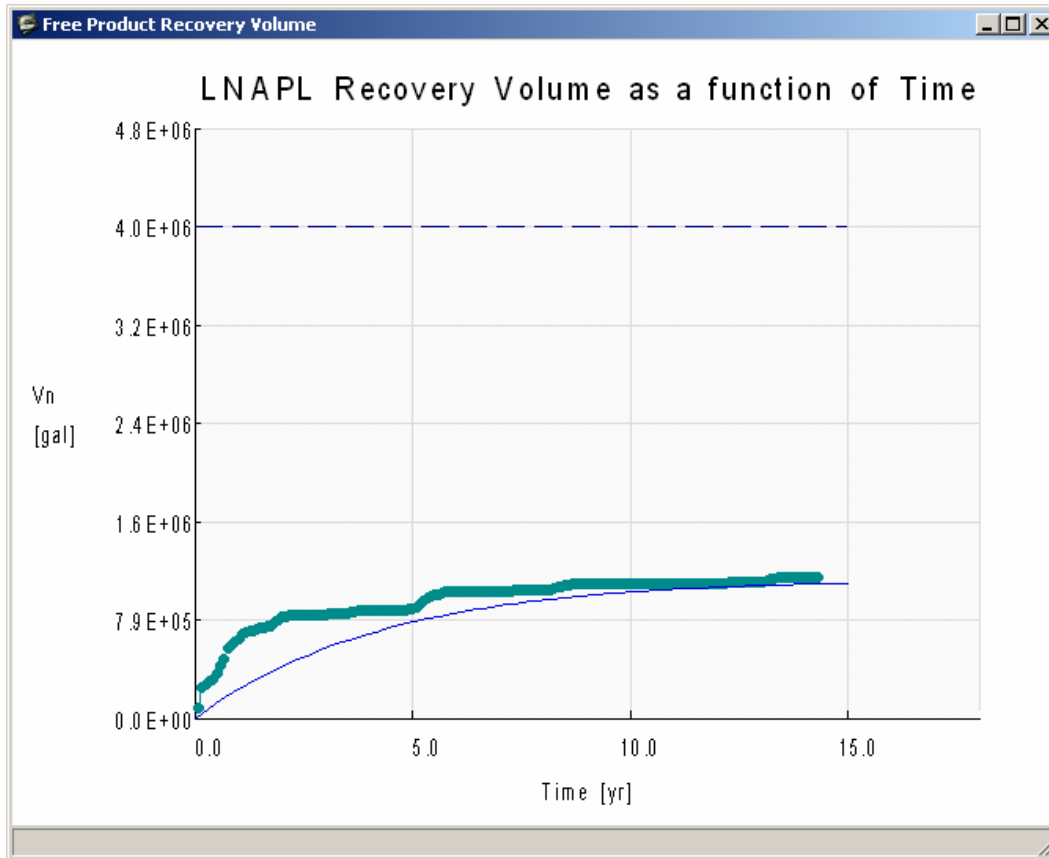


Figure 3.28—LNAPL Recovery Volume Versus Time

Inspection of plots reveals that the predicted recovery rates are lower than expected during the first two years and then are overestimated until approximately year 10. This results in a cumulative recovery curve which falls well below the field curve until approximately the 10<sup>th</sup> year.

At this point, the User could consider revisiting the input parameters in an effort to generate a better match with the field data. Attempting this would reveal that an unreasonably large van Genuchten “ $\alpha$ ”, hydraulic conductivity, and/or LNAPL well thickness values for layer one would be needed to match the recovery trends. Similarly, the user might increase the radius of capture to increase the recovery rate, only to find out that the model then over predicts the recovery volume.

Clearly something is wrong. At this juncture, the User might recall that the model greatly under predicted the LNAPL specific volume. Revisit the model conceptualization and consider the implications of the water table fluctuations. The user should be wondering what condition could explain why the model under predicted both the specific volume and recovery rates. Upon careful consideration, one conclusion may be that the LNAPL that is “missing” from the calculated specific volume might be oil (or LNAPL) that is actually present, but immobile under two-phase conditions below the water table. This condition is suggested by the fluid level observations discussed in Section 3.6.4.2. This oil, although present and contributing to the measured specific LNAPL volume, did not appear in monitoring wells and, therefore, the model’s specific volume estimates. However, upon lowering of the water table by pumping, a

fraction of this oil likely drained under three-phase conditions (due to the lower three-phase residual LNAPL saturation), thereby increasing the recovery rates. This hypothesis is supported by the LNAPL recovery “spikes” in the field data, which occurred when the water table was much lower than normal due to very dry conditions (see recovery volume plot above). In summary, the user should conclude that the water table fluctuations and trapping of residual LNAPL beneath the water table play a significant role, and the LDRM should not be expected to provide reliable results for this facility.

#### **3.6.4.5 Example Problem #4 Conclusions**

Example problem #4 exemplified the importance of comparing model results to field-based data and confirming that key model assumptions are not violated. The problem execution process showed that violation of two key model assumptions in later time periods significantly affected the model results. The first violated assumption was homogeneity, which was violated by the hydraulic conductivity contrast between the smear zone and the more permeable aquifer materials beneath. This condition was managed by developing a two-layer model to account for the hydraulic conductivity contrast. The second violated assumption was the significance of residual LNAPL trapping beneath the fluctuating water table, particularly as it influences recovery at later time frames in the data sequence. The User was left with a seemingly irreconcilable situation where the field-measured specific volume cannot be approached without changing the well thickness or capillary properties far beyond their expected range and without obtaining peak LNAPL saturations that greatly exceed field measurements. The explanation for this condition is stranded LNAPL under 2-phase conditions that becomes mobile under 3-phase conditions when the water table drops during dry years. The User is left to explore methods for producing a closer fit to the field data. Some possible methods might include piecewise fitting of the recovery data over time or developing a method to accurately represent the correct LNAPL specific volume while also maintaining representative LNAPL transmissivity values over time. Due to the transient nature of this problem, the user might also consider using numerical modeling methods to predict LNAPL recovery at this facility

As mentioned above, the main point of this example problem is the importance of comparing model results to field-based data and confirming that key model assumptions are not violated. Failure to do so can lead to erroneous forward predictions of LNAPL recovery. It is expected that most Users will utilize the LDRM model to make forward predictions of LNAPL recovery as part of a final remedy evaluation. These evaluations may be based on calibration to pilot test or interim recovery data. Again, care must be taken to compare the model results to field-based data and confirm that the key model assumptions are not violated. In this example, if all that we had were “interim” recovery data from the early period between 1986 and 1989 and we forced the model to match these data, the result would be over-prediction of the subsequent recovery rates and volume. The outcomes of overpredicting recovery rates are the unnecessary cost associated with remediation system over-design and the consequences of setting unattainable LNAPL recovery goals with the regulatory agency and stakeholders.

## 4 REFERENCES

American Geological Institute, 1984. *Dictionary of Geological Terms*, 3rd Edition, 1984.

American Petroleum Institute, 2003. Light Non-Aqueous Phase Liquid (LNAPL) Parameters Database (updated 2006), Available at: <http://www.api.org/ehs/groundwater/lnapl/index.cfm>.

Carsel, R.F. and Parish, R.S., 1988. "Developing joint probability distributions of soil water retention characteristics." *Water Resources Research*, 24(5), pp. 755- 769.

Chatzis, I., Kuntamukkala, M.S., Morrow, N.R., 1988. "Effect of capillary number on the microstructure of residual oil in strongly water-wet sandstones," *SPE Reservoir Engineering*. August, 1988, pp. 902-912

Melrose, J.C, and Brandner, C.F., 1974. "Role of capillary forces in determination of microscopic displacement efficiency for oil recovery by water flooding." *Journal of Canadian Petroleum Technology*, Vol. 13, No. 4, pp. 54-62.

Mualem, Y., 1976a. A catalogue of the hydraulic properties of unsaturated soils. Development of methods, tools, and solutions for unsaturated flow with applications to watershed hydrology and other fields. Israel Institute of Technology.

Mualem, Y., 1976b. "A new model for predicting the hydraulic conductivity of unsaturated porous media." *Water Resources Research*, Vol. 12, pp. 513-522.

M.G. Schaap, U.S. Salinity Lab, 1999. Rosetta Model. Available at: <http://www.ars.usda.gov/Services/docs.htm?docid=8953#references>

Tyler, N., and Finley, R.J., 1991. "Architectural controls on the recovery of hydrocarbons from sandstone reservoirs: In Miall, A.D., and Tyler, N. (eds.), *The three-dimensional facies architecture of terrigenous clastic sediments and its implications for hydrocarbon discovery and recovery: Society of Economic Paleontologists and Mineralogists*," Tulsa, Oklahoma, *Concepts in Sedimentology and Paleontology*, Vol. 3, pp.1-5.



**APPENDIX A**

**REVIEW OF THE LNAPL DISTRIBUTION & RECOVERY MODEL  
MATHEMATICAL VERIFICATION, CODE FIXES, & SENSITIVITY**

Prepared by:  
AQUI-VER, INC.  
Hydrogeology, Water Resources & Data Services

November 2006

## TABLE OF CONTENTS

<b>1.0 INTRODUCTION</b> .....	1
1.1 SCOPE AND OBJECTIVE .....	1
1.2 GENERAL METHODOLOGY .....	1
1.3 LIMITATIONS .....	3
1.4 MEMO STRUCTURE AND CONTENT .....	3
<b>2.0 GENERAL PROGRAM FUNCTIONALITY</b> .....	3
2.1 CODE IRREGULARITIES .....	3
2.2 CODE FUNCTIONALITY .....	4
2.3 INPUT/OUTPUT COMMENTS .....	5
<b>3.0 VERIFICATION OF MATHEMATICAL FUNCTIONS</b> .....	6
3.1 ESTIMATION OF SATURATION PROFILES .....	7
3.2 ESTIMATION OF RELATIVE PERMEABILITY FUNCTIONS .....	7
3.2.1 Mualem-Van Genuchten Relative Permeability Model .....	7
3.2.2 Burdine-Van Genuchten Relative Permeability Model .....	7
3.3 DRAWDOWN AND LNAPL RECOVERY RATE .....	8
3.4 CONCEPTUAL MODEL VERIFICATION .....	8
3.5 COMPARISON TO NUMERICAL SIMULATIONS .....	9
<b>4.0 PARAMETER SENSITIVITY</b> .....	9
4.1 LNAPL DISTRIBUTION INPUT PARAMETERS .....	10
4.1.2 LNAPL Density .....	11
4.1.3 LNAPL/Water Interfacial Tension .....	11
4.1.4 LNAPL/Air Interfacial Tension .....	12
4.1.5 Monitoring Well LNAPL Thickness .....	12
4.1.6 Ground Surface Elevation .....	12
4.1.7 Vertical Groundwater Gradient .....	12
4.2 RECOVERY MODEL INPUT PARAMETERS .....	12
4.2.1 Soil Properties .....	13
4.2.1.1 Hydraulic Conductivity .....	13
4.2.1.2 Residual LNAPL Saturations and "F-factors" .....	14
4.2.2 LNAPL Viscosity .....	14
4.2.3 Recovery Time .....	15
4.2.4 Water Production Rate .....	15
4.2.5 Well Properties .....	15
4.2.5.1 Radius of the Pumping Well .....	16
4.2.5.2 Radius of Capture .....	16
4.2.5.3 Radius of Influence .....	16
4.2.5.4 Groundwater Thickness .....	16
4.2.5.5 Air-Phase Vacuum .....	17
4.2.5.6 Screen Length for Air Flow and Radius of Capture for Air Flow .....	17
4.2.6 Trench Properties .....	17
4.2.6.1 Natural Hydraulic Gradient .....	18
4.2.6.2 Trench Length .....	18
4.2.6.3 LNAPL Lens Width .....	18
4.2.6.4 Screen Depth .....	18
4.2.7 Smear Correction .....	18
4.2.8 Relative Permeability Models .....	19
<b>5.0 SUMMARY AND CONCLUSIONS</b> .....	19

## 1.0 INTRODUCTION

Based on the work-plan dated November 1, 2004, and the subsequent contract issued December 9, 2004, AQUI-Ver, inc. (AVI) has prepared this memorandum to summarize the technical findings of the LNAPL Distribution and Recovery Model (LDRM) verification. The beta Version 2 of LDRM was verified through this work (April 2005), and the current release (Version 3.7) reflects fixes and updates based on this work, and comments to the API by others. The fundamental numerical calculations have not changed significantly, and the numerical verifications presented subsequently herein are expected to hold for the most recent LDRM version.

The problem solving and parameter selection guide, which is also part of the December 9, 2004 contract, has been provided as a separate document. Key output and summary findings are provided in the body of this report, with additional information provided in the appendices.

### 1.1 SCOPE AND OBJECTIVE

The objective of this memo is to summarize the LDRM validation process used to document any errors, anomalies, or variability within the program. Additionally, the functionality of the program was evaluated. The validation process described in this memorandum isolates each component of the combined calculation (to the degree possible) and compares the intermediate calculations against independent calculations and/or other analytic models with the same boundary conditions. Additionally, a series of LDRM simulations were evaluated to demonstrate the sensitivity of each key input parameter in the calculations and results for a set of generic simulations.

### 1.2 GENERAL METHODOLOGY

The LNAPL distribution and recovery model has been prepared for the API by Dr. Randall Charbeneau of the University of Texas at Austin. In accordance with the API's request, the following evaluations have been performed by AVI:

1. The underlying mathematical framework was verified under a range of input conditions to test important code algorithms against relevant benchmarks.
2. The LDRM was tested to verify that the software represents the conceptual model.
3. The code's operational features were tested to verify that input, output, and calculation options work as intended
4. The LDRM's parameter sensitivity was documented so that users may better understand which parameters are critical to the LDRM results and how combinations of parameters can affect outcomes.

### 1.3 LIMITATIONS

Every effort was made to test and compare each feature and combination of options to ensure that the program functions as intended. Each component of the LDRM has been explored and tested independently. However, it was not possible nor practical to compare every possible combination of options, components, and input parameters without reconstructing the full LDRM code.

Since the initial testing of the LDRM code (beta Verison 2), the code has been updated to the current distribution Version 3.7. It is AVI's understanding that the current code is mathematically similar and uses many of the same algorithms. As such, it is expected that the numerical verification portions of this work hold for the current version. However, the newer LDRM versions have not been explicitly tested.

### 1.4 MEMO STRUCTURE AND CONTENT

This memo is organized into three sections. First, the program functionality is described. Next, the individual components of the LDRM that have been compared to independent calculations are detailed (saturation profiles, relative permeability, etc.). Finally, the results of the sensitivity analysis are presented.

## 2.0 GENERAL PROGRAM FUNCTIONALITY

Overall, the program is fairly easy for a typical user to navigate and understand. However, a number of anomalies were noted throughout the testing process. These anomalies are discussed in detail in the following sections. These sections also contain suggestions and clarifications that could improve the usability of the program. It should be noted that these comments pertain to LDRM beta Version 2. As noted previously, most of the issues below have been addressed and incorporated into the current distribution version of LDRM (Version 3.7).

### 2.1 CODE IRREGULARITIES

During the testing process, ten coding irregularities were noted. A brief description of each item is provided below.

1. When residual saturations are manually entered, values are re-computed without notifying the user (the user must re-open the data input screen to determine if residual saturation values are different than the ones entered). During the testing of this method, attempts were made to force the residual saturation values into the LDRM; these attempts were unsuccessful. Modifying the "F-factor" under the "Help" pull-down menu is the only way that was found to alter the residual saturation values.
2. The graphs (for example, "total volume recovered") only use six digits on the Y- scale labels; therefore 1,800,000 appears as 800,000 on the display. In other instances, large numbers print as "\*\*\*\*\*", and the Y-axis text is not always legible.
3. Each time the user makes parameter changes and re-prints the graphs, six additional windows are displayed and the original graph windows do not automatically close. Once



new graph windows are opened, the older windows are empty and cannot be closed manually.

4. The  $S_n$ ,  $S_w$ , and  $K_m$  graph is color-coded incorrectly.  $S_n$  and  $S_{nr}$  are red in the legend and brown on the graph, and it may be difficult to differentiate the output.
5. When the program is closed by the "X" in the upper right hand corner (or alt+F4), the program is still listed in the "Running Programs" section of the Windows Task Manager. Every time the program is open and closed in this manner, another copy is entered into the Task Manager. Eventually, this affects Windows memory and the computer must be re-booted (or the user can open the Task Manager and terminate each copy manually).
6. When entering field data, the instructions read, "open the spreadsheet file (\*.csv) and ...". The associated file is named "field\_data.csv". Providing the current path to the file and additional instructions on the same screen would be helpful.
7. The text in the main window becomes illegible if the window is re-sized. This problem is more prominent in Windows 98 than in Windows XP, although it occurs in both operating systems. Scroll bars and fixed text-size would be one method to correct this problem.
8. The "Tab" order on the Data Input Screen is not sequential. For example, the conductivity value is skipped while tabbing through inputs. It would be helpful if the user could tab through the input screen in a logical and sequential manor.
9. Many of the inputs lack error trapping. For example, porosity and residual saturations values can be entered as 35 or 0.35. When values greater then 1 are entered (i.e., 35) the program calculates erroneous values. Error trapping the inputs with easy to understand error messages may help users successfully navigate the program.
10. On a similar note to #9, positive vacuum on recovery wells are ignored. No warnings are provided to indicate that the user has made an error.

## 2.2 CODE FUNCTIONALITY

As previously noted, the program is fairly easy to navigate and understand. However, a few components of the program do not behave as a typical Windows user might expect. These items are listed below, and again, have predominantly been addressed in the current release version of the LDRM (Version 3.7).

1. It is not immediately clear to the user that the LDRM works in two distinct, sequential steps: 1) LNAPL distribution and 2) LNAPL recovery. This may be confusing to some users.
2. Upon startup, most programs open to a "start screen" where the user can either open an existing file or begin a new file. When the LDRM program opens, the user is not presented with a start screen. As a result, there is no clear starting point for calculations. Including basic directions or a "file new" or "file open" option on the initial screen may help the first-time user to begin.

3. The first three options under the "Help" menu ("LNAPL residual F-factor," "LNAPL residual sat model," and "break points") are not really "Help" functions. The current location for these items is confusing and they could be moved to a separate pull-down menu. They might fit better under menus such as "Options," "Features," or "Program Settings."
4. The graphing component of the program is an excellent method for the user to quickly view the results of the calculations. However, when the user selects "graphs," all graphs (up to six) are simultaneously displayed on the screen. This large amount of information is often unnecessary and potentially confusing. Allowing the user to choose which graph(s) to display could simplify the process. Similarly, a option to display tabular output may also be useful to some users.
5. Some of the pull-down menus do not function as a typical user would expect. The pull-down menu for "well," "trench," "graphs," and "exit" do not display menu options. When these menus are selected, the application is instantly launched, which may be confusing to some users. As an alternative, the "well" and "trench" menus could be replaced with a "recovery options" menu that contains "well" and "trench" options. The "graphs" menu could be modified to provide a list of the available graphs, as well as allow the user to select a single graph, multiple graphs, or all graphs. The "exit" menu can be removed, as the exit feature is already available under the file menu (the location where most Windows users will first look).

### 2.3 INPUT/OUTPUT COMMENTS

Parameters are directly entered into the LDRM through input screens. These screens are fairly easy to understand and use, with a few exceptions noted below.

1. The capillary soil properties (van Genuchten parameters) will have different values for the same soil, depending on which relative permeability model is selected for the soil layer. The input screen does not make any distinction between the Van Genuchten parameters (used with the Mualem relative permeability) and the Burdine-Van Genuchten equation (used with the Burdine-Van Genuchten relative permeability model). The multiphase soil properties "n," "m," and "S<sub>rw</sub>" are dependent upon the relative permeability model selected and would be better noted as different variables in the LDRM input and output.
2. The process of entering field data may be confusing to some users. When the user begins the process of entering field data, the program produces a file called "field\_data.csv" in the same directory in which the LDRM model .exe file is stored. The user is required to open the .csv file, enter the data, and save the file while the LDRM is open. The user cannot close or minimize the program while opening the .csv file. This potential point of confusion could be eliminated if the program were to open the .csv file automatically.
3. Currently, the help screens are not available without first closing the data input screen. Including links to the help options from the input menus might be useful for many of the users. These links could allow a user to look up typical values for a given parameter by accessing the help screens from within the input screens.

4. The help screens, intended to aid users in selecting input parameters, do not reflect the most recent values for the van Genuchten soil properties for in-situ environmental applications. Updating the references within the help screens (perhaps by recommending the same default values as the API-LNAPL guide) may help users better select input parameters.
5. The water production rate used to increase the gradient in the vicinity of a well or trench is a user-input parameter. This allows for input of unrealistic water recovery rates. It would be helpful if the LDRM had an option to automatically calculate the water production rate that will produce the optimal drawdown.

The output features within the program are somewhat limited. For example, the program lacks a print feature, and graphs cannot be copied to the clipboard. The user has two output options: using screen capture or copying and interpreting the tabular results from the .txt file. If the graphs will be used or manipulated to produce report-quality graphics, the best option is to extract the output from the .txt file and paste it into a spreadsheet to process the data. However, the current file structure contains formatting inconsistencies that make it more difficult to import and plot the file in another program. It would be helpful if the file were formatted in such a way that the results can easily imported be into a spreadsheet. Recommendations for improving the formatting are listed below.

1. Two possible ways to improve the process of exporting files to another program would be to: 1) store the input parameters in a constant column (for example, column 20) within the data file; or 2) add an export feature to the program that would produce a delimited file of the tabular data (e.g. tab or comma delimited).
2. The table headings in the text file would be easier to understand if a consistent format were used. The best method available (with the current LDRM files) is to import the output tables by using a space delimiter (tab, comma, and other common delimiters are not able to separate the columns). The header rows for these tables should be formatted consistently such that the variable name, units, and data fall within the same column as the appropriate header. The current structure uses two formats and the data is often not in the same column as the header.
3. The text file uses standard numbers with three digits of precision (0.000). If the text file saved numbers in scientific notation, rounding errors could be minimized.

### **3.0 VERIFICATION OF MATHEMATICAL FUNCTIONS**

Where possible, the individual mathematical functions were tested against analytic benchmarks to compare for consistency. The results of these comparisons are discussed below and presented in Appendix A. As mentioned previously, the mathematical aspects of the LDRM beta Version 2 are generally the same as the current release Version 3.7, except as noted in the program documentation. As such, the numerical verification results should hold, in general, for the current release version except in limited areas where the program has changed from beta Version 2.

### 3.1 ESTIMATION OF SATURATION PROFILES

The basic equations used in the LDRM code to compute the saturation profiles appear to be consistent with published equations. The equations used within the LDRM code were isolated and compared to published equations from Farr et al. (1990). The equations used to compute the LNAPL saturation profiles are consistent with the equations from published sources. The complete results are shown in Appendix A. Additionally, the results of the isolated equations were compared to output from the LDRM. For the special case of 0 residual saturation values, with no advanced options or features selected, the LDRM code output agrees with the associated published equations from peer-reviewed literature.

The isolated equations were tested for the simple case of 1 layer. Multi-layer models are based on the same equations verified above with different inputs for the individual layers. The LDRM was also tested to confirm that the proper inputs were used for the different layers in the multi-layer analysis. The feature also appears to function correctly.

### 3.2 ESTIMATION OF RELATIVE PERMEABILITY FUNCTIONS

Relative permeability is a function of the LNAPL saturation. To verify the accuracy of the LDRM, the equations used to compute the relative permeability within the LDRM were compared to published equations. The relative permeability is computed within the LDRM using either the Burdine equation (the default) or the Mualem equation. The results of both equations are discussed below and presented Appendix A. To further complicate the comparisons, when the Burdine model is selected, the van Genuchten soil properties must be calculated differently than when the Mualem model is selected. The results presented in Appendix A do not fully account for this complication. Instead of recalculating the van Genuchten parameters, a value of 1 was added to the van Genuchten "n" term to ensure that the criteria for the Burdine model would be satisfied for the purposes of this mathematical verification.

#### 3.2.1 Mualem-Van Genuchten Relative Permeability Model

When the Mualem relative permeability option is selected, the LDRM uses the equations shown in Appendix A to calculate the relative permeability to LNAPL. As shown in Appendix A, the equations produce an equivalent output to the Mualem equation published in van Genuchten 1980, once it has been transformed to account for the presence of LNAPL. The results of the comparisons, shown in Appendix A, demonstrate that both the LDRM and published equations produce the same output. The Mualem model appears to function correctly within the LDRM.

#### 3.2.2 Burdine-Van Genuchten Relative Permeability Model

When the Burdine relative permeability option is selected, the LDRM uses the equations shown in Appendix A to calculate the relative permeability to LNAPL. Note that the subscript "b" has been added to all the variables related to the Burdine model, including the water and LNAPL saturation equations in Appendix A. The "b" denotes that the equations are specific to the Burdine model, which uses alternate van Genuchten parameters to estimate fluid saturations and relative permeability. The equations shown in Appendix A produce equivalent output to the Burdine equation published in van Genuchten 1980, once it has been transformed to account for the presence of LNAPL.

### 3.3 DRAWDOWN AND LNAPL RECOVERY RATE

The LDRM predicted drawdown due to water production (dual phase extraction) as well as the LNAPL production rate were compared to the Theim Equation (1906), shown below.

$$Q = 2 * \pi * T * \frac{dH}{\ln\left(\frac{r_i}{r_w}\right)}$$

Where:  $Q$  is the production rate;  $T$  is transmissivity;  $dH$  is the change in head (drawdown);  $r_i$  is the radius of the influence; and  $r_w$  is the effective radius of the well.

To test the accuracy of the drawdown estimate, the Theim Equation was solved for  $dH$  (drawdown) and the water transmissivity, production rate, radius of influence, and radius of the well were input for a range of conditions. The same conditions were entered in a series of LDRM runs and the predicted drawdown at the well was compared between the LDRM and the Theim equation. The drawdown between the two calculations showed no error over the tested range of conditions. The LDRM code used to predict the steady state drawdown is consistent with the Theim Equation and appears to be functioning properly.

The Theim Equation was also applied to the LNAPL production rate over a range of conditions, shown in Appendix B. The LNAPL transmissivity and water drawdown (verified above) were calculated using the LDRM and used in the Theim Equation. The LDRM recovery rate was then compared to the results from the Theim Equation. The results of the analysis demonstrate that the LDRM recovery rates and the Theim Equation produce similar LNAPL production rates. The minor differences (less than 0.05%) noted in Appendix B are due to rounding error associated with the drawdown and LNAPL transmissivity calculations. It appears the LDRM code calculates LNAPL production rate as intended according to the modifications of the Theim equation and variants.

### 3.4 CONCEPTUAL MODEL VERIFICATION

The LDRM uses a conceptual model of vertical equilibrium (VEQ) assumptions to define the vertical extent and distribution of the LNAPL. When the well is selected as the recovery method, the vertical extent and the radius of capture are used to define a cylindrical model domain. When the trench is selected, the simulated domain is defined by the trench length, LNAPL lens width, and vertical LNAPL extent. LNAPL is recovered uniformly from the domain, resulting in a decrease in LNAPL thickness and saturation through time.

To verify that the LDRM accurately represents the conceptual model, the initial LDRM calculations of LNAPL volume per unit area ( $D_n$  and  $R_n$ ) were used to confirm that the total LNAPL volume estimates for the model domain were accurate. Next, as the recovery operations removed LNAPL from the domain, the updated LNAPL-specific volume numbers were used to determine the amount of remaining LNAPL. The results of the conceptual model verification indicate that the LDRM accurately represents the conceptual model.

### 3.5 COMPARISON TO NUMERICAL SIMULATIONS

To further evaluate the recovery estimates from the LDRM, four scenarios have been compared to numerical simulations. The results of the analysis are presented in Appendix C and discussed below.

The analysis indicates that the LDRM generally predicts higher early time recovery rates than the numerical simulations. As a result, the LDRM estimates that more LNAPL can be recovered in a shorter period of time than the equivalent numerical simulations. The analysis also demonstrates that the LDRM results most closely agree with the numerical simulations when high conductivity soils with high LNAPL saturation are input. The difference in LNAPL recovery for the course sand is within 20% for both the LDRM simulations (Burdine and Mualem) and the numerical analysis. The fine sand simulation indicates that the recovery for Burdine and Mualem models are 21% and 41%, respectively, more than the numerical simulation. For the silty sand, more than an order of magnitude difference exists between the numerical simulations and the Mualem LDRM.

The differences between the LDRM and the numerical simulations are in part due to the LDRM's simplification of the LNAPL distribution within the model domain. The LDRM averages the LNAPL depletion over the model domain through time, while the numerical simulation computes the LNAPL depletion at various points throughout the model domain. The LDRM also estimates the LNAPL volume with the assumption that the LNAPL is in vertical equilibrium (VEQ). When the LNAPL conductivity is high, which occurs in course-grained soils and high LNAPL saturations, the VEQ assumptions are fairly accurate. However, when the LNAPL conductivity is low, the VEQ is often not maintained, resulting in an over prediction of the LNAPL recovery.

Overall, the LDRM compares reasonably well to numerical simulations for relatively high conductivity soils with moderate to high LNAPL saturations. However, as with other analytic models that use VEQ assumptions, the LDRM results become less accurate when fine-grained soils or low-LNAPL saturations are modeled for recovery.

### 4.0 PARAMETER SENSITIVITY

A parameter sensitivity screening is provided in this section to give the user a feeling for which parameters are important and sensitive in the LDRM evaluations. The quantitative sensitivity to each parameter obviously varies with problem conditions, so these sensitivity results are germane only to the examples discussed. Sensitive parameters discussed below can be important at any site for which LDRM or other multiphase evaluations are conducted. However, the degree of site specific sensitivity may be different than that discussed in the examples that follow. Do not arbitrarily apply these sensitivity results, or non-representative statements may result.

The parameter sensitivity analysis consists of a matrix of LDRM runs. A range of inputs for each parameter is selected, based on parameter ranges from the API-LNAPL parameters database. The first LDRM run is a "base case," for which the input is comprised of the middle value for each varied parameter. The base case run provides a point of reference against which all subsequent LDRM outputs are compared. The remainder of the matrix runs consist of inputs identical to the base case except for one variable, which is either increased or decreased. The effect of increasing or decreasing each variable is then determined relative to the base case for the given examples.

The LDRM inputs and key outputs are presented in Appendix D. The effect of each parameter is described in the following sections. The base case properties chosen for the well and trench sensitivity analyses represent an LNAPL similar to a diesel fuel, with soil properties that are similar to a sand (representing intermediate soil and fluid values).

The LDRM requires 22 input parameters to estimate the LNAPL saturation profile and LNAPL volume. When a well is selected as the recovery method, an additional six parameters are required. When a trench is selected as the recovery method, an additional four parameters are required. To simplify the analysis, two separate parameter sensitivity matrices were used, the first with a well and the second with a trench as the recovery method. This strategy resulted in 57 simulations in the well matrix and 53 simulations in the trench matrix, for a total of 110 runs.

The sections below describe how each input parameter affects the LDRM output. The parameters have been divided into two groups. The first group includes parameters that affect the fluid saturation profiles (LNAPL distribution) and the LNAPL volume estimates. The second group of parameters are necessary to compute the recovery rate.

#### 4.1 LNAPL DISTRIBUTION INPUT PARAMETERS

The following section describes the effects that soil/fluid input properties and program settings have on the LNAPL distribution ( $S_{max}$  and  $S_{avg}$ ) and specific volume estimates ( $R_n$  and  $D_n$ ). To quantify the effects of each parameter, the maximum and average saturation values from the well sensitivity matrix are discussed below and shown in Table 1 below.

**Table 1**

Variable	Input values			Maximum Saturation			Average Saturation		
	Low	Base	High	Low	Base	High	Low	Base	High
van Genuchten alpha [ $m^{-1}$ ]	1	3	6	0.05	0.4	0.63	0.03	0.23	0.39
van Genuchten n	2.1	3	4	0.06	0.4	0.59	0.04	0.23	0.33
Swr1	0.05	0.15	0.25	0.45	0.4	0.35	0.26	0.23	0.2
LNAPL Density [ $g/cm^3$ ]	0.65	0.8	0.95	0.59	0.4	0.02	0.32	0.23	0.01
LNAPL/Water Interfacial tension	15	25	35	0.58	0.4	0.26	0.33	0.23	0.14
LNAPL Surface tension [dyne/cm]	15	25	35	0.39	0.4	0.41	0.23	0.23	0.23
Monitoring Well LNAPL thickness [m]	0.5	1	1.5	0.14	0.4	0.54	0.07	0.23	0.33
Ground surface elevation [m]	1	3	5	0.4	0.4	0.4	0.23	0.23	0.23
Water vertical gradient (+up)	-0.01	0	0.01	0.38	0.4	0.42	0.22	0.23	0.24

#### 4.1.1 Soil Capillary Parameters

The LDRM uses the van Genuchten equation to represent the soil capillary properties. The van Genuchten equation has three key parameters:  $\alpha$ , which is roughly inversely proportional to the capillary fringe height;  $n$  (some scientists use “ $S$ ” instead of “ $n$ ”), which is a measure of pore-size uniformity (with higher values indicating more uniform pore-sizing); and  $S_{wr}$ , which is the residual saturation of the wetting phase. To test the LDRM model, each of the three parameters were varied over a range of values. The effect of each input on the LDRM output is discussed below.

The  $\alpha$  parameter has an exponential effect on the average and peak LNAPL saturation calculations because it is part of the capillary head calculation, which itself is exponential. When  $\alpha$  was decreased from the base value of  $3 \text{ m}^{-1}$  to a value of  $1 \text{ m}^{-1}$ , the average and peak LNAPL saturation decreased by 88% and 86% from the base case values, respectively. When  $\alpha$  was increased from the base value to  $6 \text{ m}^{-1}$ , the average and peak LNAPL saturation increased by 71% and 57%, respectively.

The  $n$  parameter is the exponent to which the capillary head/saturation equation is raised. Therefore, the  $n$  parameter also has an exponential effect on the average and peak LNAPL saturation calculations for the given conditions. When  $n$  was decreased from the base value of 3 to a value of 2.1, the average and peak LNAPL saturation decreased by 84% and 85% from the base case values, respectively. When  $n$  was increased from the base value to 4, the average and peak LNAPL saturation increased by 44% and 48%, respectively.

The  $S_{wr}$  has a fractional effect on the average and peak LNAPL saturation calculations because it affects only pore saturation volumetrics. When  $S_{wr}$  was decreased from the base value of 15% to a value of 5%, the average and peak LNAPL saturation increased by 12%. When  $S_{wr}$  was increased from the base value to 25%, the average and peak LNAPL saturation decreased by 12%.

#### 4.1.2 LNAPL Density

The LNAPL density has a non-linear effect on the average and peak LNAPL saturation calculations because it is used in the non-linear capillary head estimation. When LNAPL density was decreased from the base value of  $0.8 \text{ g/cc}$  to a value of  $0.65 \text{ g/cc}$ , the average and peak LNAPL saturation increased by 38% and 48%, respectively. When the LNAPL density was increased from the base value to  $0.95 \text{ g/cc}$ , the average and peak LNAPL saturation decreased by 96% and 95%, respectively.

#### 4.1.3 LNAPL/Water Interfacial Tension

The LNAPL/water interfacial tension has an inverse, non-linear effect on the average and peak LNAPL saturation calculations. This is because interfacial tension scales the non-linear capillary function between different fluid couplets (air-water, oil-water). When LNAPL/water interfacial tension was decreased from the base value of  $25 \text{ dyne/cm}$  to a value of  $15 \text{ dyne/cm}$ , the average and peak LNAPL saturation increased by 45%. When LNAPL/water interfacial tension was increased from the base value to  $35 \text{ dyne/cm}$ , the average and peak LNAPL saturation decreased by 39% and 35%, respectively.



#### 4.1.4 LNAPL/Air Interfacial Tension

The LNAPL/air interfacial tension has a fractional effect on the average and peak LNAPL saturation calculations. This factor affects primarily the oil/water/air capillary fringe, and therefore only affects a small portion of the saturation profile. When LNAPL/air interfacial tension was decreased from the base value of 25 dyne/cm to a value of 15 dyne/cm, the average and peak LNAPL saturation both decreased by 2%. When LNAPL/air interfacial tension was increased from the base value to 35 dyne/cm, the average and peak LNAPL saturation increased by 1% and 2%, respectively.

#### 4.1.5 Monitoring Well LNAPL Thickness

At VEQ, the observed LNAPL well thickness is part of the non-linear capillary head/saturation calculation. Therefore, the monitoring well LNAPL thickness has a non-linear effect on the average and peak LNAPL saturation calculations. When the monitoring well LNAPL thickness was decreased from the base value of 1 m to a value of 0.5 m, the average and peak LNAPL saturation decreased by 68% and 65%, respectively. When the monitoring well LNAPL thickness was increased from the base value to 1.5 m, the average and peak LNAPL saturation increased by 44% and 37%, respectively. The total LNAPL volume in the formation is proportional to the LNAPL thickness. A doubling of the LNAPL thickness results in slightly less than a doubling of the total volume in place.

#### 4.1.6 Ground Surface Elevation

When the LNAPL is near the ground surface, this factor will truncate the saturation functions at the ground surface. The ground surface term may affect the LNAPL volume estimate when LNAPL is near the surface. No effects from the ground surface elevation were noted in the sensitivity matrix.

#### 4.1.7 Vertical Groundwater Gradient

The vertical groundwater gradient is used to alter the saturation profile to account for the different capillary pressures under a vertical gradient. This can occur in fine-grained soils near the surface (according to the LDRM documentation). The vertical water gradient has a minimal effect on the average and peak LNAPL saturation calculations, with an approximately linear sensitivity as the vertical water gradient is increased. When the vertical water gradient was decreased from the base value of 0 to a value of -0.01, the average and peak LNAPL saturation decreased by 2% and 3%, respectively. When the vertical water gradient was increased from the base value to +0.01, the average and peak LNAPL saturation increased by 2% and 3%, respectively.

### 4.2 RECOVERY MODEL INPUT PARAMETERS

The input parameters discussed below are necessary to calculate the average fluid conductivity and transmissivity, LNAPL recovery rate, total recoverable LNAPL volume, etc. from the LNAPL saturation calculations that have been discussed above. The parameters discussed below do not affect the initial conditions for the LNAPL (or water) saturation calculations. To simplify the discussion, the values provided in the following sections are from the well sensitivity matrix, with the exception of trench-specific parameters. Both the trench and well sensitivity matrices demonstrate similar trends and values.

The effects of the input parameters are described below and presented in Table 2 using the values for total LNAPL recovery and initial recovery rate. The total LNAPL recovery is a measure of the total recoverable LNAPL volume, given sufficient time. The initial recovery rate is an indication of the rate that LNAPL will be recovered over the first modeled time interval. Since the model time intervals are the same between simulations, the initial recovery rate provides some insight to which parameters will speed up or impede the recovery rate of LNAPL. The initial recovery rate should not be used to compare LDRM simulations with different time scales.

#### 4.2.1 Soil Properties

The soil properties that effect the recoverability of LNAPL are conductivity and residual LNAPL saturation. These input parameters are discussed below, with variable ranges presented in Table 2.

**Table 2**

Variable	Input values			Initial Recovery Rate (L/day)			Total Recovery Volume (L)		
	Low	Base	High	Low	Base	High	Low	Base	High
Hydraulic conductivity [m/d]	1	10	100	505	925	5,124	199,161	199,245	199,245
* LNAPL Residual	1	2	2	732	925	925	207,150	199,245	199,245
Residual-f (vadose)	0.1	0.2	0.3	896	925	956	202,952	199,245	195,531
Residual-f (saturated)	0.2	0.3	0.4	777	925	1,101	204,969	199,245	193,516
LNAPL Viscosity [cp]	0.5	2	5	3,699	925	370	199,245	199,245	198,590
Recovery time [yr]	2	10	20	925	925	925	188,304	199,245	199,245
Water production rate [l/min]	10	50	100	558	925	1,383	199,208	199,245	199,245

##### 4.2.1.1 Hydraulic Conductivity

The aquifer hydraulic conductivity affects the LNAPL recovery calculations in two ways. First, the hydraulic conductivity is used to calculate the LNAPL transmissivity by integrating relative permeability and fluid properties, which then directly controls the LNAPL recovery rate. Second, the hydraulic conductivity affects the drawdown and gradient caused by water production in a dual-phase extraction system. Given sufficient time, the same total volume of LNAPL can be recovered, regardless of conductivity (except for minor variability due to LNAPL potential smearing).

The effect of hydraulic conductivity is a fractionally proportional to the initial LNAPL recovery rate. When conductivity was decreased from the base value of 10 m/day to a value of 1 m/day, initial LNAPL recovery rate and total recovery estimates decreased by 45% and 0%, respectively. When conductivity was increased from the base value to 100 m/day, the initial recovery rate and total volume recovered increased by 454% and 0%, respectively. The total recovery volume is not effected because 1) LNAPL smearing is not taken into account and 2) the simulations were run for sufficient time.

#### 4.2.1.2 Residual LNAPL Saturations and "F-factors"

The residual LNAPL saturation parameters control the fraction of the total LNAPL volume that is immobile and non-recoverable within the formation. The program uses two values for residual saturation: 1) two-phase residual " $S_{nrs}$ " to quantify the residual or entrapped LNAPL below the watertable; and 2) three-phase residual " $S_{nrV}$ " to quantify the residual LNAPL above the watertable in the vadose zone (note: this has now been changed in Version 3.7). The residual saturation values are calculated by the program as a fraction of the initial saturation (F-factors). The user cannot directly input residual LNAPL values; however, the user can still control the residual LNAPL values through "F-factors." The F-factors are simply the fraction of the initial saturation that is residual LNAPL. There are two F-factors, one factor for the two-phase residual or entrapped LNAPL and one for the three-phase residual LNAPL above the watertable.

The residual LNAPL saturations are calculated from the F-factors using one of two methods. The first method, "constant residual saturation," computes the residual saturations as the maximum saturation value multiplied by the F-factors to determine the two- and three-phase residual saturation values.

When the constant residual saturation method is selected, the F-factors have a fractionally proportional effect on the initial recovery rate and total LNAPL recovery, with a linear sensitivity as the F-factors are increased. When the F-factors (vadose and saturated) are decreased from the base values of 0.2 and 0.3, respectively, to values of 0.1 and 0.2, the initial recovery rates decreased by 3% and 6%, while the total recovery volumes increased by 2% and 3%. When the F-factors (vadose and saturated) are increased from the base values to values of 0.3 and 0.4, respectively, the initial recovery rates increased by 3% and 19%, while the total recovery volumes decreased by 2% and 3%. These findings are consistent with the anticipated effect of altering the F-Factors.

The second option, "variable residual saturation," computes the residual saturation at every point along the saturation profile. The variable method calculates a greater recoverable volume and thus a greater total recovery than the constant residual saturation method. When the variable residual saturation option was selected, the total LNAPL volume recovered increased by 4%. Again, note that these results are very much specific to the simulations provided, and a much wider range may be anticipated in site specific applications for other conditions.

#### 4.2.2 LNAPL Viscosity

Viscosity has an inverse linear effect on the initial recovery rate. When the viscosity was decreased from the base value of 2 cp to a value of 0.5 cp, the initial recovery rate increased by 300%. When viscosity was increased from the base value to 5 cp, the initial recovery rate is decreased by 60%. Given sufficient time, the same total LNAPL recovery can be achieved, though a higher viscosity LNAPL will require a longer design time. These findings are consistent with the anticipated effect of altering the viscosity parameter.

### 4.2.3 Recovery Time

The recovery time is the time the system is expected to operate. The LDRM creates 60 evenly-spaced time intervals from 0 to the design time in the data file. At each of the 60 time steps, the program reports the LNAPL thickness, total volume recovered to date, and current recovery rate. The percent recovery displayed on the main program window is computed as the total volume recovered at the last time step divided by the total recoverable LNAPL. A display of "100% recovery" indicates that all of the mobile fraction can potentially be removed. Within the sensitivity analysis, three design times were explored. The results show no change in the initial recovery rates for any of the design times, and only a small decrease (5%) in the total volume recovered for the smallest design time (two years).

### 4.2.4 Water Production Rate

The water production rate is the rate at which water is extracted from a well or trench in an effort to increase the LNAPL gradient (dual-phase extraction). A larger water production rate will cause a larger drawdown and result in a higher gradient, which can increase the rate at which LNAPL will be recovered. The larger drawdown can also cause additional smearing of the LNAPL (provided the smear correction is on) that will decrease the total LNAPL recovery volume.

The water production rate has a fractional effect (2:1) on the initial recovery rate calculations when the smear correction is not active (well sensitivity matrix). When the water production rate was decreased from the base value of 50 L/min to a value of 10 L/min, the initial recovery rate decreased by 40%. When the water production rate was increased from the base value to 100 L/min, the initial recovery rate increased by 50%. The smear correction was not active for the sensitivity matrix, so the total volume recovered was not affected for the well sensitivity matrix.

### 4.2.5 Well Properties

The following section discusses the input parameters that are specific to the well recovery method. The effects of each input parameter are shown in Table 3 and discussed below.

**Table 3**

Variable	Input values			Initial Recovery Rate (L/day)			Total Recovery Volume (L)		
	Low	Base	High	Low	Base	High	Low	Base	High
Radius of pumping well [m]	0.03	0.06	0.12	862	925	1,011	199,245	199,245	199,245
Radius of capture [m]	10	30	60	925	925	925	22,138	199,245	775,330
Radius of influence [m]	20	60	120	925	925	925	199,245	199,245	199,245
Groundwater thickness [m]	1	5	15	2,758	925	619	199,245	199,245	199,231
Suction pressure [atm]	0	0.1	0.2	458	925	1,391	199,074	199,245	199,245
Screen length for air flow [m]	1	5	10	925	925	925	199,245	199,245	199,245

#### 4.2.5.1 Radius of the Pumping Well

The well radius has a fractional effect on the initial recovery rate. When the well radius was decreased from the base value of 0.06 m to a value of 0.03 m, the initial recovery rate decreased by 7%. When the well radius was increased from the base value to 0.12 m, the initial recovery rate increased by 9%. Given sufficient time, the total recovery is unaffected.

#### 4.2.5.2 Radius of Capture

The radius of capture is used to define the total volume of LNAPL in place that can be potentially recovered by the well. The total recovery increases linearly with area within the radius. The radius of capture has an exponential effect on the total recovery rate. When the radius of capture was decreased from the base value of 30 m to a value of 10 m, the total recovery decreased by 89%. When the well radius was increased from the base value to 60 m, the total recovery increased by 289%.

#### 4.2.5.3 Radius of Influence

The radius of influence is used to determine the drawdown and gradient. Radii of influence of 20 m, 60 m, and 120 m were utilized in the sensitivity matrix. No significant changes in the initial production rate or the total production were noted. The radius of influence is not generally a sensitive parameter unless it becomes small relative to the domain, and the results of the sensitivity matrix support that finding.

#### 4.2.5.4 Groundwater Thickness

The groundwater thickness parameter is used to determine the screened interval below the LNAPL. A shorter screened interval results in a lower transmissivity that increases the drawdown for a given pumping rate.

Groundwater thickness has an inverse non-linear effect on the initial recovery rate, with a decreasing sensitivity as the groundwater thickness is increased. When the groundwater thickness was decreased from the base value of 5 m to a value of 1 m, the initial recovery rate increased by 198%. When the groundwater thickness was increased from the base value to 15 m, the initial recovery rate decreased by 33%. Given sufficient time, total recovery is not affected by the groundwater thickness. Additionally, groundwater thickness does not affect the LNAPL recovery rate under ambient (no water pumping) conditions.

#### 4.2.5.5 Air-Phase Vacuum

A vacuum can be applied to enhance LNAPL recovery. The vacuum is the negative pressure (in atm) applied to the well head to enhance LNAPL recovery. The larger the vacuum, the higher the initial rates of LNAPL recovery. However, given sufficient time, the same volume of LNAPL can theoretically be recovered, regardless of the applied vacuum.

The vacuum has a linear effect on the initial recovery rate. When the vacuum is decreased from the base value of 0.1 atm to a value of 0 atm, the initial recovery rate decreased by 50%. When the vacuum was increased from the base value to 0.2 atm, the initial recovery rate increased by 50%.

#### 4.2.5.6 Screen Length for Air Flow and Radius of Capture for Air Flow

Two additional parameters that relate to the vacuum are screen length for air flow and the radius of capture for air flow. These parameters are necessary to determine the air flow rate required to maintain the vacuum pressure in the well. For example, when the screen length was decreased from 5 m to 1 m, the required air flow rate decreased from approximately 1018 L/min to approximately 509 L/min.

#### 4.2.6 Trench Properties

The following sections and Table 4 describe the effects of each input parameter specific to trench recovery. These parameters control the initial recovery rate and total volume of LNAPL that can be recovered, but they do not affect the saturation distribution.

**Table 4**

Variable	Input values			Initial Recovery Rate (L/day)			Total Recovery Volume (L)		
	Low	Base	High	Low	Base	High	Low	Base	High
Natural hydraulic gradient (Jw)	0	0	0.01	41	63	256	438,475	460,222	467,228
Trench length [m]	50	75	100	56	63	70	310,281	460,222	604,573
LNAPL lens width [m]	50	100	150	63	63	63	233,557	460,222	659,306
Screen depth [m]	1	5	10	228	63	42	467,228	460,222	440,054

#### 4.2.6.1 Natural Hydraulic Gradient

The natural gradient is the ambient gradient from the LNAPL body toward the trench. The program assumes that the trench is installed directly down gradient from the LNAPL body. The gradient affects the flow of water and LNAPL toward the trench.

The gradient has a fractional effect on the initial recovery rate, with a linear sensitivity as the gradient is increased. When the gradient was decreased from the base value of 0.001m/m to a value of 0.0001 m/m, the initial recovery rate decreased by 34%. When the gradient was increased from the base value to 0.01m/m, the initial recovery increased by 308%. Given sufficient time, the same volume can be recovered.

#### 4.2.6.2 Trench Length

The trench length is used to define the width of the LNAPL body transverse to flow (similar to the radius of capture for a well). The trench length has a linear effect on the total recovery and initial recovery rate. When the trench length was decreased from the base value of 75 m to a value of 50 m, the total recovery decreased by 33%. When the trench length was increased from the base value to 100 m, the total recovery increased by 31%.

#### 4.2.6.3 LNAPL Lens Width

Lens width is the length of the LNAPL body parallel to the direction of flow (similar to the radius of capture for a well). The longer the lens width, the more LNAPL is present. The LNAPL lens width has a linear effect on the total recovery. When the lens width was decreased from the base value of 100 m to a value of 50 m, the total recovery decreased by 49%. When the LNAPL lens width was increased from the base value to 150 m, the total recovery increased by 43%. The longer the lens width, the longer the recovery will take; the effects of the large LNAPL lens width have been slightly skewed by an insufficient recovery time.

#### 4.2.6.4 Screen Depth

The screen depth is equivalent to the groundwater thickness for the well. Larger screened intervals result in larger water transmissivity values, which in turn results in less drawdown and a smaller gradient. The screen length is not a sensitive parameter for a skimming trench (no water production).

#### 4.2.7 Smear Correction

The smear correction is a feature used to account for LNAPL smearing that occurs from dual-phase recovery by recalculating the saturation profile to account for the average drop in the watertable across the domain. When the smear correction feature is selected, the program accounts for the increased volume of soil that will be impacted by the LNAPL. The smear correction increases the volume of residual LNAPL and results in slower and smaller recovery than when the option is not selected. When this option is not selected, the program will compute increasingly faster recovery rates as the water production rate is increased. Activating this parameter allows the user to explore the effects of under/over pumping. As shown in Table 5, the total recovery and initial recovery rate decreased by 9% and 5%, respectively, when the smear correction was activated in the well matrix.

**Table 5**

Variable	Input values			Initial Recovery Rate (L/day)			Total Recovery Volume (L)		
	Low	Base	High	Low	Base	High	Low	Base	High
* Smear Correction	0	0	1	925	925	810	199,245	199,245	182,147
Relative permeability model	0	0	1	925	925	4,905	199,245	199,245	299,515

#### 4.2.8 Relative Permeability Models

The LDRM program has two options to compute the relative permeability to LNAPL. The default method is a modified Burdine model. Alternatively, the Mualem model can be selected to compute the relative permeability. Given the same input parameters (which is not the recommended procedure), the Mualem model results in a higher initial recovery rate than the Burdine model. As shown in Table 5, the recovery rate for the Burdine model does not decrease as rapidly as the Mualem model. When the Mualem model was selected, the initial recovery rate increased 430% over the Burdine model, while the total recovery increased by 50%. The increase in total volume is a result of the different soil property inputs required for the Burdine and Mualem models. This example demonstrates the error that would occur if a user were to switch relative permeability models without changing the soil properties. When the alternate van Genuchten parameters are input, as recommended in LDRM documentation, both relative permeability functions produce the same total volumes.

### 5.0 SUMMARY AND CONCLUSIONS

The objective of this report is to summarize the processes used to validate the LDRM and document the anomalies within the program, the majority of which have been addressed through code updates to beta Version 2 (current Version 3.7). The validation process isolated each component of the combined calculations, to the degree possible, and compared the intermediate calculations to other relevant calculations, analytic models, and numerical models. Additionally, LDRM simulations were evaluated to determine the sensitivity that each input parameter had on the resulting calculations. The general functionality of the program and recommended improvements have also been discussed.

In general, the LDRM produced reasonable estimates for LNAPL recovery from a well and trench. The intermediate calculations for the LNAPL saturation, relative permeability, and LNAPL recovery rates are consistent with published methods. The LDRM's recovery rates compared reasonably well to numerical simulations under certain conditions. When the LNAPL transmissivity is high, VEQ assumptions are valid and the LDRM calculations agree with the numerical simulations. However, when the LNAPL transmissivity is low, VEQ conditions are not maintained, and the LDRM predicts more LNAPL recovery than the numerical simulations.

The results of the sensitivity analysis demonstrate that the LDRM generally performs as expected. Varying input parameters affect the LDRM in a predictable and logical way. Additionally, the different features of the LDRM have consistent and expected results.



Overall, the program is fairly easy to understand and use. A few minor glitches, such as graphs not printing correctly, were noted; however, none of these glitches causes serious errors in the final results of the LDRM. With the implementation of some recommended improvements to the user-interface, the program will be simple for most users to understand and use.



**Additional copies are available through IHS**

Phone Orders: 1-800-854-7179 (Toll-free in the U.S. and Canada)  
303-397-7956 (Local and International)  
Fax Orders: 303-397-2740  
Online Orders: [global.ihs.com](http://global.ihs.com)

Information about API Publications, Programs and Services  
is available on the web at [www.api.org](http://www.api.org)



1220 L Street, NW  
Washington, DC 20005-4070  
USA

202.682.8000

Product No. I47600